Spring 6-17-2021

Life Cycle Climate Performance Assessment for R1234yf As a Low GWP Drop-In Alternative for R134a in Domestic Refrigerators

Mohamed Ragab Senosey Khaled Zain
The American University in Cairo AUC, mohamed_ragab@aucegypt.edu

THE AMERICAN UNIVERSITY IN CAIRO
SCHOOL OF SCIENCES AND ENGINEERING

Life Cycle Climate Performance Assessment For R1234yf As A Low GWP Drop-In Alternative For R134a In Domestic Refrigerators

BY

Mohamed Ragab Senosey Khaled Zain

A thesis submitted in partial fulfillment of the requirements for the degree of

Master of Science in Mechanical Engineering

Under the supervision of:

Dr. Mohamed El-Morsi

Professor, The Dept. of Mechanical Engineering

The American University in Cairo

Dr. Nabil Mahmoud

Professor, Mechanical Engineering Power Dept.

Ain Shams University

Dr. Omar Abdelaziz

Assistant Professor, The Dept. of Mechanical Engineering

The American University in Cairo

Dr. Asmaa Ramadan

Assistant Professor, Mechanical Engineering Power Dept.

Ain Shams University

May 2021

Dedication

To

My parents and sisters
for their patience, support, and continuous encouragement.

Acknowledgments

I Would like to express my ultimate gratitude to my advisors Professor Mohamed El-Morsi, Professor Omar Abdelaziz, Professor Nabil Abdelaziz, Professor Asmaa El-Sayed. My sincere appreciation is extended to the professors in the Mechanical Engineering Department, AUC. They taught me a lot and enriched my study journey. My cordial thanks are due to Professor Mohamed El-Morsi and Professor Omar Abdelaziz. They always provided candid and critical comments that assisted me in getting out with this work in a presentable way. I have greatly profited from their advice, interactions, and discussions. Professor Mohamed El-Morsi generously made available to me his lab facilities and paid for the expensive experimental setup components that the AUC research grant did not cover. Without using his lab facilities and the components, I could not have completed the experiment of my thesis.

I would particularly wish to thank the members of the Fluid Mechanics and Solar Energy Laboratories members Eng. Osama Mohamed and Hamdy for their help. Special and sincere thanks are due to Haitham Mohamed Awad, Fluid Mechanics Lab Technician, for his precious help. Haitham sacrifices his relaxation time after the official working hours and during weekends to let me access the laboratory after my working hours and during weekends.

Last but not least. I would like to express appreciation to Mohamed El Banna and Khaled Terzaki who helped me build the current measurement output modification circuit. Also, I wish to thank Ashraf Talaat, Mohamed Osman, Omar Osama, Mohamed Al-Shehabi, Ashraf Bazan, Islam Hamdy, and the other friends and colleagues who contributed with either inspirational or actual work in this research effort.

Abstract

Aligning with the global movements towards mitigating CO_2 emissions and regulations to phase out HFC refrigerants, many low GWP refrigerants are being tested and proposed as fourth-generation refrigerants. R1234yf is a refrigerant with a GWP of less than one and has a high potential to replace R134a, which has a GWP of 1300, and it is the most commonly used refrigerant in domestic refrigerators. In this study, an energy performance evaluation and a life cycle climate performance assessment for R1234yf were conducted and compared to those of R134a based on a baseline domestic defrost refrigerators. Four different charges of R1234yf (166.5g, 185g, 202g, and 221g) were tested on three thermostat points (low, medium, and high) and compared with the recommended manufacturer charge of R134a. This study ended up with R1234yf can reduce daily energy consumption by 5 to 2% depending on the thermostat setting. Also, the R1234yf charge optimization to the lowest life cycle CO_2 emissions shows that reducing the charge from the baseline value of 185g to 166.5g proves to be the best option. In addition, all R1234yf charges achieved lower evaporation temperature than R134a at all thermostat settings. Also, R1234yf charges were able to achieve similar freezer and refrigerator air temperatures to that of R134a.

Table of Contents

Table of Contents

List of Figures

List of Tables

List of Nomenclature and Abbreviations

Nomenclatures

C	Refrigerant Charge (Kg)
E	Energy (Wh)
h	Enthalpy (KJ/Kg)
I	Current (A)
m	Refrigerant Mass (kg)
N	System’s Lifetime (year)
P	Pressure (bar)
T	Temperature (°C)
V	Voltage (V)

Subscripts

cond	Condensation
evap	Evaporation

Abbreviations

AEC	Annual electricity consumption (kWh)
Adp. GWP	Adaptive global warming potential

AFEAS	Alternative fluorocarbons environmental acceptability study
ALR	Annual leakage rate (%)
CFC	Chlorofluorocarbons
COP	Coefficient of performance
ED	Efficiency defect
EDR	Exergy destruction ratio
EEC	Ejector/expansion cycle
EEG	Emissions of electricity generation ($kgCO_2/kWh$)
EELSHXC	Ejector/expansion with liquid suction heat exchanger cycle
EES	Engineering Equation Solver
EOLL	End of Life Leakage (%)
ERD	Emissions of Refrigerant Disposal (CO_2/ kg of refrigerant)
ERM	Emissions of refrigerant manufacturing (CO_2/ kg of refrigerant)
ESMM	Emissions system's material manufacturing ($kgCo_2$/kg of material)
GWP	Global warming potential
HC	Hydrocarbon
HCFC	Hydrochlorofluorocarbons

HFC	Hydrofluorocarbon
HFO	Hydrofluoroolefin
IPCC	Intergovernmental panel on climate change
LCCP	Life cycle climate performance
LSHX	Liquid suction heat exchanger
MAC	Mobile air conditioning
Max.	Maximum
Min.	Minimum
MRE	Material recycling emissions (CO_2/kg of recycled material)
MRM	Mass of recycled material (kg)
ODP	Ozone depletion potential
P. F	Power factor
SM	System’s mass (kg)
TEWI	Total equivalent warning impact
VCC	Volumetric cooling Capacity

Chapter 1 Introduction

In 1997, several countries signed the Kyoto protocol in Kyoto city, Japan. Targeting, for the second time in the 20th century, the gradual reduction of and banning the usage of some widely used fluids, especially those used for refrigeration [1]. A refrigeration process could be defined as the process of cooling a particular space and maintaining its temperature below the temperature of the surroundings [2]. The fluids used to carry out the refrigeration processes are called refrigerants. Generally, refrigerants are substances that serve as a cooling agent by absorbing heat from the desired space or object [2]. In vapor compression refrigeration cycles, the refrigerant is the working fluid that vaporizes when it absorbs heat from a heat source (cooling load) and condenses when releases this heat to a heat sink or the environment.

From the beginning of the artificial refrigeration in 1834, the year in which the first patent for an ice-making machine was granted [3], until 1929, the known refrigerants were natural substance like sulfur dioxide (SO_2), methyl chloride (CH_3Cl), carbon dioxide (CO_2), chloroethane (C_2H_5Cl), and ammonia (NH_3) [4]. These early used refrigerants have severe detrimental effects on human health; thus, Thomas Migdley and his research team in 1929 derived and produced, from petroleum, in a laboratory the first molecules of dichlorodifluoromethane (CCl_2F_2). Afterward, this chemical compound was manufactured at scale by Dupont de Nemours in 1932 under the name of Freon to replace the early toxic refrigerants [4]. At this point, the era of chlorofluorocarbons (CFC) refrigerants and hydrochlorofluorocarbons (HCFC) has begun.

In the 1970s, the world recognized the role of refrigeration activities in the ozone layer depletion problem [5]. In fact, CFC and HCFC refrigerants leakage to the atmosphere with significant amounts caused negative effects on the environment, especially the ozone layer [6] [3]. The term Ozone Depletion Potential (ODP) was introduced to quantify the harmful ability of a certain gas on the ozone layer. ODP measures the contribution of a certain gas to the depletion of the ozone layer relative to that of dichlorodifluoromethane (R-12). CFCs and HCFCs refrigerants have an ODP ranging from 1 to 16 and 0.001 to 0.2, respectively [6].

In light of this, in 1987, the Montreal Protocol was signed to gradually reduce the use of CFC and HCFC refrigerants to reach total phase-out by 2010 for CFCs Refrigerants and 2040 for HCFC Refrigerants, for developing countries [7]. That was the first time to develop a phase-out plan against the usage of a refrigerant; consequently, the era of hydrocarbon refrigerants (HCs) and hydrofluorocarbon refrigerants (HFCs) has begun. Nevertheless, HC refrigerants are not widely used in refrigeration due to their high flammability. Therefore, HFCs were developed and used extensively as third-generation refrigerants, especially R134a [8] [9].

After a short time, the correlation between HFC refrigerants and global warming has been raised. As a result, the Kyoto protocol was signed and updated with the Kigali amendments to accelerate the phase-out process of CFCs and HCFCs, as well as schedule a phase-out for HFCs (the assigned refrigerants to replace CFCs and HCFCs), which has a global warming potential (GWP) of 1300 [10]. The GWP is a criterion created to measure the contribution of a certain amount, 1 ton, of a gas on global warming with respect to the contribution of the same amount of CO_2 [11]. Also, the European Parliament developed regulations like 2037/2000 and 842/2006 to set a

gradual phase-out for HFCs, improve the refrigeration process efficiency to reduce refrigerants charging amount and energy consumption by the systems, and put a GWP limit for the gases to be used such as banning the gases with GWP more than 150 by 2015 [12].

Such a global movement towards low GWP refrigerants made many scientists search for and test new refrigerants taking into consideration the following important selection criteria [4]:

1. ODP, which is an indicator of how harmful a specific refrigerant to the ozone layer.
2. GWP, which is an indicator of how much a specific refrigerant warms the Earth for 100 years.
3. Adp. GWP, which is the GWP of the degradation product of a refrigerant in the atmosphere.
4. Total Equivalent Warming Impact (TEWI), an assessment designed to calculate the contribution of a refrigeration system in global warming during its working life.
5. Life Cycle Climate Performance (LCCP), a holistic approach that counts the CO_2 emissions throughout the system life cycle. It is a cradle-to-grave approach.

According to the later refrigerant selection criteria and the old one that states that the working refrigerant should have no detrimental effects on human health, hydrofluoroolefin refrigerants (HFOs) appear as potential replacements for HFC refrigerants. These refrigerants, HFOs, are chemical compounds composed of unsaturated organic compounds composed of hydrogen, fluorine, and carbon. HFO

refrigerants are characterized by their zero ODP and low GWP; therefore, they are being developed as fourth-generation refrigerants [9].

HFO-1234yf (R1234yf) is one of the promising alternatives to replace HFC-134a (R134a) as it has almost the same thermodynamics properties. However, R1234yf has less cooling effect than R134a at the same working temperatures (condensation and evaporation temperatures). Besides, R1234yf has a GWP of less than 1 [13].

This study examines the LCCP and the energy consumption of R1234yf and R134a using a domestic refrigerator. In the following chapters, a review of the previous work, research objectives, and experimental setup and procedures necessary to study the performance of R1234yf and R134a are presented. Chapter 2 presents a review of the relevant work in addressing R1234yf as a low GWP replacement for R134a. In Chapter 3, the experimental setup of the conducted experiment to study the performance of R1234yf and R134a is presented. Chapter 4 presents the results of this study. Finally, Chapter 5 presents the conclusions and recommendations of this work.

Chapter 2 Literature Review

The environmental aspects act as the main drivers for change, causing phase-outs of systems and introducing new systems. Refrigeration systems have been subject to phase-out plans and the introduction of environmental processes since the industrial refrigeration era. Problems like public health problems, the ozone layer depletion problem, and the global warming played a significant role in moving from a commonly used group of refrigerants to another group of refrigerants. Due to the active contribution of HFCs in the severity of global warming, HFCs are currently subjected to a phase-down plan. R134a, which is the commonly used refrigerant in domestic refrigeration, belongs to the HFC refrigerants; thus, many alternatives are being proposed and investigated to replace R134a to cope with the planned phase-down plan for the HFCs. R1234yf appears to be a promising alternative to replace R134a.

R1234yf is a synthesized refrigerant that belongs to the HFO family with a chemical name: 2,3,3,3-tetrafluoropropene. It is a fluorinated gas, yet it is not among those gases that EU F-gas regulations combat. Moreover, R1234yf has a high potential in the EU to replace restricted fluorinated gases. The reason behind such an exception for R1234yf is the fact that R1234yf is an environmentally friendly refrigerant with no ODP and very low GWP. Table 2.1 summarizes some important chemical properties of R1234yf and R134a.

Table 2.1: R1234yf and R134a properties.

Property	R1234yf	R134a
GWP	0.31 [14]	1300 [15]
Adp. GWP [16]	3.3	1.6
ODP [15]	0	0
Critical Temperature [17]	94.7 °C	101.06 °C
Critical Pressure [17]	33.822 bar	40.593 bar
Safety Class [18]	A2L	A1
Atmospheric Lifetime [15]	0.0288 years (10.5 days)	13.4 years
Refrigerant Manufacturing Emissions [19]	13.7 kg CO_2/kg	9.4 kg CO_2/kg
Chemical Composition [15]	CF3CF=CH2	CH2FCF3
Price*	204.58 $/Kg	78.7 $/Kg

*According to the Egyptian market

In terms of the thermodynamic and heat transfer properties, S. Daviran et al. [20] and S. Jarall [21] studied the heat transfer properties of R1234yf compared with R134a. S. Daviran et al. [20] concluded that the thermal conductivity of R1234yf is 20% lower than that of R134a; As a result, R1234yf exhibited 18–20% lower overall heat transfer coefficient than that of R134a. On the other hand, S. Jarall [21] showed that R1234yf has higher evaporation and convection heat transfer coefficients than R134a. Regarding the thermodynamic properties, R1234yf demonstrated lower specific volume compared to R134a [22]. That means that R1234yf has a higher density than R134a, resulting in a higher mass flow rate for R1234yf per unit volume [20-24]. The refrigerants' latent heat vs. saturation temperature, and thermal conductivity vs. saturation temperature are presented in figures (2.1-2.2) [17]

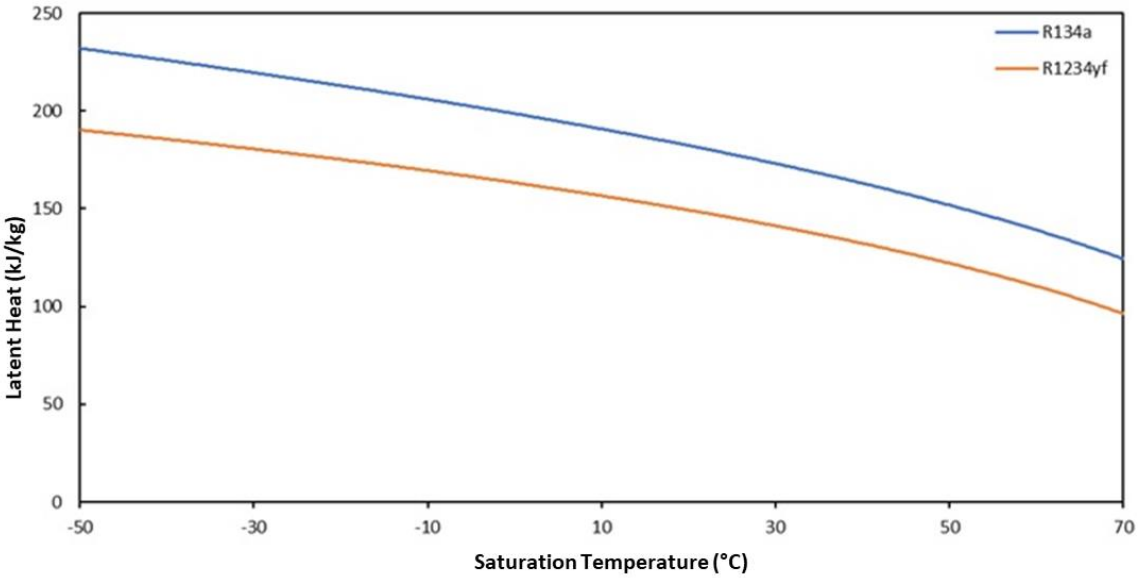

Figure 2.1: R134a and R1234yf latent heat variation with saturation temperature [17].

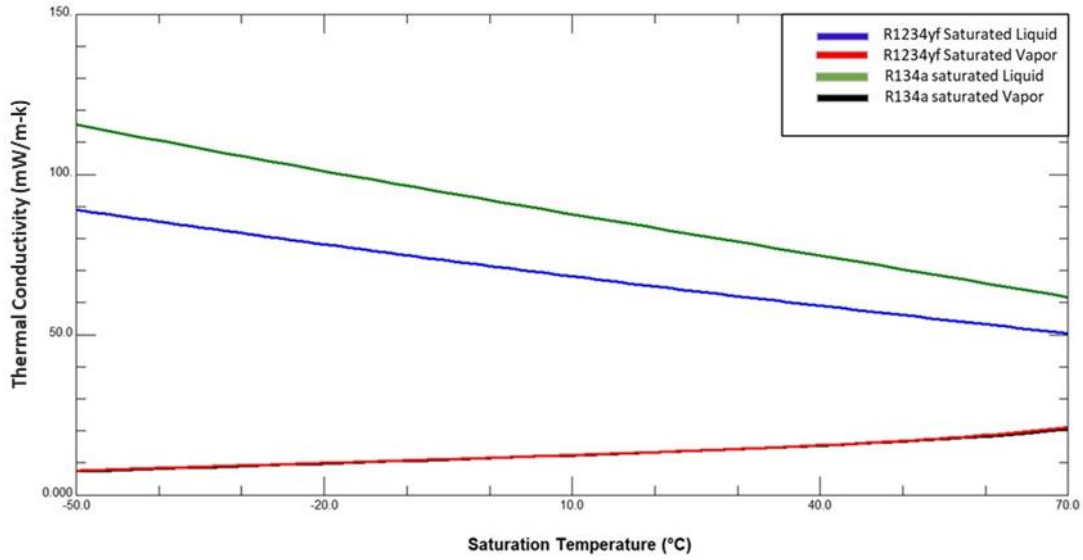

Figure 2.2: R1234yf and R134a thermal conductivity [17].

In addition to studying the chemical and physical properties of R1234yf against R134a, many researchers studied R1234yf from different aspects such as energetic performance, exergitic performance, and the overall contribution to global warming.

2.1. R1234yf Energetic Performance

The investigation of R1234yf energetic performance as an alternative for R134a in the literature can be categorized into a theoretical comparison of R1234yf's performance, experimental investigation of R1234yf, and both theoretical and experimental investigation. In the former category, Mole´s et al. [25] compared the basic cycle and other configurations of the R1234yf system to the basic cycle of R134a. On the other hand, Daviran et al. [20] studied R1234yf behavior in running a mobile air conditioning (MAC) system. Moreover, Zhaogang [26] modeled the effects of subcooling, superheating, compressor's volumetric efficiency, and compressor isentropic efficiency on R1234yf MAC system performance.

In the second category, Sánchez et al. [22] experimented R1234yf in a single-stage vapor-compression plant with the same charging amount of each refrigerant. On the other hand, Cho et al. [23] studied R1234yf in a variable speed MAC system. Aprea et al. [27] investigated R1234yf behavior in domestic refrigerators with an optimized charging amount for R1234yf. Mota-Babiloni et al. [10] examined R1234yf at various evaporation and condensation temperatures and with and without a liquid suction heat exchanger (LSHX).

In the latter category, Jarall [21] studied the feasibility of using R1234yf as a drop-in replacement for R134a working in a basic refrigeration cycle. Sethi et al. [13] tested R1234yf in a vending machine under different ambient and return air temperatures. Navarro-Esbrí et al. [1] examined R1234yf at various evaporation and condensation temperatures and with and without a liquid suction heat exchanger (LSHX). Details of the above references are discussed hereinafter.

2.1.1. Theoretical Investigation

Mole´s et al. [25] modeled R1234yf under several configurations for vapor-compression refrigeration systems besides the basic cycle with and without LSHX Mole´s et al. compared the COP and the cooling capacity of these configurations to their counterparts of the basic vapor compression cycle that works by R134a taking constant refrigerant volumetric flow rate. The proposed configurations are presented in figure 2.3 and include:

1- Ejector/Expansion cycle (EEC), Fig. 2.3-a
2- Ejector/expansion with LSHX cycle (EELSHXC), Fig. 2.3-b
3- Expansion work recovery cycle (WRC), Fig. 2.4-c
4- Expansion work recovery with LSHX cycle (WRLSHXC), Fig. 2.3-d

Mole´s et al. found that the basic cycle with R1234yf has 7% lower COP than that working with R134a. The introduction of LSHX to R1234yf's basic cycle led to higher compressor work and less COP. For WRC configuration, the expander was used to reduce the system's power consumption and elevate the refrigerating effect to increase the system's COP. In all the proposed configurations, introducing LSHX demonstrated a positive effect on the systems' COP. Finally, Mole´s et al. concluded that the optimum configuration was the EEC configuration which exhibited 15% higher COP than the basic cycle that works with R134a.

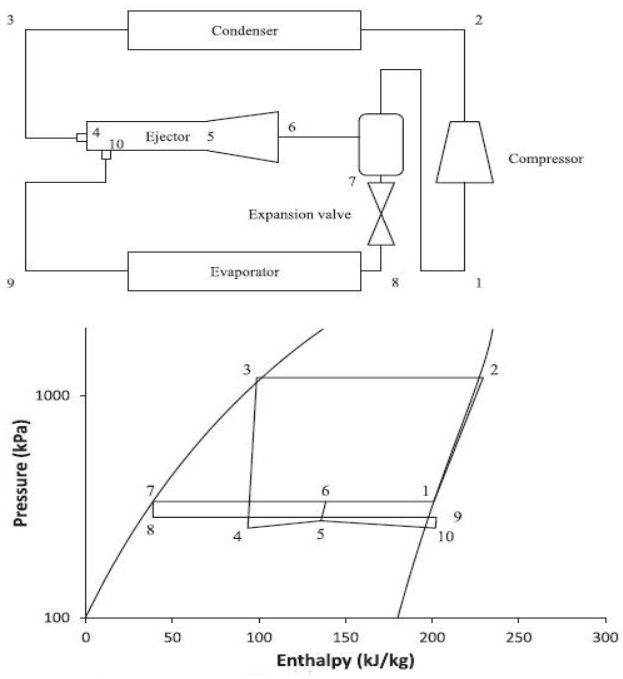

a) Ejector/Expansion cycle (EEC).

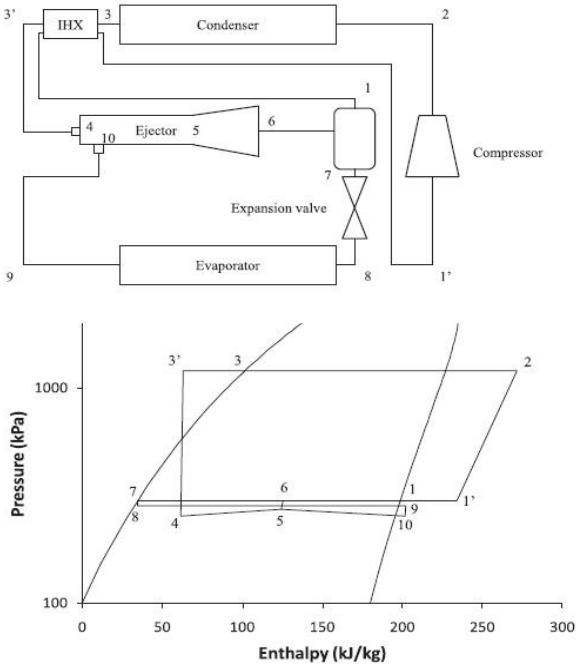

b) Ejector/expansion with LSHX cycle (EELSHXC).

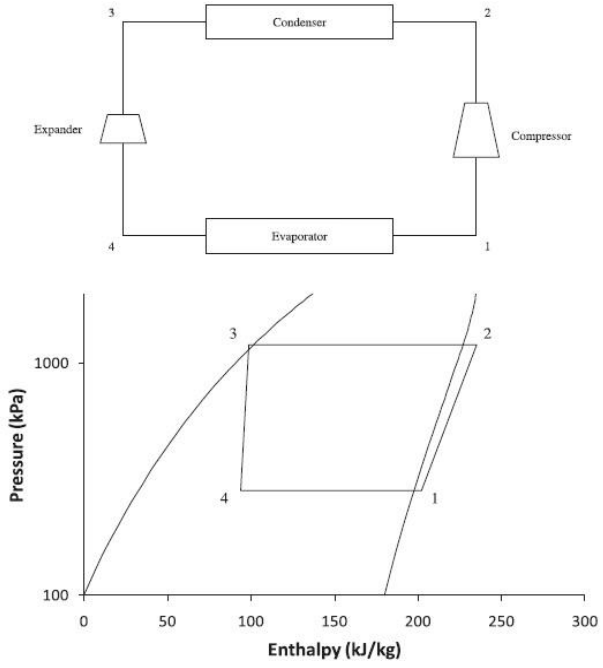

c) Expansion work recovery cycle (WRC).

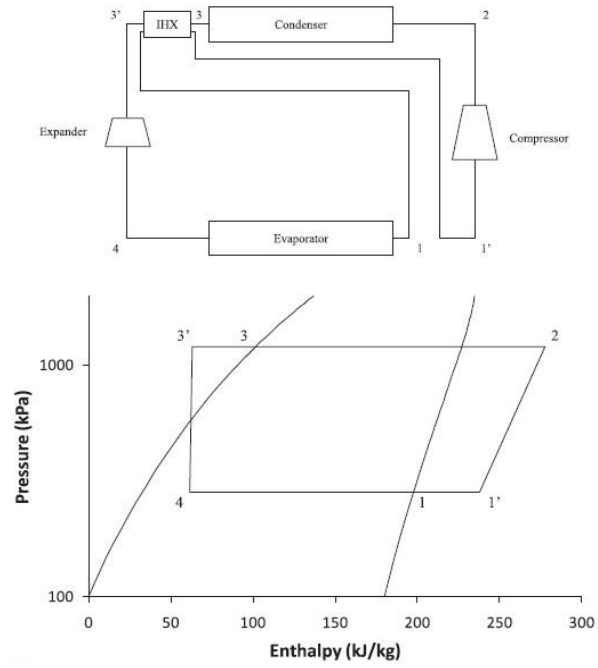

d) Expansion work recovery with LSHX cycle (WRLSHXC).

Figure 2.3: The proposed configurations by Mole´s et al. [25] to improve R1234yf cycle performance [25].

Daviran et al. [20] developed a simulation model to test R1234yf as a drop-in replacement for R134a in an automobile air conditioning system. R1234yf was evaluated against R134a in two states: in the first state, the cooling capacity was constant at 3.6 kW, while the second state was conducted based on a constant refrigerant mass flow rate at 113 kg/h. The constant cooling capacity state was achieved by increasing the R1234yf mass flow rate by 27% over R134a's mass flow rate. Therefore, the compressor work increased for R1234yf and affected its system COP by up to 5% less than R134a. On the other hand, R1234yf revealed 18% higher COP than R134a in the state of constant refrigerant mass flow rate.

Zhaogang [26] tested the effects of subcooling, superheating, compressor's volumetric efficiency, and compressor isentropic efficiency on an automobile air conditioning cycle working with R1234yf compared to that working with R134a. In the basic cycle, R1234yf revealed defect up to 7, 10.6, and 3.8% in terms of system COP, cooling capacity, and compressor energy consumption, respectively. During studying the influence of superheating on the cycle performance, the cooling capacity and COP only increased respectively by 3.7% and 2.6% when the superheat increased by 9°C, which implies that superheating had no significant effect on the system performance. On the other hand, increasing the subcooling by 9°C dramatically increased the cooling capacity and the system COP by 15% at fixed power consumption. This increase was in favor of the decreased refrigerant quality at the evaporator inlet, which was caused by the increased subcooling, causing a more considerable enthalpy difference between the evaporator outlet and inlet. More subcooling could have happened if a LSHX was used at the evaporator outlet. Concerning the impact of the compressor performance on the system performance, increasing the volumetric efficiency from 55% to 95% resulted in 72.8% increase in cooling capacity; however, no changes in COP have been revealed

because the power consumption proportionally increased with the volumetric efficiency. On the other hand, increasing the isentropic efficiency revealed no effect on the cooling capacity, yet the COP increased by 72.7% when the isentropic efficiency increased from 55% to 95% as the later increase reduced the power consumption. Therefore, it can be concluded that increasing subcooling degrees and compressor isentropic efficiency should be considered if an R1234yf system was targeted to be improved.

2.1.2. Experimental Investigation

Sánchez et al. [22] tested the performance of R1234yf and four other alternative refrigerants, representing three groups of refrigerants, to replace R134a as direct drop-ins in refrigeration facility with hermetic compressor. The tests conducted addressed different operating conditions: at two evaporating temperatures (0 and -10°C) and three condensation temperatures (25, 35, and 45°C). The same charging amount (900g) was applied for all refrigerants during the test. R1234yf had a 28.4% higher mass flow rate driven by the compressor due to its lower specific volume than R134a. However, no significant difference in terms of the volumetric efficiency of the compressor has been found between R1234yf and R134a. Even though R1234yf obtained 28.4% higher mass flow rate, it exhibited 4.5% - 8.6% less cooling capacity than R134a. Moreover, R1234yf exhibited 6.7% higher power consumption and 10% less compressor's global efficiency compared to R134a. Regarding the compressor's power consumption and the global efficiency, the R1234yf system showed 6.7% higher power consumption and 10% less compressor's global efficiency. As a result of the reduced cooling capacity and the increased power consumption R1234yf showed, R1234yf resulted in 10% COP defect. Figure 2.4 summarizes the Sánchez et al. [22] findings.

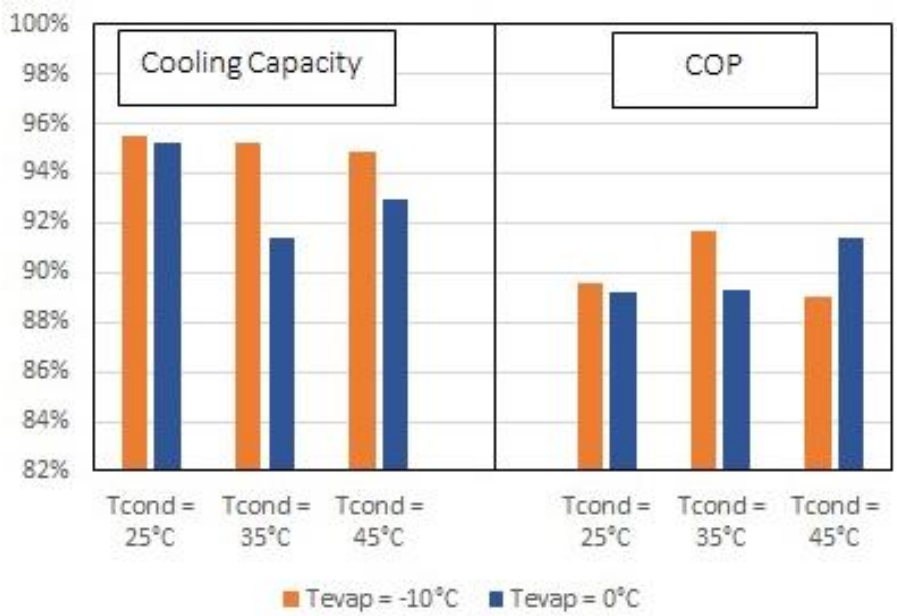

Figure 2.4: R1234yf cooling capacity and COP as a percentage of that of R134a according to Sánchez et al. [22].

Cho et al. [23] experimentally studied the cooling capacity, power consumption, and COP of an automotive air conditioning system working with R134a and R1234yf with and without LSHX. In the beginning, the optimum refrigerant charge for each system was determined based on the highest COP obtained in each system. R1234yf systems pronounced 10% less charging amount. In terms of the discharging pressure, the R1234yf system had 4.7% less discharge pressure than the R134a system; however, introducing the LSHX to the R1234yf system increased the discharge pressure in the R1234yf system by 1.4% due to the higher compressor inlet temperature. This increase in the compressor inlet temperature decreased the gap in mass flow rate between the R1234yf and R134a systems. R1234yf revealed up to 17% higher mass flow rate than that of the R134a system due to the lower specific volume of R1234yf, but the increase of the refrigerant temperature at the compressor inlet, which presented in favor of the LSHX, increased R1234yf's specific volume which let less refrigerant amount in compressor suction. With respect to power consumption, the R134a system consumed more power than both R1234yf systems at all compressor speed ranges. Due to the

higher compressor inlet temperature, the LSHX system of R1234yf consumed more power than that of the basic system of the same refrigerant. Despite the higher mass flow rate that the R1234yf system revealed, the R1234yf system had up to 7% less cooling capacity than the R134a system. Increasing the compressor speed negatively affected the basic R1234yf system's cooling capacity only; however, it expressed zero influence on the cooling capacity of the R1234yf system with the LSHX. For the system's COP, the R1234yf system expressed 4.5% less COP than that of the R134a system. Adding LSHX to the R1234yf system did not decrease the COP gap significantly; the R1234yf system with LSHX showed almost 3% less COP than the R134a system.

Aprea et al. [27] investigated the feasibility of replacing R134a with R1234yf as a working fluid in domestic refrigerators experimentally. In this experiment, two identical no-frost domestic refrigerators with a refrigerator cabinet and freezer were used. The freezer's and the refrigerator's set points during the experiment were -18°C and 5°C, respectively. The experiment was built up on two types of tests. The first test was a pull-down test to determine the suitable amount of R1234yf, and the second test was an energy consumption test. Most of the measurement instruments were inserted inside the refrigerant tubes except the thermo-resistances inserted outside the tubes with a layer of aluminum oxide plus silicon as a heat transfer compound to ensure appropriate thermal contact between the sensors and the tubes. A zero-pressure drop; also was assumed thought out the condenser and the evaporator. As a result, the measured condensation and evaporation pressures were recorded using piezoelectric sensors at the discharge and the charge lines of the compressor, respectively. The surrounding environment was taken into account during the experiment using a thermo-hygrometer to record the surrounding temperature and relative humidity. Concerning

the pull-down test, they measured how long a refrigerator takes to achieve the set point of the air inside the freezer (-18°C). The goal behind this test was to identify the equivalent charging amount of R1234yf to achieve a similar pull-down time similar to R134a. Firstly, the pull-down time was measured for the R1234yf refrigerator by charging the refrigerator with an amount of R1234yf equal to the manufacturer-assigned charging amount of R134a (85g). The pull-down times were recorded while the R1234yf charging amount was increased gradually by steps of 5 grams until 110g, which allowed a pull-down time less than the pull-down time recorded for R134a by almost 7.3%. Afterward, the energy consumption test was carried out throughout 24 hours using charging amounts 85g and 110g for R134a and R1234yf, respectively. R1234yf showed 3% energy saving compared to R134a in addition to a higher cooling capacity due to the higher charging amount of R1234yf, which led to a higher discharge temperature, but it still within the safe temperature range.

Mota-Babiloni et al. [10] examined R1234yf as an alternative for R134a at three evaporation temperatures, three condensation temperatures, and with and without LSHX. The plant consisted of a vapor-compression plant with a reciprocating compressor derived by variable speed 5-KW electric motor. The refrigeration load was simulated by a heated water/propylene glycol brine (65/35% by volume) using electrical resistances controlled by a PID controller. Both condenser and evaporator were shell and tube heat exchangers; in addition, the plant contained LSHX to do a heat exchange activity between the condenser and evaporator's outputs in half of the tests run during the experiment. R134a exhibited higher volumetric efficiency than R1234yf by 3% at a compression ratio 2.5. This percentage of the higher volumetric efficiency is subjected to an increase if the compression ratio increased. In terms of cooling capacity and COP, both of these energy performance indicators were tested under two

scenarios with many evaporation and condensation temperatures. In the first scenario (while the LSHX in turned off), R1234yf found to has 13.71% and 3.34% less cooling capacity at evaporation temperatures of -13°C and 7°C and condensation temperatures of 57°C and 37°C, respectively. At evaporation temperature of 7°C and condensation temperature of 47°C, the R1234yf system COP was less than that of R134a by 10.5%, and it was less by 4.96% at -13°C as evaporation temperature and 47°C as condensation temperature.

When the LSHX was turned on, R134a achieved higher cooling capacity and COP in this case also. The highest percentage gap in terms of cooling capacity was 10.46% at evaporation temperature of -13°C and condensation temperature of 57°C, while the lowest difference percentage was 1.83% at evaporation temperature of 7°C and condensation temperature of 47°C. The highest difference percentage in terms of COP was 8.36% at evaporation temperature of -3°C and condensation temperature of 37°C, while the lowest difference percentage was 2.98% at evaporation temperature of 7°C and condensation temperature of 37°C. Figure 2.5 summarizes the output of Mota-Babiloni et al. [10].

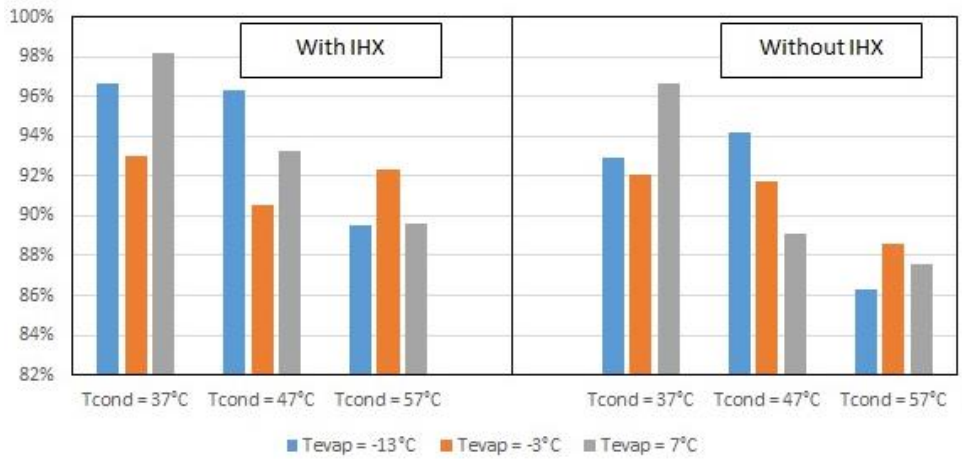

a) R1234yf cooling capacity with and without LSHX as a percentage of that of R134a.

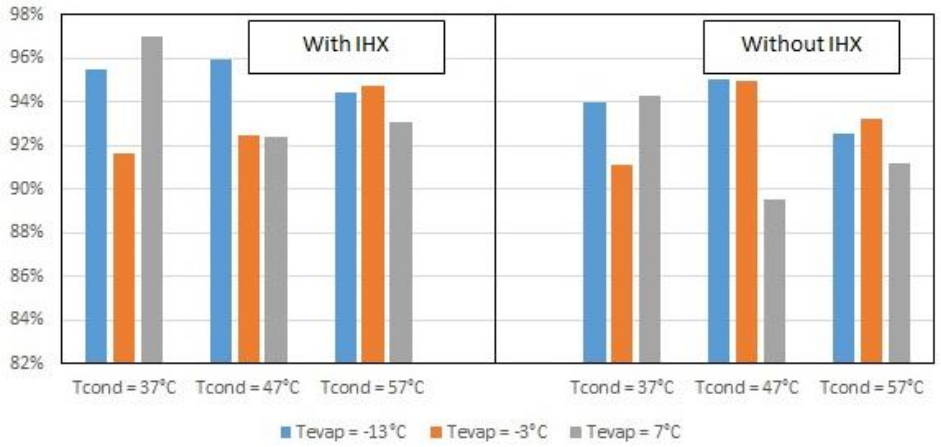

b) R1234yf COP with and without LSHX as a percentage of that of R134a.

Figure 2.5: R1234yf cooling capacity and COP as a percentage of that of R134a according to Mota-Babiloni et al. [10].

2.1.3. Theoretical and Experimental Investigation

Jarall [21] studied the feasibility of using R1234yf as a drop-in replacement for R134a theoretically and experimentally on a basic refrigeration cycle of a vending machine. Jarall theoretically concluded that R1234yf exhibited lower pressure ratio, discharge temperature, COP, and Carnot efficiency, and higher evaporation and convection heat transfer coefficients than R134a. Jarall [21] also concluded that R1234yf is more positively sensitive to sub-cooling and superheating as R1234yf is an isentropic refrigerant. The experimental tested cycle consisted of a condenser cooled by an open-loop of water from a water tap, a control valve to ensure constant condensation pressure, an evaporator with a hot brine to mock a refrigeration load, an expansion valve, and a hermetic compressor. The condensation temperature during the test was 40°C and 45°C while the evaporating temperature varied between -8°C and 15.5°C. At 40 °C condensation temperature, the R1234yf system's cooling capacity, COP, and Carnot efficiency were lower than those of R134a by 3.4-11.15%, 0.35-8.4%, and 0-4%, respectively. At 45°C condensation temperature, the values of cooling capacity, COP, and Carnot efficiency for R1234yf were lower than those of R134a by 7.6-13.7%, 3.7-

11.88%, and 0-6.3%, respectively. Regarding the system's COP, R1234yf consumed less power; however, its cooling capacity was lower than R134a. Thus, R1234yf had less COP than R134a. Figures 2.6-a and 2.6-b show the variation of cooling capacity and COP according to the variation of the evaporating and condensation temperatures in Jarall [21].

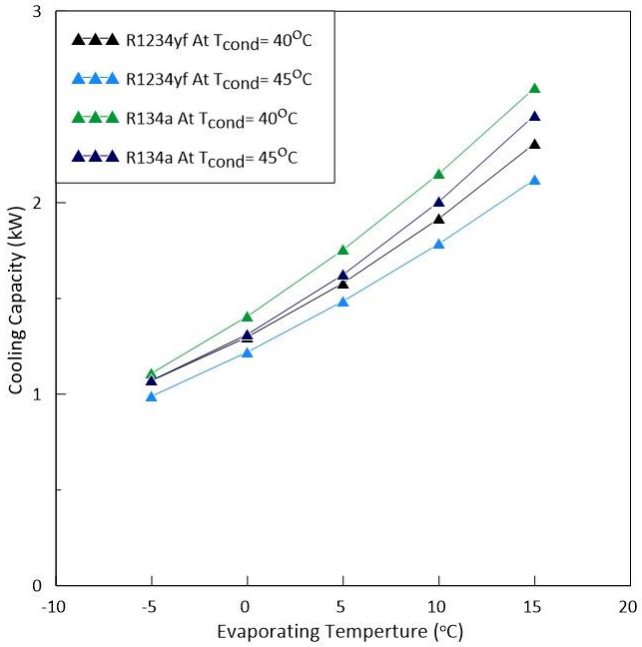

a) The effect of the condensing and evaporating temperatures on the cooling capacity

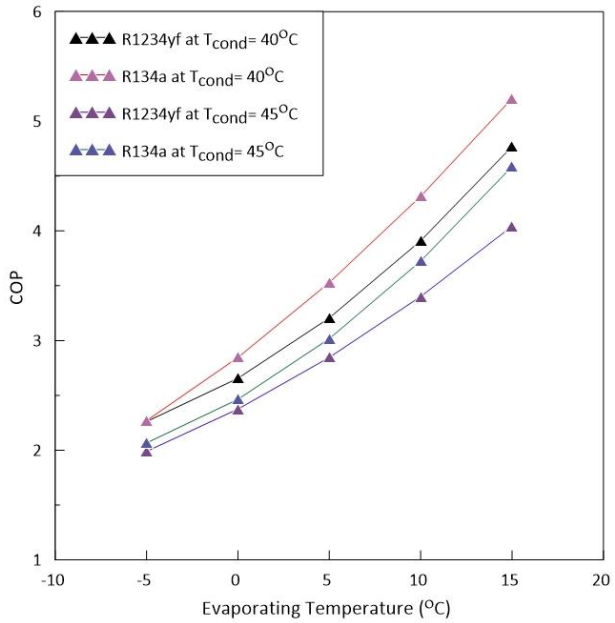

b) The effect of the condensing and evaporating temperatures on the COP

Figure 2.6: The effect of the variation of the condensing and evaporating temperatures on the cooling capacity and COP in Jarall [8].

Sethi et al. [13] examined R1234yf in a basic cycle of a vending machine. The theoretical study was performed under two different outdoor ambient temperatures, three different return air temperatures, and with and without LSHX with 40% effectiveness. R1234yf demonstrated 4% and 7% less volumetric cooling capacity and COP than R134a at 30°C and 40°C ambient temperature, respectively. After applying the LSHX to the refrigeration circuit, the volumetric cooling capacity and COP of R1234yf improved to show similar values to R134a at 30°C ambient temperature and about 4% lower at 40°C ambient temperature.

Experimentally, the experiments were performed under two different outdoor ambient temperatures, three different return air temperatures, and with and without LSHX with 40% effectiveness. The refrigeration circuit components were the same except for the expansion device; a needle valve was used in testing R1234yf, while a thermostatic expansion valve was used in the R134a system. Sethi et al. [13] optimized the charging

amount of each refrigerant to maximize the COP of each system. Surprisingly, this led to using the same charging amount (650g) for R1234yf and R134a. Experimental results showed that R1234yf had a slightly lower cooling capacity and COP than R134a despite having 19% more mass flow rate and higher compressor efficiency. Also, R1234yf had 20% higher pressure drop in the suction line than that of R134a. Also, Sethi et al. theoretically examined R1234yf performance if the suction line's outer diameter was increased by 0.125 inches to overcome a 20% pressure drop (compared to R134a) showed in the suction line during the experimental testing. In favor of this modification, the performance of the R1234yf refrigeration system improved by 1-2%.

Navarro-Esbrí et al. [1] tested R1234yf as a drop-in replacement for R134a, theoretically, at a wide range of evaporating and condensation temperatures. The cooling capacity of R1234yf was 8-11% and 3-6% lower cooling capacity with and without using an LSHX, respectively. R1234yf showed 5-10% less COP without LSHX and 2-4% less COP when applying the LSHX. Experimentally, plenty of tests were carried out at a wide range of evaporating and condensation temperatures. R1234yf showed 9% less cooling capacity regardless of the variation of the evaporating temperatures, condensing temperatures, and the super heating degrees. This difference in cooling capacity reduced to 7% when a LSHX was applied for both systems and 5% when the LSHX was applied for the R1234yf system only. The variation between R1234yf and R134a in COP was from 5 to 27%, proportionally with the condensing temperature during the experiment. The latter gap increased as the superheating degree increased and decreased to 6-17% when LSHX was used. In terms of power consumption, R1234yf consumed 2% more energy at the higher condensing temperature and 18-27% at the lowest condensing temperature during the experiment.

Additionally, the power consumption for R1234yf decreased when the superheating degree increased.

2.2. Exergy Performance Investigation

Exergy is defined as the amount of work that can be performed by a system when it is brought into thermodynamic equilibrium with the surroundings [28]. Therefore, the exergetic efficiency can be called second law efficiency and would be defined as the ratio between the minimum power required by a reversible system and the actual power supplied to the system [29]. Also, it would be calculated by dividing the actual COP of a cycle by the maximum COP of that cycle [30]. For a system with more than one component, the contribution of each component in the overall system exergy destruction is called efficiency defect [31].

In light of the precious definitions of exergy and exergetic efficiency, many researchers examined R1234yf exergy against R134a. All the reviewed articles revealed that the compressor is the most contributor to exergy destruction for all systems. Golzari et al. [32] conducted a theoretical exergy analysis for a MAC plant working with R1234yf and compared it to another plant working with R134a based on JIS D1618-1986 Standard [33]. Also, Yataganbaba et al. [30] developed a computer code to compare exergy efficiency and exergy destruction of R134a and 1234yf. Experimentally, Cho et al. [23] experimentally analyzed the exergy destruction in a MAC system, while Belman-Flores et al. [34] conducted an exergy analysis for R1234yf and R134a working in a domestic refrigerator with forced convection air distribution.

Golzari et al. [32] conducted an exergy analysis for an automotive refrigeration plant working with R1234yf and compared it to another plant working with R134a. The

performance of both cycles was calculated theoretically based on JIS D1618-1986 Standard [33]. This standard states that a refrigeration plant performance assessment should be conducted under the following conditions: Air temperature entering evaporator = 27°C, Air temperature entering condenser = 35°C, Volumetric flow rate of air streams in evaporator = 500m^3/hr., Degree of superheat = 5°C, Velocity of air streams in condenser = 4m/s, Compressor Volumetric Displacement =154.9cc/s, Rotational speed of compressor = 1800rpm, Air side heat transfer area = 4.2m^2, and Degree of superheat = 5°C. The compressor was the highest contributor to exergy destruction in both systems. It was found that the with about 53% followed by the condenser and the expansion valve with 21% and 15%, respectively.

In contrast, the evaporator was the lowest contributor with about 11%. For the condenser, the exergy destruction inversely proportional to the air's inlet temperature enters the condenser. On the other hand, it proportional directly to air inlet velocity. When comparing exergy destruction of the two systems, R1234yf exhibited 35% less exergy destruction than R134a. This less exergy destruction was revealed because R1234yf had higher exergy efficiency than R134a at low dead state temperatures and vice versa. Finally, R1234yf had a higher COP than R134a.

Yataganbaba et al. [30] developed a computer code to compare R134a and 1234yf in terms of exergy efficiency and exergy destruction. Yataganbaba et al. model was a vapor compression refrigeration system with one compressor, two evaporators to cover different cooling demands, and an evaporator pressure regulator to maintain the same pressure in the inlet of the mixing chamber for each evaporator. The function of the mixing chamber is to collect the refrigerant from each evaporator before entering the compressor. A set of equations was developed presenting the exergy efficiency and

exergy destruction for each component in the cycle (compressor, evaporator-1, evaporator-2, condenser, expansion valve-1, expansion valve-2, evaporator pressure regulator, and mixing chamber). After building these equations, EES (Engineering Equation Solver) software [35] was used to solve these equations considering 35 to 45°C as a condenser temperature range, evaporator-1 temperature varies between 0 and -5°C, and evaporator-2 temperature varies between -10 and -18°C. Some observations have been concluded after running the program, such as the highest exergy destruction occurs in the compressor while the lowest occurs in the mixing chamber. Besides, the temperatures of evaporator-2 and the condenser play the primary role in exergy efficiency; the exergy efficiency decreases when the condenser temperature increases while it increases by the increase of evaporator-2 temperature. However, exergy efficiency is not noticeably affected by evaporator -2 temperature; besides, as the sub-cooling temperature increases, the exergy efficiency increases by increasing the specific refrigerant effect, which leads to a reduction in the mass flow rate of the refrigerants for constant refrigeration capacity. Finally, R1234yf showed 2-3% less exergy efficiency than R134a.

Cho et al. [23] experimentally studied the exergy destruction in a variable speed MAC system working with R134a and R1234yf with and without LSHX. During the exergy destruction test, a significant portion of the exergy destruction took place in the evaporator and the compressor in all systems. However, introducing the LSHX to the R123yf system decreased the exergy destruction in the evaporator by 21.7%, but increased those of the compressor and the condenser almost by 8%. The second low efficiency was decreasing with increasing the compressor speed. R134a system achieved 7.76% second low efficiency at 800 rpm, while the R1234yf system and the R1234yf system with LSHX had 7.42% and 7.53% second low efficiency, respectively.

At 2500 rpm, the second low efficiency was 3.62% for the R134a system, 3.5% for the R1234yf system, and 3.66% for the R1234yf system with LSHX. A 4.6%-improvement took place in the R1234yf system by adding the LSHX. Concerning exergy destruction ratio (EDR), at compressor speeds range of 800 – 1800 rpm, the R1234yf system exhibited 3.6 – 5% higher EDR than the R134a system but introducing the LSHX decreased the EDR difference to 0.5 – 3.3%. However, at 2500 rpm, the R1234yf system with LSHX presented lower EDR than the R134a system by 1.2%.

Belman-Flores et al. [34] conducted an exergy analysis for R1234yf and R134a working in the same domestic refrigerator with forced convection air distribution. In the beginning, an exergy analysis was conducted for 100g charging mass of R134a while R1234yf charge was optimized to minimize the exergy destruction using different charges starting from 70g and increased in steps of 7g until reaching 119g. For the effect of cycle parameters on R1234yf cycle performance, the COP increased by 13% as the evaporator temperature increased from -25 to -10 °C. On the other hand, increasing the condensation temperature presented a negative influence on the system's COP. Increasing the condensation temperature led to a smaller value of cooling effect and higher energy consumption. However, the efficiency defect, which measures the influence of the exergy of each component on the overall efficiency of the system, in the compressor is not affected by this variation of the condensation temperature. In this experiment, the optimum charge of R1234yf was 92.2g (7.8% lower than R134a), leading to optimum exergy destruction. Also, for R1234yf, the condenser was the minor contributor to the exergy destruction, while the evaporator was the higher contributor. Concerning the energy consumption, the refrigerant with lower GWP consumed 1.03 kWh/d while the other refrigerant consumed 0.99 kWh/d, which means that 4% more energy was consumed by R1234yf. Regarding the exergy destruction, the ED of all

components, except the compressor, is almost the same for both refrigerants. For the compressor performance, the efficiency defect in the compressor in the R1234yf system was 50% higher than it in the R134a system.

2.3. R1234yf Environmental Impact Evaluation

GWP, TEWI, and LCCP are the most common and currently used matrices to compare refrigerants. GWP is used for evaluating refrigerants as a chemical composition leaked to the atmosphere; however, TEWI and LCCP are used for revaluating a whole refrigeration system, but LCCP is more holistic than TEWI.

2.3.1. Global Warming Potential (GWP)

GWP is the simplest and the quickest way to compare two refrigerants [36]. It was used in 1990 in the first scientific evaluation of the Intergovernmental Panel on Climate Change (IPCC) to estimate greenhouse gas emissions' potential effects on climate [37]. GWP measures the influence of a specific amount of greenhouse gas emissions (the radiative force of these gases) on global warming relative to the influence of the same amount of carbon dioxide emissions (the radiative force of carbon dioxide) during a time horizon, mostly 100 years [36-38]. GWP can be calculated by dividing the integration of the radiative force of an amount of traced greenhouse gas released in the air over a specific time on the integration of the radiative force of the same amount of carbon dioxide released in the air over the same period of time, and it can be calculated by equation (2.1) [39].

$$GWP = \frac{\int_0^n a_i * C_i \, dt}{\int_0^n a_{Co_2} * C_{CO_2} dt} \tag{2.1}$$

Where a_i is the radiative force of a greenhouse gas i. C_i is the concentration of the traced greenhouse gas i that last in the air at time t after the release of the traced greenhouse gas [39]. The dominator has the same variables corresponding to carbon dioxide.

Further, GWP was used as categorizing factor to determine which greenhouse gases should be phased out by the Kyoto protocol in 1997 [40]. Nevertheless, GWP is subjected to criticism due to its inability to include the harms and abatement costs [41]. Therefore, there is a need for comprehensive tools to evaluate refrigerants against each other and provide an in-depth assessment of the harm that might be caused by using these refrigerants. Such approaches are like TEWI and LCCP.

2.3.2. Total Equivalent Warming Impact (TEWI)

In light of the fact that the significant contribution of refrigeration practices in global warming comes from the electricity consumption in order to run these systems [42], TEWI was introduced by the Alternative Fluorocarbons Environmental Acceptability Study (AFEAS) and the U.S. Department Of Energy in the early 90s of the 20th century [43]. TEWI approach takes into account the indirect CO_2 emissions related to the refrigeration system. Therefore, TEWI equals the sum of the indirect emissions related to running refrigeration equipment and the direct emissions resulting from the refrigerant leakage throughout the system lifetime, and it can be calculated by equation (2.2-2.3) [44].

$$\text{TEWI} = \text{direct emissions} + \text{Indirect emmisions} \tag{2.2}$$

$$\text{TEWI} = \text{GWP} * \text{ALR} * \text{L} + \text{AEC} * \text{EEG} * \text{L} \tag{2.3}$$

Even though the TEWI approach gives a more comprehensive evaluation for a refrigerant's impact on global warming and accounts for direct and indirect emissions,

TEWI does not consider the embodied energy and greenhouse gases emission in system materials manufacturing, manufacturing of the refrigerant, and end of life disposal of the system components [16].

2.3.3. Life Cycle Climate Performance (LCCP)

The term LCCP was introduced by Montreal Protocol Technology and Economic Assessment Panel in 1999 [45]. LCCP is a cradle-to-grave approach that monitors the impact of using a refrigerant on the environment [46]. LCCP take into account many sorts of CO_2 emissions that TEWI does not consider, such as the following CO_2 emissions:

1- CO_2 emissions during refrigerant manufacturing.
2- CO_2 emissions during the system manufacturing.
3- CO_2 emissions during transporting the refrigerant.
4- CO_2 emissions during recycling the refrigerant and the system.

Therefore, LCCP is the most comprehensive matrix to evaluate the embodied emissions of using a refrigerant and a refrigeration or an air conditioning system. LCCP can be calculated by equation (2.4) [47]

$$\text{LCCP} = \text{Direct Emissions} + \text{Indirect Emissions} \tag{2.4}$$

$$\text{Direct Emissions} = \text{C}[(\text{N} * \text{ALR} + \text{ELL}) + (\text{GWP} + \text{Adp. GWP})] \tag{2.5}$$

Where, *C* is the refrigerant charge, Kg; *N* is system life, years; *ALR* is Annual Leakage Rate, % of refrigerant charge; ELL is End of life Leakage Percentage, % of refrigerant charge.

$$\text{Indirect Emissions} = \text{RMDE} + \text{ECM} + \text{SME} \tag{2.6}$$

Where, RMDE is Refrigerant Manufacturing and disposal Emissions $KgCO_2/Kg$ of refrigerant; ECM is Energy Consumption Emissions, $KgCO_2/kWh$; SME is System material Emissions, $KgCO_2/Kg$ of material.

$$\text{RMDE} = \text{C} * (\text{ERM} + \text{N} * \text{ALR} * \text{ERM} * +(1 - \text{ELL}) * \text{ERD}) \tag{2.7}$$

Where, ERM is Emissions of Refrigerant Manufacturing, $KgCO_2/Kg$ of refrigerant.; ERD is Emissions of refrigerant Disposal, $KgCO_2/Kg$ of refrigerant.

$$\text{ECE} = \text{N} * \text{AEC} * \text{EEG} \tag{2.8}$$

Where, AEC is Annual Electricity Consumption, kWh/year; EEG is Emissions of Electricity Generation $kgCO_2/kWh$

$$\text{SME} = \sum \text{ESMM} * \text{SM} + \sum \text{MRE} * \text{MRM} \tag{2.9}$$

Where, ESMM is Emissions of Systems Materials Manufacturing, $KgCO_2/Kg$ of material; SM is Systems materials Mass, Kg; MRE is Material Recycling Emissions, $KgCO_2/Kg$ of recycled material; MRM is Mass of Recycled Material, Kg.

2.3.4. Environmental Impact Investigation Literature

Belman-Flores et al. [31] established a comparison between R1234yf and R134a in terms of the power consumption and the total equivalent warming impact (TEWI). Three domestic refrigerators with a freezer compartment and fresh food compartment were used in this experiment inside a climate chamber with a temperature of 32.2°C ±0.6 and 56% relative humidity. For data collection, data regarding refrigerants'

behavior and refrigerators' performance were collected by measuring temperatures in various places inside each compartment in addition to the evaporator, condenser, and compressor inlet and outlet. The charging mass for R134a was fixed at 100g as mentioned by the refrigerator manufacture; on the other hand, the charging mass for R1234yf was optimized. Eight different charges, starting from 70g and adding 7g until reaching 119g, were tested to reach the optimum charge, which provides the lowest power consumption in a day. The absolute majority of R1234yf charges have been tested at a single point on the thermostat, which set 1.6°C as fresh food compartment temperature and -21.1°C as freezer compartment temperature. The results were extracted based on the three successive cycles of the compressor right before a defrost cycle to ensure high stability in readings. Although the three refrigerators were identical and from the same manufacturer; yet, the optimum R1234yf charge was not the same for the three refrigerators. Thus, they end up with 92.2g as the optimum R1234yf charge based on the average optimum charge of each of the three refrigerators. In terms of the power consumption, this optimal charge of R1234yf led to yearly energy consumption evaluated by 375.95 kWh while R134a led to 361.35 kWh, 4% less than R1234yf. Finally, the TEWI test was conducted to evaluate the effect of using these refrigerants on global warming. Based on this test, they found that, even though the GWP of the direct emissions of R1234yf is negligible compared to the GWP of R134a emissions, the result of the TEWI test showed that R1234yf has 1.07% higher warming impact than R134a. Therefore, the power consumption due to using R1234yf must be reduced by utilizing the R1234yf refrigeration circuit.

Aprea et al. [24] studied the energetic performance and LCCP of R1234yf based on UNI-ISO15502 standard [48] in which the steady-state tests must last for 24-h under a surrounding temperature of 25°C and 45% - 75% relative humidity. The optimum

charging amount of each refrigerant and mixture was assigned based on a pull-down time test, the charge that gives the shortest 1st pull-down time, while the R134a charge was 100g as designed by its manufacture. The used refrigerator has two compartments; a freezer was set at -18°C and a cold cell was set at 5°C. R1234yf showed higher compressor outlet pressure than that of R134a. This higher compressor outlet pressure made the R1234yf circuit subjected to higher mechanical losses. The mass flow rate of R1234yf was higher than that of R134a in favor of their lower compression ratio and higher density at the compressor's inlet. The power consumption when the compressor was running of R1234yf was higher than that of R134a.

On the other hand, the duty time, the cumulative time in which the compressor is working, of R1234yf was noticeably lower than R134a. Consequently, the daily energy consumption of R1234yf was significantly lower than that of R134a. Concerning LCCP, R1234yf presented lower CO_2 emissions than R134a. R1234yf showed around 6% emissions reduction. The reason behind this reduction of LCCP is the noticeably lower direct emission; R1234yf showed 99.4% lower direct emission than R134a.

2.4. Literature Summary

Table 2.2: Summary for the reviewed studies.

Reference	Study Type	R1234yf outcomes relative to that of R134a
[20]	Theoretical on MAC	• 5% less COP at constant cooling capacity (3.6 kW) • 15% higher COP at a constant mass flow rate (113 kg/hr)
[32]	Theoretical on MAC	At 27 and 35°C air temperature entering the evaporator and condenser respectively, and 5°C superheat degrees: • 35% less exergy destruction • Higher COP

Table 2.2: Summary for the reviewed studies.

Reference	Study Type	R1234yf outcomes relative to that of R134a
[26]	Theoretical on MAC	At Basic cycle W/O LSHX: • 7% less COP • 10.6% less cooling capacity • 3.8% less power consumption
[30]	Theoretical on vapor compression refrigeration system with two evaporators	At 35 to 45°C condenser temperature, 0 to -5°C evaporator-1 temperature, and -10 to -18°C evaporator-2 temperature: • 2-3% less exergy efficiency
[21]	Theoretical & Experimental on the basic cycle	At 40°C and 45°C condensation temperature and -8°C to 15.5°C evaporation temperature: • 3.4-11.15% and 7.6-13.7% less cooling capacity at T_{cond} = 40 and 45°C, respectively. • 0.35-8.4% and 3.7-11.88% less COP at T_{cond} = 40 and 45°C, respectively.
[1]	Theoretical & Experimental on a basic cycle of a vapor compression system	At 40°C, 50°C, and 60°C condensation temperature and -7.5°C, 0°C, and 7.5°C evaporation temperature: ◊ Theoretically • 8-11% and 3-6% less cooling capacity W/O and with LSHX, respectively. • 5-10% and 2-4% less COP W/O and with LSHX, respectively. ◊ Experimentally • 9% and 7% less cooling capacity W/O and with LSHX, respectively. • 5-27% and 6-17% less COP W/O and with LSHX, respectively. • 2% and 18-27% less energy consumption W/O and with LSHX, respectively.

Table 2.2: Summary for the reviewed studies.

Reference	Study Type	R1234yf outcomes relative to that of R134a
[13]	Theoretical & Experimental on a vending machine	At the same charging amount, 2°C, 20°C, and 38°C return air temperatures, and 30°C, 35°C, and 40°C ambient temperature: ◊ Theoretically • 4% less VCC and COP at T_{cond} = 30°C W/O LSHX • 7% and 4% less VCC and COP at T_{cond} = 40°C W/O and with LSHX, respectively. ◊ Experimentally • 2% and 2.75% less cooling capacity and COP, respectively. • 19% higher more mass flow rate
[22]	Experimental on a refrigeration facility with a hermetic compressor	At 25°C, 35°C, and 45°C condensation temperature and 0°C and -10°C evaporation temperature: • 4.5% - 8.6% less cooling capacity • 10% COP defect • 6.7% higher power consumption
[23]	Experimental on MAC	At optimized charging amount to maximize COP and a variable speed compressor: • 17% higher mass flow rate W/O LSHX • less energy consumption with and W/O LSHX • 7% less cooling capacity W/O LSHX • 4.5% and 3% less COP W/O and with LSHX, respectively • 3.6 – 5% and 0.5 – 3.3% higher EDR at low and medium speeds W/O and with LSHX, respectively • 1.2% lower EDR at high speed with LSHX

Table 2.2: Summary for the reviewed studies.

Reference	Study Type	R1234yf outcomes relative to that of R134a
[24]	Experimental on a domestic Refrigerator	At Optimized charging amount for Min. 1st pull-down, 25°C and 45%-75% surrounding temperature and RH, 5°C fresh food compartment temperature, and -18°C freezer compartment temperature: • 4% less CO2 emissions in LCCP • shorter duty time • less power consumption
[27]	Experimental on a domestic Refrigerator	At Optimized charging amount for similar 1st pull-down, 5°C fresh food compartment temperature, and -18°C freezer compartment temperature: • 7.3% less pull-down time • 3% energy saving • Higher cooling capacity • higher discharge temperature
[34]	Experimental on a domestic Refrigerator	At optimized charging amount for R1234yf for Min. exergy destruction and forced convection air distribution: • 4% more energy consumption • 50% higher exergy efficiency defect in compressor
[31]	Experimental on a domestic Refrigerator	At Optimized charging amount for Min. energy consumption, 32.2°C and 56% surrounding temperature and RH, 1.6°C fresh food compartment temperature, and -21.1°C freezer compartment temperature: • 4% higher power consumption • 1.07% higher TEWI

2.5. Research Objectives

In an effort to complete and extend some of the previously reported results in the literature, an experimental investigation of R1234yf performance as a drop-in replacement for R134a is conducted and followed by an LCCP analysis for both

R1234yf and R134a. The current research aims to help find a suitable alternative to replace R134a by holistic evaluation of R1234yf compared with R134a.

The specific goals of the research are:

1. Verify the ability of R1234yf to carry the same refrigeration load as R134a.
2. Study the energy performance of R1234yf while satisfying a refrigeration load at different thermostat settings.
3. Quantifying all possible saved/extra CO_2 emissions resulted from changing from R134a to R1234yf

Chapter 3 Experimental Setup

3.1. Introduction

HFOs are generally known for their low GWP and zero ODP. R1234yf is now replacing R134a in automotive air conditioning systems; however, there is no clear decision regarding R1234yf to replace R134a in domestic refrigerators due to many aspects like its lower refrigeration effect and significantly higher price compared to R134a. In this study, the energetic performance of R1234yf is tested experimentally as a drop-in replacement for R134a. Also, this study is meant to study the life cycle climate performance to define precisely the total CO_2 emissions saving in case of replacing R134a with R1234yf as the direct and indirect effects of both refrigerants are investigated over the course of refrigerants' life from the primary production steps until the end of life disposal or recycling.

3.2. Experimental Setup

An experimental setup is constructed to evaluate the performance of R1234yf in a domestic refrigerator compared to that of R134a. The experimental setup consists of a refrigerator, refrigerant tanks (R1234yf and R134a), sight glasses, compression fitting connectors, and a measuring system to measure performance parameters. Both refrigerants were tested using the same refrigerator. R134a performance was tested at 185g (170g) recommended by the manufacturer plus 15g to account for the increased system volume due to the sight glasses, connections, and measuring devices. On the other hand, R1234yf was tested at different charges.

3.2.1. The Refrigerator

Both refrigerants were tested using the same defrost refrigerator with a total gross volume of 0.32 m^3 and a freezing capacity of 4 kg/24hr originally designed and produced to work with R134a as a refrigeration medium. Each refrigerator has a separate freezer compartment with 0.065 m^3 capacity and a refrigerator compartment with a capacity of 0.215 m^3. Figure 3.1 depicts the used refrigerator.

The refrigeration cycle of the refrigerator used in the experiment consists of:

1- Compressor
2- Wire-on-tube condenser
3- Capillary tube
4- Liquid-suction heat exchanger
5- Flat plate evaporator
6- Anti-sweat tube
7- Filter drier

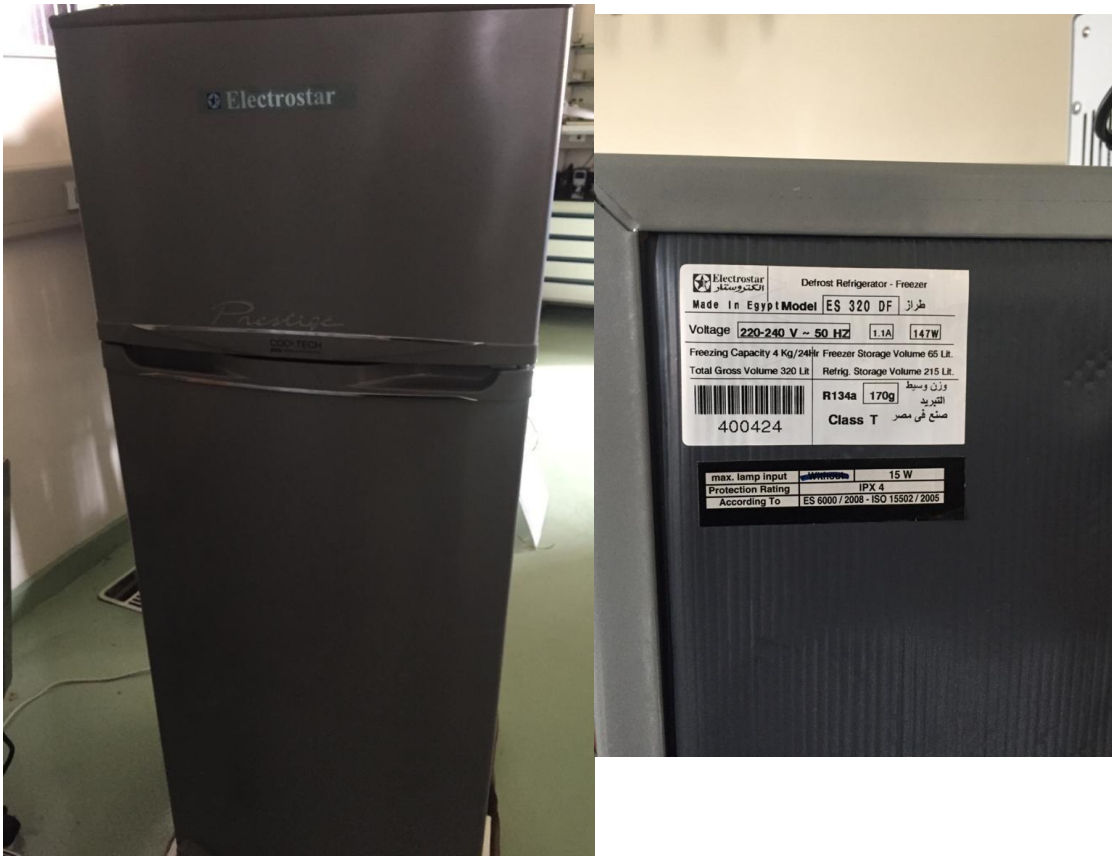

Figure 3.1: The used refrigerator.

3.2.1.1. Compressor

The used compressor is Cubigel GL90AA with 9.09 cm^3 stroke volume and operating evaporating range -35 to -10 °C. The compressor runs by a 0.25 hp RSIR motor supplied by 220-240V 50Hz single-phase power supply.

3.2.1.2. Condenser

The condenser carries out the process of transforming the refrigerant from the superheated gas state, at the compressor exit, to subcooled liquid at the condenser exit. The condenser used in this experiment is a wire-tube condenser with an outer tube diameter of 4.76mm (3/16inch), an inner diameter of 3.36mm, and 10.4m in length. Seventy-one wires have been welded on each side of the condenser tubes. Each wire has 1.4mm diameter and 822mm length. The heat rejection process in the condenser

was done through free convection with the help of the 142 wires (extended surface) to allow for a higher heat rejection rate and amount. The condenser used for the experiment is presented in figure 3.2.

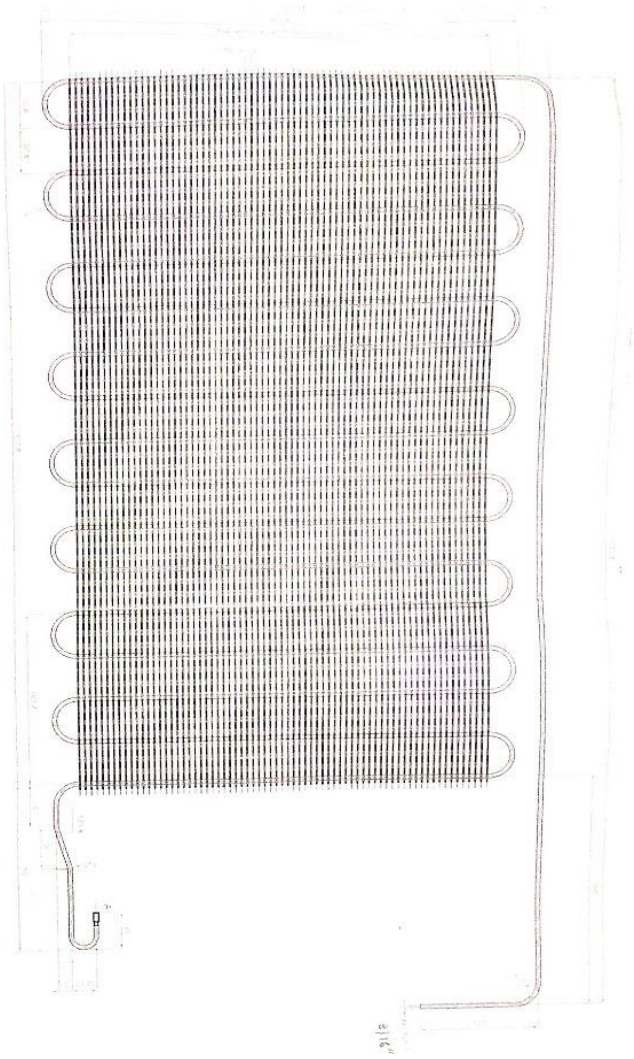

Figure 3.2: CAD drawing for the used condenser.

3.2.1.3. Capillary tube

The capillary tube carries out the refrigerant expansion process. The capillary tube in the experiment is 3m long, 0.66 mm inner diameter, and 1.6 mm (1/16 inches) outer diameter. The capillary receives the subcooled liquid refrigerant from the filter drier and delivers it to the evaporator as a 2-phase mixture. A portion of the capillary tube,

1.5175m, passes through the liquid-suction heat exchanger to transfer heat with the refrigerant exit from the evaporator. The part that exits from the liquid-suction heat exchanger has wounded 11 turns around the liquid-suction heat exchanger tube. The assembly of the capillary tube and the liquid-suction heat exchanger is presented in figure 3.3.

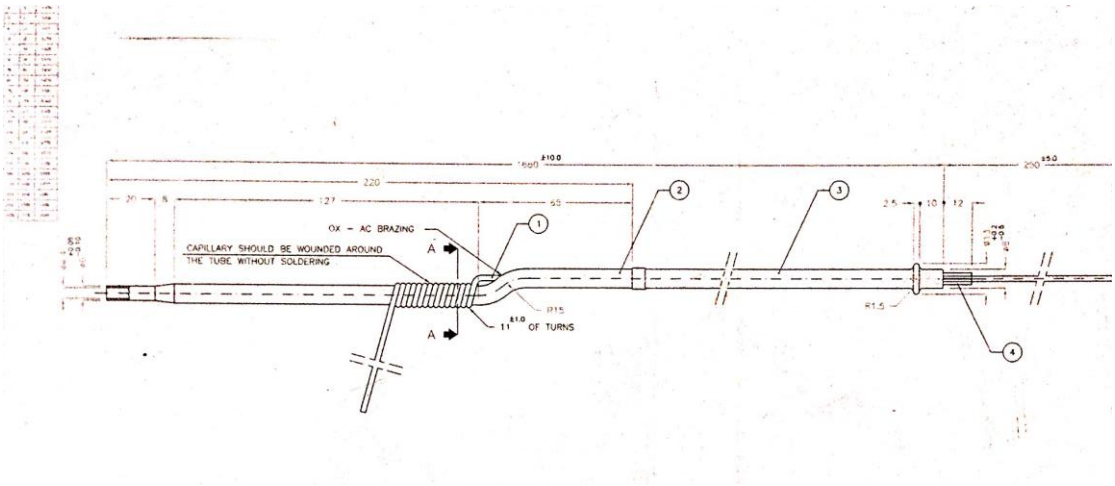

Figure 3.3: The liquid-suction heat exchanger assembly with the capillary tube.

3.2.1.4. Liquid-Suction Heat Exchanger (LSHX)

The function of the liquid-suction heat exchanger is to transfer heat from the first part of the capillary tube (starting from length 0.25 m to capillary exit from liquid-suction heat exchanger at length 1.5175 m) to the vapor exit from the condenser. By this process, the refrigeration effect of the refrigerant increase, and the compressor receives superheated vapor. The total length of the liquid-suction heat exchanger is 1.680 m with an 8 mm outer diameter (5/16 inches). The capillary paths through 1.5175m and wounded in 11 turns around liquid-suction heat exchanger in a distance equals 17.6mm, approximately as shown in Figure 3.3.

3.2.1.5. Evaporator

The evaporator in this study is a flat plate type with theoretical channels cross-section 0.172 – 0.275 cm^2 and theoretical channels development of 16.09 m^2. The evaporator carries out the process, which the whole refrigeration system is built to achieve, of cooling the freezer and refrigerator compartments. The heat transfer in the freezer compartment is done through conduction as cooling loads touch the freezer compartment's walls. Also, free convection is the other way of heat transfer in the freezer compartment. Regarding the refrigerator compartment, free convection is the only mode of heat transfer. The design of the used evaporator is presented in figure 3.4.

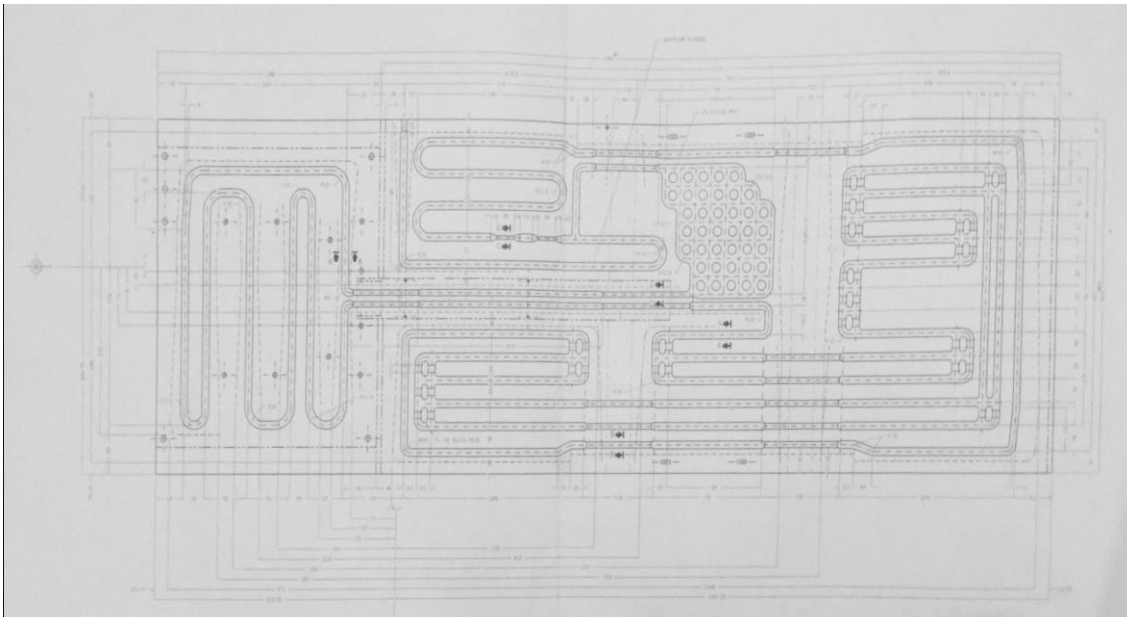

Figure 3.4: Drawing for the used flat plate evaporator.

3.2.1.6. Anti-Sweat heater

The Anti-Sweat heater is a 4.8 mm (3/16 inches) diameter stainless-steel tube that receives the refrigerant exit from the condenser and passes under the area at which the doors close to prevent moister condensation at the refrigerator frame and to keep the gasket, which is made from rubber, in a good and functional condition. The area that

the anti-sweat heater passes under it is presented in figure 3.5, with green arrows refers to it. After that, Anti-Sweat heater delivers the refrigerant to the filter drier.

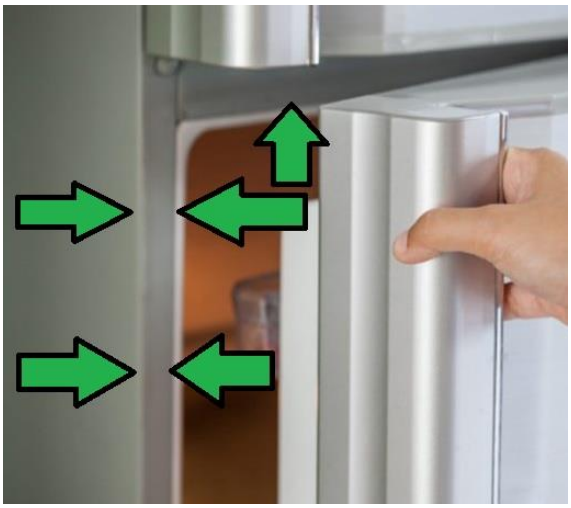

Figure 3.5: The area under which the anti-sweat heater tube paths.

3.2.1.7. Filter Drier

A copper filter drier is used in the experiment to ensure no moisture in the refrigeration cycle and prevent any tiny particle of dirt or copper chips from entering the capillary tube as it may block the tube and result in a non-functional refrigeration cycle. Therefore, the filter drier is locater right before the capillary tube. Figure 3.6 presents a copper filter drier similar to the one used in the experiment.

Figure 3.6: Copper filter drier

3.2.2. Measuring System

The measuring system in the experiment was used to quantify the outputs of the experiment and save them to a data acquisition system. The outputs of this experiment are temperature, pressure measurements, current, voltage, and energy measurements. Thermocouples were used to measure the refrigerant temperatures at five critical points in the cycle and to measure the surrounding environment temperature and the temperature inside the two compartments of the refrigerator. The current measurement was done using a current transducer. It was also used to determine the ON/OFF states of the refrigerators. The voltage was measured using a voltmeter. The Three pressure transducers were used to measure the pressure at 3 points in the cycle. All the measurements were recorded and saved every 4 seconds using a data acquisition system.

3.2.2.1. Thermocouples

the thermocouples used in the experiment are Omega J-type (iron-constantan) thermocouples. These thermocouples have almost 52μV/°C Seebeck coefficient, temperature range from 0 to ±750°C with ±2.2°C tolerance. These thermocouples are located at the compressor inlet, compressor outlet (condenser inlet), anti-sweat tube outlet (filter drier inlet/ capillary tube inlet), evaporator inlet, evaporator outlet, the refrigerator cabinet, and the freezer cabinet (to measure the air temperature in the air temperature in the two cabinets), and at five points around the refrigerator to measure the surrounding temperature. The list of the used thermocouples and their locations are presented in table 3.1 and figure 3.7.

Table 3.1: Thermocouples Locations.

Thermocouple No.	Measurement Point	Attachment Method
C1	Compressor inlet	Instream
C2	Compressor outlet	Instream
C3	Anti-Sweat tube exit	Instream
C4	Refrigerator left ambient temperature	hanging
C5	Evaporator inlet	Surface-mount
B3	Freezer cabinet temperature	Surface-mount
B5	Refrigerator cabinet temperature	Surface-mount
A1	Refrigerator front ambient temperature	hanging
A2	Refrigerator back ambient temperature	hanging
A3	Refrigerator top ambient temperature	hanging
A4	Refrigerator right ambient temperature	hanging
A5	Evaporator outlet	Surface-mount

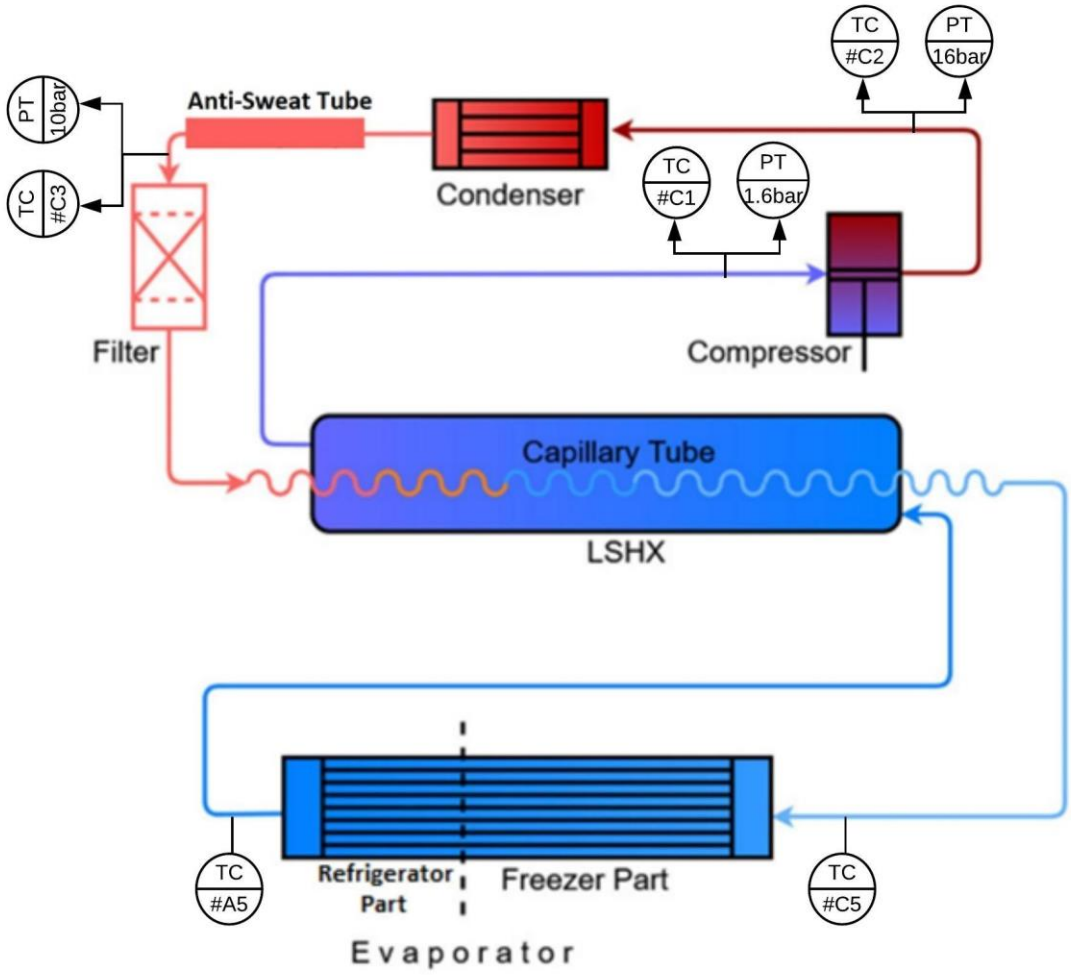

Figure 3.7: Thermocouples and pressure transducers distribution on the refrigeration cycle.

The thermocouples that measure refrigerant temperatures at the compressor inlet, compressor outlet, and capillary tube inlet were located inside sight glasses to measure the stream temperature as the compressor outlet thermocouple presented in figure 3.8.

Figure 3.8: Compressor outlet thermocouple inside a sight glass.

On the other hand, the thermocouples that measure refrigerant temperatures at the evaporator inlet and outlet are attached to the outer surface of the evaporator and covered by two layers of insulation tape. Each thermocouple is forced upward using a wood cube to ensure perfect contact between the thermocouple and the evaporator surface, as shown in figure 3.9.

Figure 3.9: Evaporator inlet and outlet thermocouples attachment.

Regarding the surrounding temperature, four thermocouples are distributed on the front, back, right, top of the refrigerator with a distance of more than 20cm between the thermocouple and the refrigerator body. Concerning the cabinets' temperatures, these temperatures are measured by a thermocouple in each cabinet attached to 500g of Propylene Glycol (Presented in figure 3.11) /water mixture (M- package) [49] with a ratio of 35% Propylene Glycol to 65% water as presented in figures 3.11 and 3.12 for the freezer cabinet and the refrigerator cabinet. Also, these thermocouples are covered by two layers of insulation tape. The water/ Propylene Glycol mixture is located at more than 5cm apart from the cabinet walls, as mentioned in IEC 62552 standard [49]. The Calibration data and curve of the thermocouples are presented in the appendix.

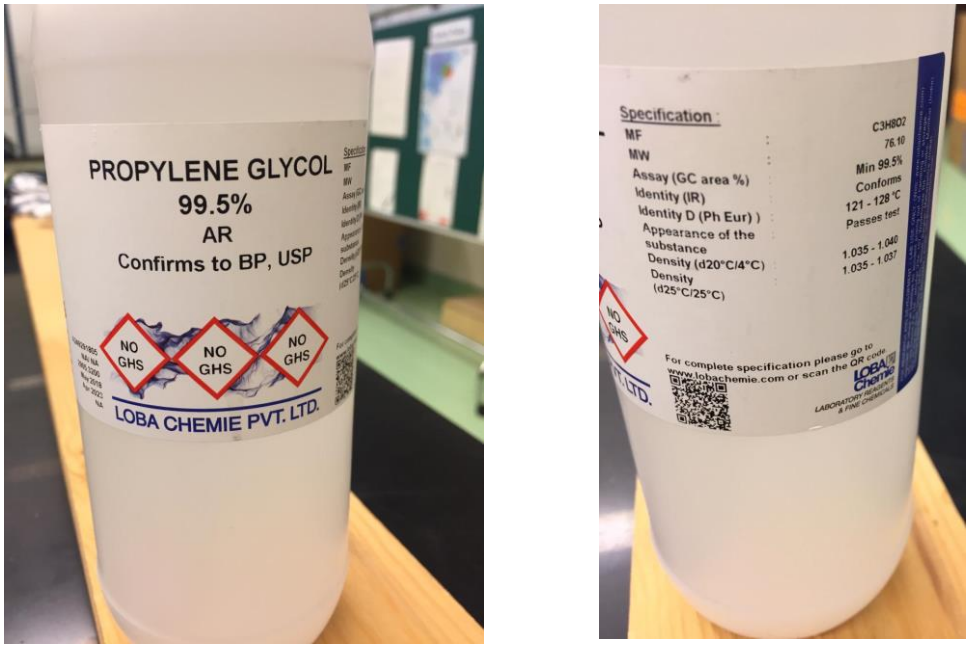

Figure 3.10: Propylene glycol

Figure 3.11: Freezer cabinet M-package.

Figure 3.12: Refrigerator cabinet M-package.

3.2.2.2. Current Transducer

SENSITEC CMS3005ABA current transducer [50] mounted on CMK3005ABA demoboard [51] for easy output reading has been used for this experiment. The current transducer has an operating range from 0 to 5 A, and it is working based on Anisotropic Magneto Resistive (AMR) effect with ±30 mA typical accuracy. Figures (3.13-3.16) show the current transducer output voltage with different power supply given that our range is 1 I_{PN}, the used current transducer and the demoboard, the current transducers mounted on the power measurement box, and the circuit diagram of the current transducer and the demoboard [51], respectively. The Calibration data and curve of the current transducer are presented in the appendix.

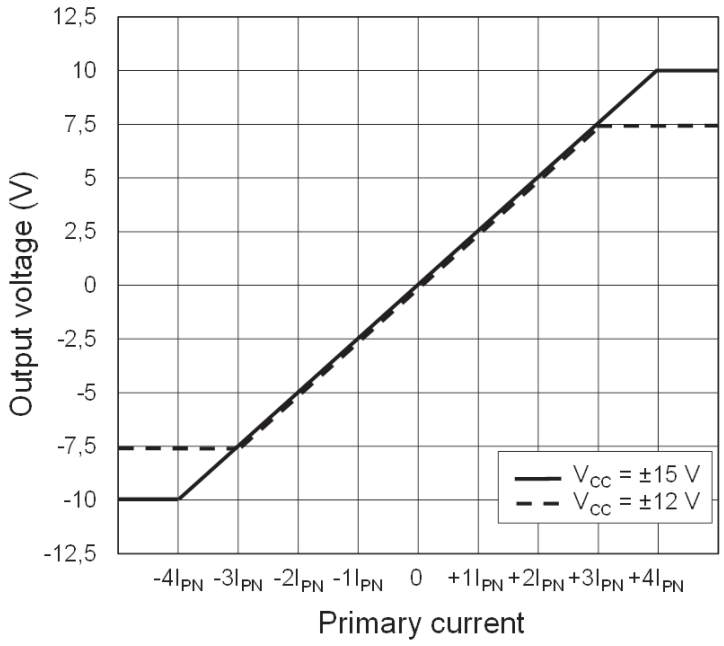

Figure 3.13: Output AC voltage range for different supply voltages for the used current transducer.

(a) (b)

Figure 3.14: (a) the used current transducer. (b) The current transducer mounted on the demoboard

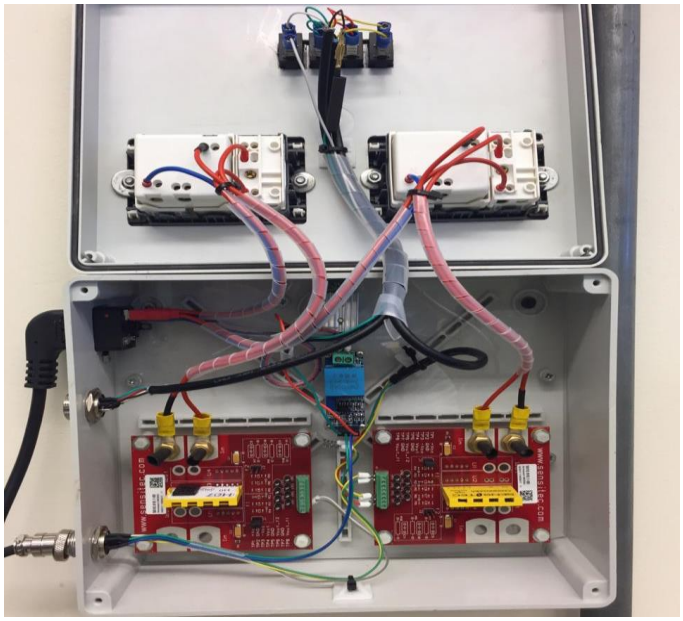

Figure 3.15: The power measurements box containing the current transducer and a voltage sensor.

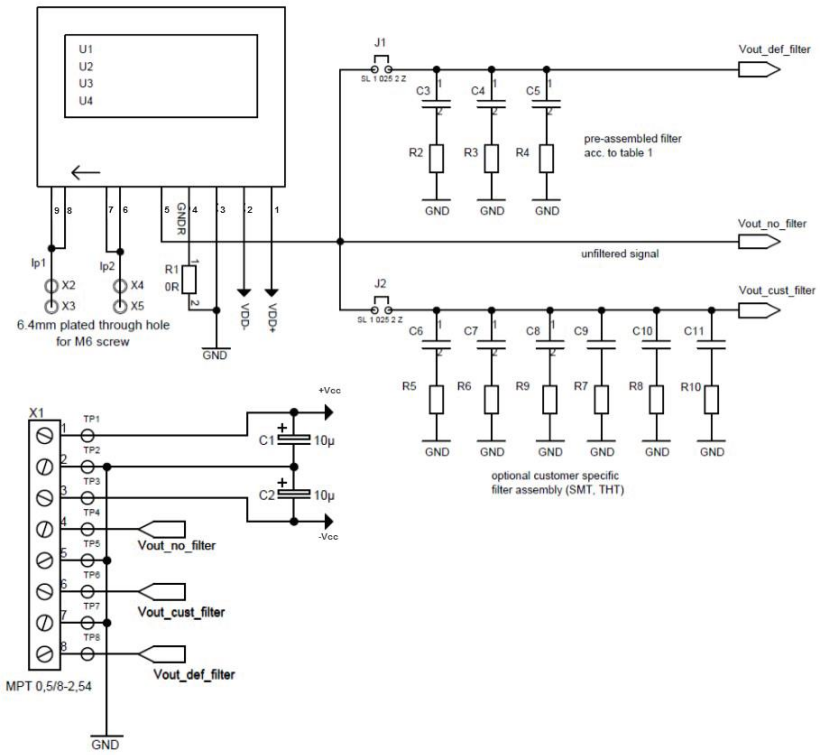

Figure 3.16: Circuit diagram of the current transducer and the demoboard

3.2.2.3. Voltage Transformer

ZMPT101B voltage transformer module presented in figure 3.17 was used to measure the voltage during the experiment. The module has a potentiometer mounted to its board to control the corresponding AC output voltage to the measured AC voltage. The Calibration data and curve of the ZMPT101B voltage transformer are presented in the appendix.

Figure 3.17: ZMPT101B voltage transformer module.

3.2.2.4. Batteries

Four 6V-lithium batteries connected in series as presented in figure 3.18 were used to supply the instruments used during the experiment with the needed power.

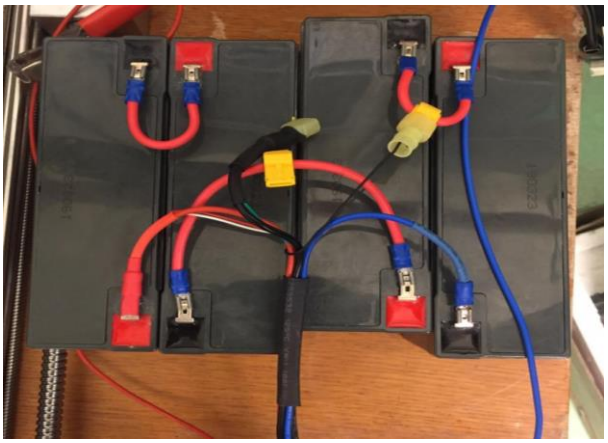

Figure 3.18: The used lithium batteries.

3.2.2.5. Pressure Transducers

Three Druck Pressure Sensors, as presented in figure 3.19, with 4 – 20mA analog output, 20mS response time, and ±0.2% accuracy were used to measure the pressure at three points of the cycle as presented in Figure 3.7 above. These pressure sensors are connected to the cycle via an on/off valve widely used for refrigeration applications and sight glass to act as a cross-connection and monitor the refrigerant state. Figure 3.19 presents the compressor's outlet pressure transducer attachment connection to the refrigeration cycle. The datalogger in volts read the output of every transducer, so a 100Ω resistance was connected to every transducer output wire to allow the datalogger to read the output volt instead of the output current. The ranges of the pressure transducers and their locations are mentioned in table 3.2.

Table 3.2: Pressure transducers ranges and locations.

Transducer range (bar gauge)	Location
-1 – 1.6	Compressor Inlet
0 – 10	Anti-Sweat Tube Outlet
0 – 16	Compressor Outlet

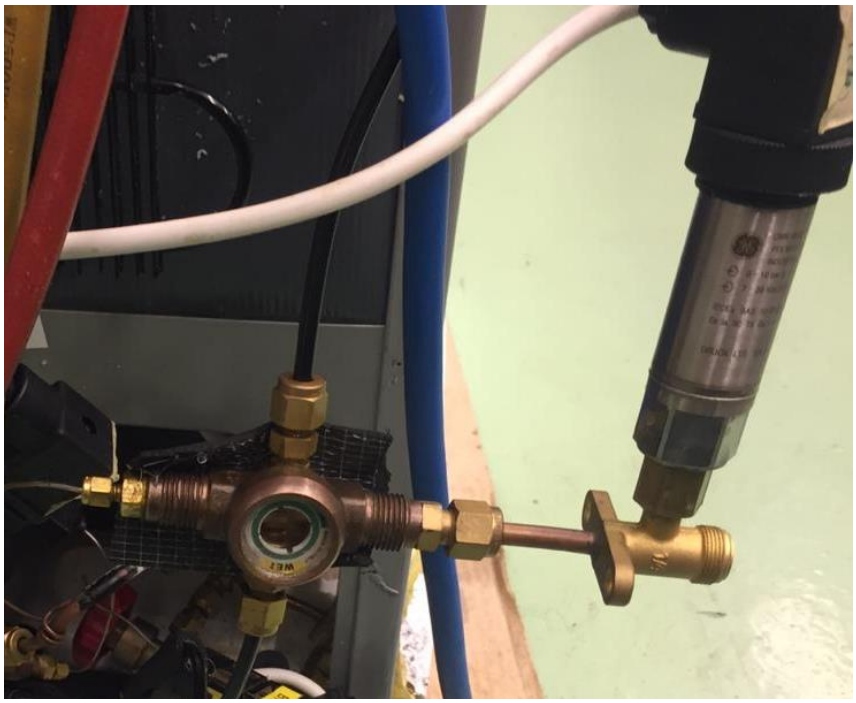

Figure 3.19: Pressure transducer attachment to the cycle.

3.2.2.6. Data Acquisition System

A Campbell Scientific CR3000 datalogger [52] was used to collect, restore, and monitor temperatures, pressure, voltage, and current readings. Campbell Scientific CR3000 has 14 differential configured input channels. One of these channels is connected to a Campbell Scientific AM25T multiplexer [53] to increase the number of channels by 24 more channels. The used Campbell Scientific CR3000 data logger has a 3ms measurement speed, an operating range of ±5Vdc, and analog voltage accuracy of

±0.09% of reading+0.5mV. Figure 3.20 shows the used Campbell Scientific CR3000 data logger.

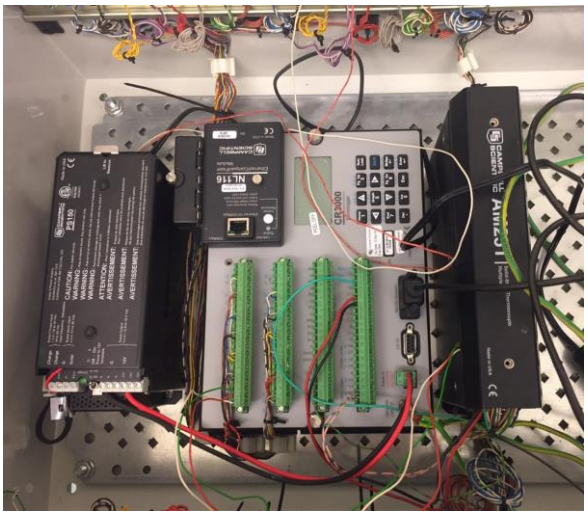

Figure 3.20: The used Campbell Scientific CR3000 datalogger and MA25T multiplexer.

3.2.2.7. Voltage modification Circuit

As the current transducer output is in AC voltage, which the data logger cannot read, the voltage modification circuit presented in figure 3.25 is built to allow the current transducer output voltage to be read by the data logger. The circuit consists of an OPAMP741, bridge rectifier, two 1KΩ resistances, a ten µF capacitor, and a zener diode. These components are mounted on a printed circuit board (PCB), as presented in Figure 3.21.

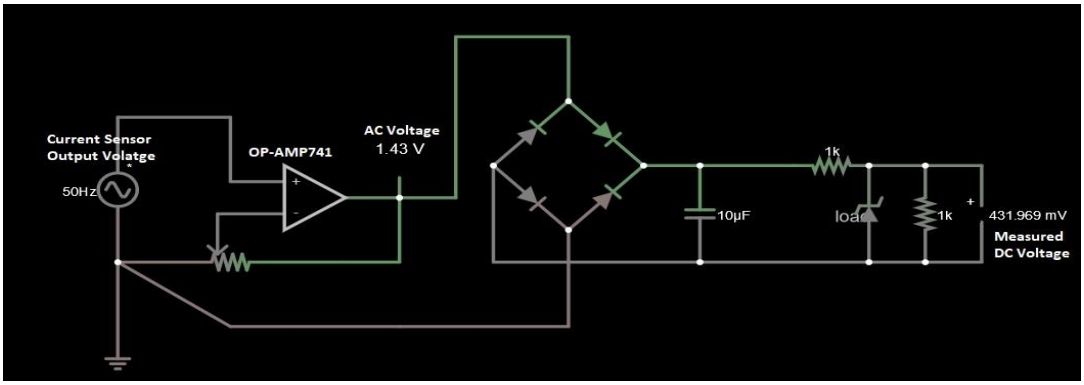

Figure 3.21: The voltage modification circuit.

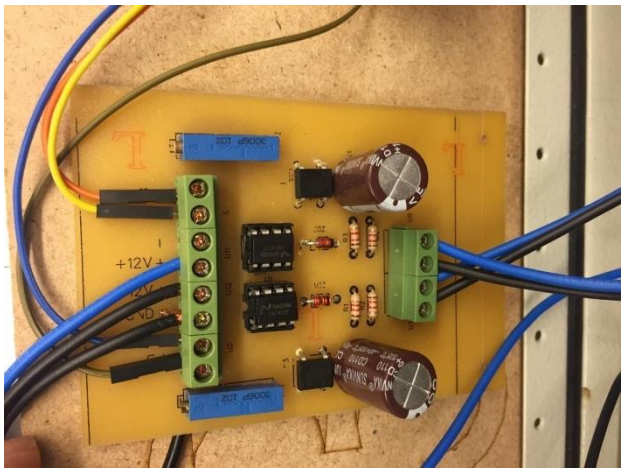

Figure 3.22: The components of the voltage modification circuit mounted on a PCB.

3.2.3. Sight Glass compression fitting connections

Sight glasses are used to form the cross-connection as presented in figure 3.19 and to indicate the refrigerant state. The sight glassed were drilled, and four NPT ¼" threads were made in the four directions of each sight glass, as presented in figure 3.23, to allow the tightening of the compression fitting connections to avoid soldering while connecting the cycle tubes.

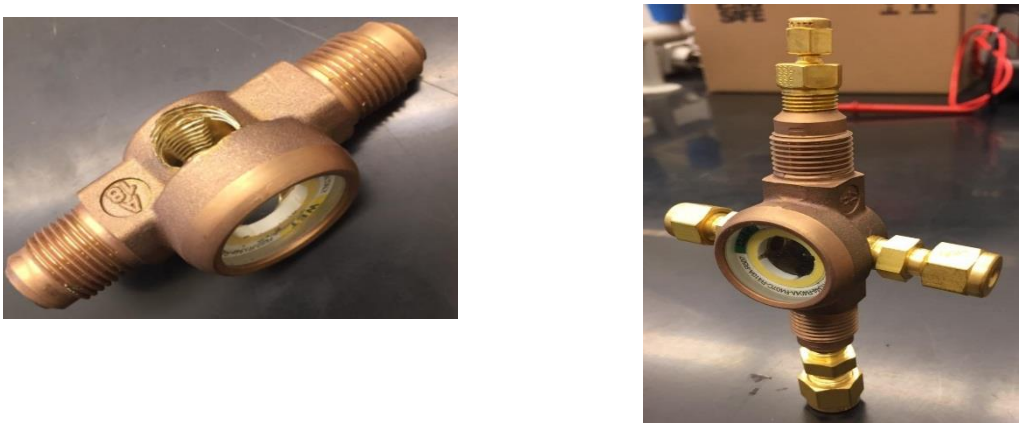

Figure 3.23: Sight glass with thread drills and with the connections tightened in it.

Table 3.3: Measuring devices summary.

device	Location	Range	Accuracy
Current Transducer		0-5A	±30 mA
Voltage Transducer		0-250VAC	±0.2%
High-pressure transducer	Compressor outlet	0-16bar	±0.2%
Medium pressure transducer	Anti-sweat tube outlet	0-10bar	±0.2%
Low pressure Transducer	Compressor suction	-1-1.6bar	±0.2%
Thermocouple C1	Compressor inlet	0-±750°C	±2.2°C
Thermocouple C2	Compressor outlet	0-±750°C	±2.2°C
Thermocouple C3	Anti-Sweat tube exit	0-±750°C	±2.2°C
Thermocouple C4	Refrigerator left ambient temperature	0-±750°C	±2.2°C
Thermocouple C5	Evaporator inlet	0-±750°C	±2.2°C
Thermocouple B3	Freezer cabinet temperature	0-±750°C	±2.2°C
Thermocouple B5	Refrigerator cabinet temperature	0-±750°C	±2.2°C

Table 3.3: Measuring devices summary.

device	Location	Range	Accuracy
Thermocouple A1	Refrigerator front ambient temperature	0-±750°C	±2.2°C
Thermocouple A2	Refrigerator back ambient temperature	0-±750°C	±2.2°C
Thermocouple A3	Refrigerator top ambient temperature	0-±750°C	±2.2°C
Thermocouple A4	Refrigerator right ambient temperature	0-±750°C	±2.2°C
Thermocouple A5	Evaporator outlet	0-±750°C	±2.2°C

3.3. Experimental Procedure

The performance of R1234yf is studied as a drop-in alternative for R134a in a defrost domestic refrigerator. The test is conducted with different charges of R1234yf at three thermostat points and compared against the manufacturer's recommended charge of R134a. This performance study includes studying the daily energy consumption and LCCP. Figures 3.24 – 3.26 shows the refrigerator with all the measuring system mounted on it.

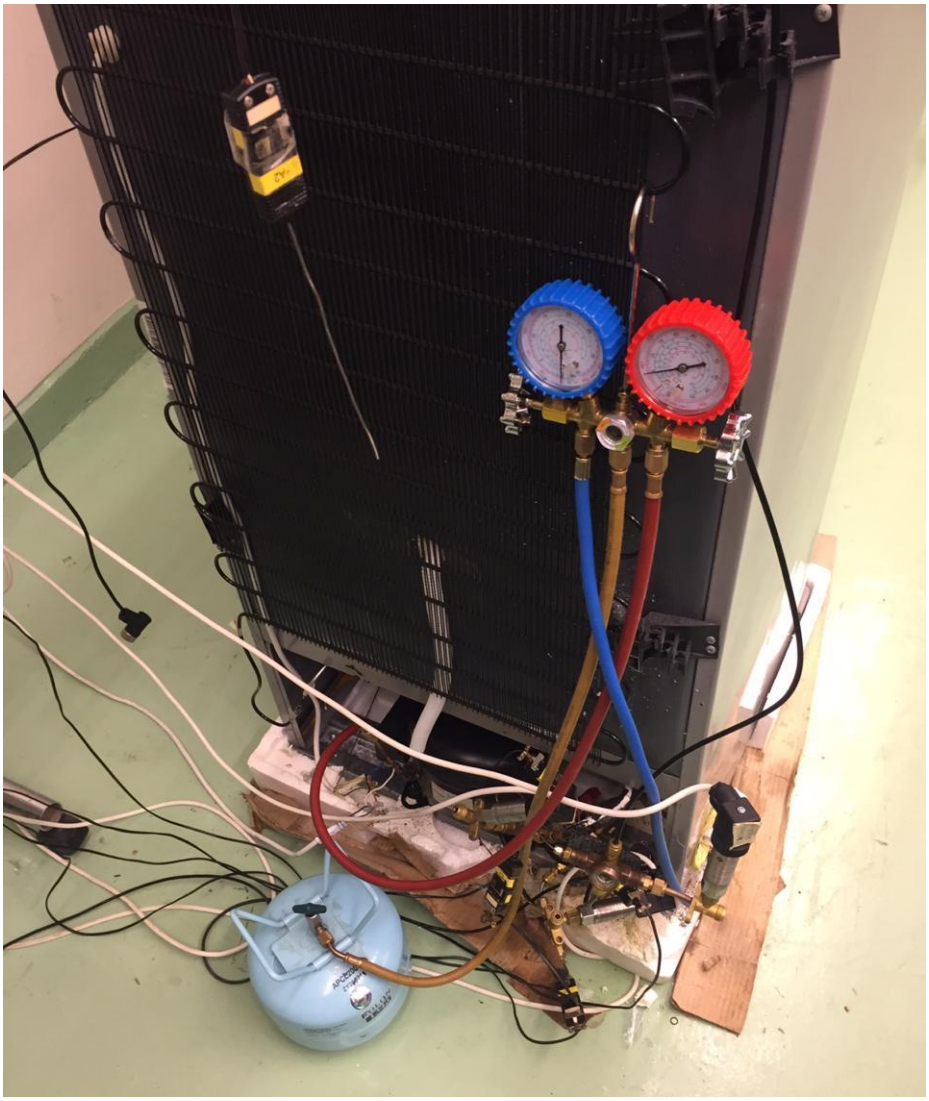

Figure 3.24: The back of the refrigerator with all the setup instruments.

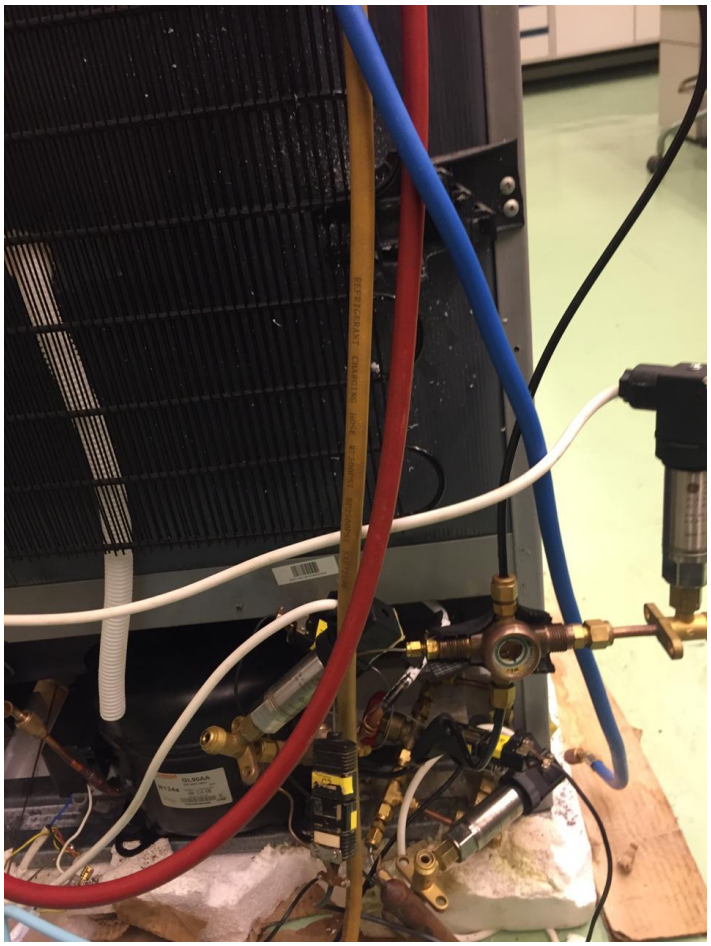

Figure 3.25: The pressure transducers, thermocouples, and sight glasses fixtures to the cycle.

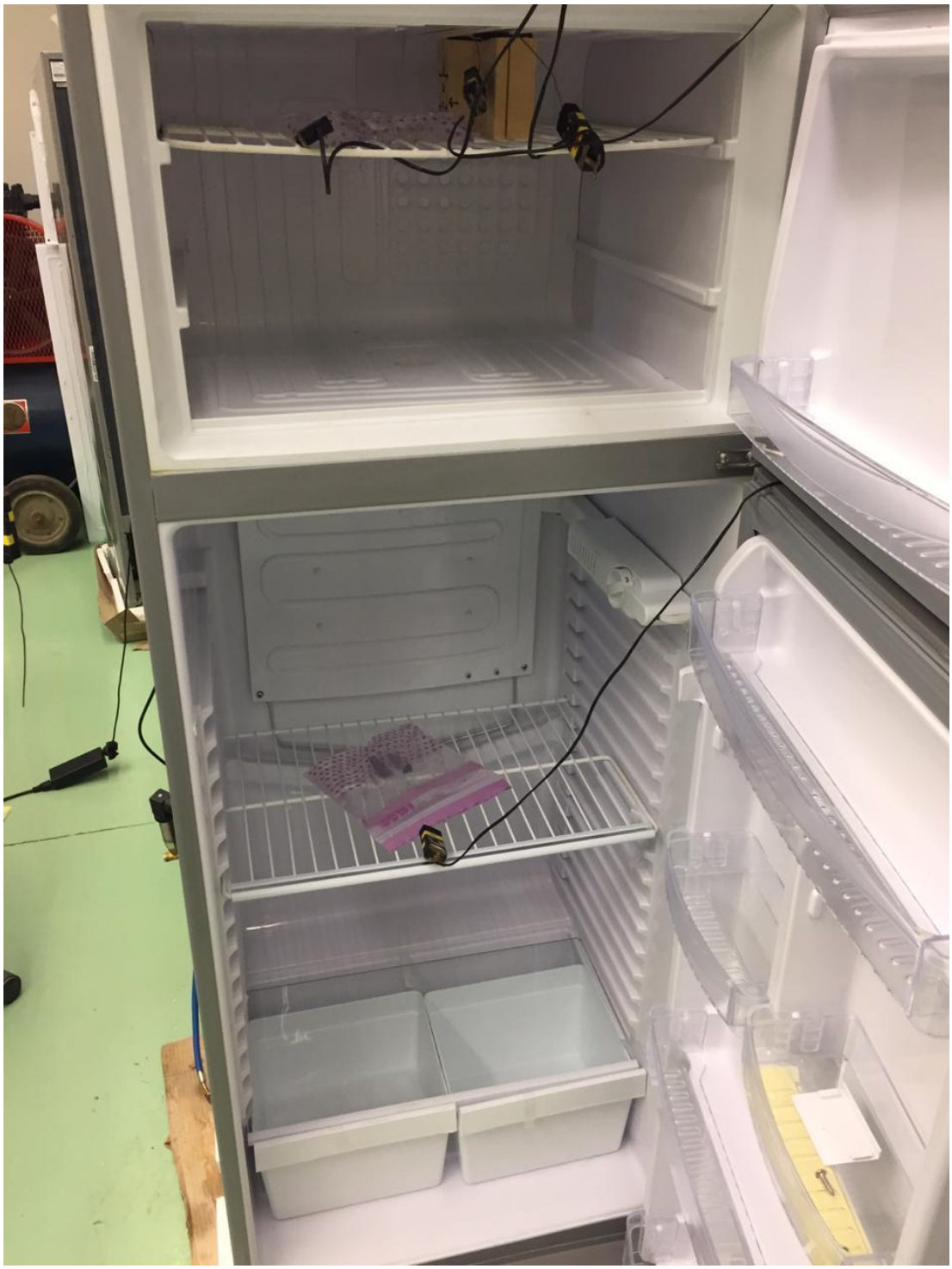

Figure 3.26: The setup of the thermocouples and the M-packages in the freezer and refrigerator cabinets.

After making sure that the experimental setup is ready, the following procedures were followed:

1- Calibrate the measuring equipment. (calibration charts are presented in the appendix)
2- Conduct a leakage test using Nitrogen and tracking potential leakage. If system pressure is reduced – sign for leakage – use foam to spot the leakage and fix it. If no leakage is detected, move to step No. 4.
3- Pull vacuum for 30 minutes.
4- Charge the refrigerator with the manufacturer recommended charge of R134a (170g) and add 15g to make up the increase in the liquid line's volume due to measurement instruments.
5- Run the test at three thermostat setpoints (low, medium, and high) for 24 hours at every thermostat setpoint.
6- Open the refrigerator doors for a day before running the experiment with the next thermostat setpoint to allow the evaporator surface and cabinet air temperature to reach the ambient temperature.
7- Repeat the test for the other two thermostat setpoints.
8- Pull vacuum.
9- Recharge the cycle with R1234yf at a charge equal 90% of the R134a charge.
10- Repeat steps 6 to 9.
11- Increase R1234yf charge by 10%
12- Repeat steps 10 and 11.
13- Repeat steps 12 and 13 until completing the four charges of R1234yf.
14- Analyze the data and draw the performance charts.

3.4. Calibration

All the measuring equipment is calibrated using different types according to the nature of the equipment. Thermocouples are calibrated against a NIST certified mercury thermometer [54] using a boiling water bath and water with an ice bath. Regarding the current transducer and the voltage transformer, both are calibrated against Keithley multimeter 2001 [55] with an accuracy of 0.0018%. The current transducer was calibrated using a set of ten 40W and 100W Incandescent lamps, as shown in figure 3.27. For the voltage transformer, it was calibrated using a Voltac variac as presented in figure 3.28. Finally, the pressure transducers were calibrated against Budenberg dead-weight tester. All calibration curves are attached in Appendix (A).

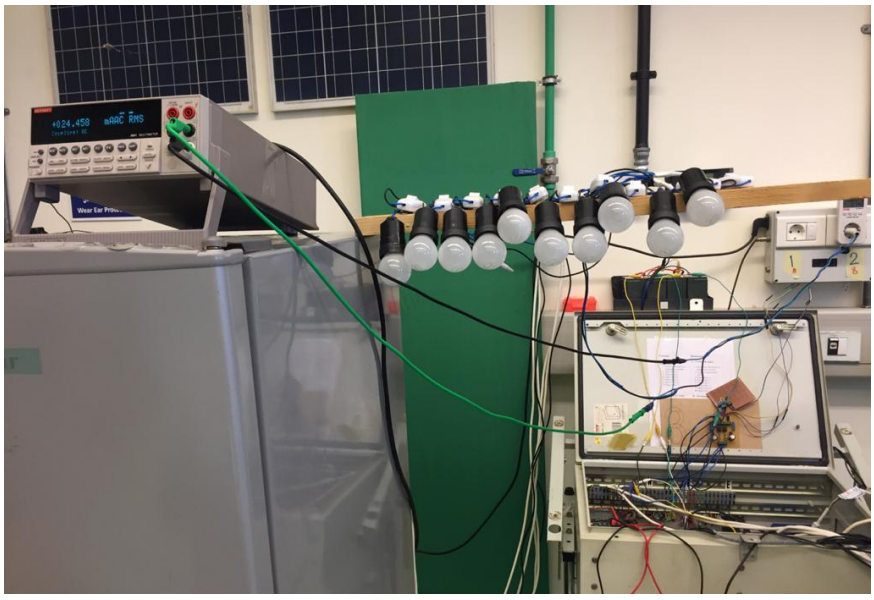

Figure 3.27: Current transducer calibration setup.

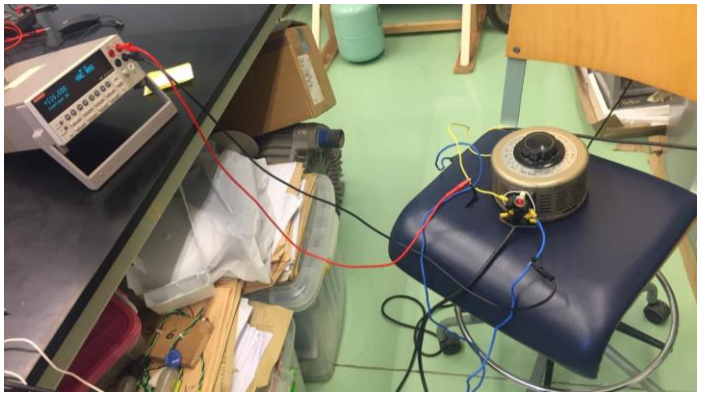

Figure 3.28: Voltage transformer calibration setup.

3.5. Uncertainty Analysis

The uncertainty analysis is done according to equation (3.1) [56]

$$\left(\frac{\sigma_f}{f}\right)^2 = \left(\frac{\sigma_a}{a}\right)^2 + \left(\frac{\sigma_b}{b}\right)^2 \tag{3.1}$$

where, $\left(\frac{\sigma_f}{f}\right)$, $\left(\frac{\sigma_a}{a}\right)$, and $\left(\frac{\sigma_b}{b}\right)$ is the uncertainty of the functions f, a, and b, respectively.

3.5.1. Energy consumption uncertainty

Several components contribute to the energy consumption measurement, especially the components of the current transducer output modification circuit. Table 3.3 list the components affected the accuracy of the energy consumption measurement and the measurement uncertainty.

Table 3.4: Energy consumption uncertainty.

Component/Transducer	Range/Value	Accuracy
Current Transducer	0-5A	±30 mA
ZMPT101B Voltage Transducer	0-250VAC	±0.2%
Two Resistors	2kΩ	±5%
3006P-102 Potentiometer	1kΩ	±10%
Total uncertainty		**±12.487%**

Chapter 4 Results and Discussion

4.1. Introduction

A per the research objectives and the test procedures, four charges of R1234yf (166.5g, 185g, 202g, and 221g) were tested against the manufacturer's recommended charge of R134a (185g) in a baseline defrost domestic refrigerator. All the alternative refrigerant charges were tested continuously for 24 hours at each thermostat point. The investigated performance indicators (the 24-hours energy consumption and the lifetime CO_2 emissions (LCCP)) of each R1234yf charge, compared to its counterpart of R134a at three thermostat points (low, medium, and high). No modifications were introduced to the cycle or the lubricating oil throughout the experiment.

4.2. Cabinets air temperature

The air temperature in the refrigerator cabinet was measured using M-Package as described in section 3.2.2.1. and presented in figure 3.12. The air temperature profile in the refrigerator cabinet for the R1234yf charges and the baseline R134a charge throughout the test period (24 hours) are presented in figures (4.1-4.3), and figures (4.4-4.6) present the air temperature profile in the freezer cabinet for the R1234yf charges and the baseline R134a charge. These figures tell that each refrigerant charge reaches different steady-state pull-down temperatures. Tables 4.1 and 4.2 summarizes the freezer and the refrigerator steady-state pull-down temperatures, respectively, for the charges under investigation at the three thermostat points.

Table 4.1: Freezer air steady-state pull-down temperatures.

Thermostat Point	steady-state pull-down temperatures (°C)				
	R134a	R1234yf			
		166.5g	185g	202g	221g
Low	-14.24	-15.24	-15.21	-15.36	-15.16
Medium	-16.90	-17.45	-17.54	-17.71	-17.34
High	-23.02	-22.38	-23.27	-22.71	-22.59

Table 4.2: Refrigerator air steady-state pull-down temperatures.

Thermostat Point	steady-state pull-down temperatures (°C)				
	R134a	R1234yf			
		166.5g	185g	202g	221g
Low	5.79	6.16	5.94	5.79	5.74
Medium	3.29	3.70	3.61	3.55	3.67
High	-3.96	-1.39	-3.14	-2.08	-2.30

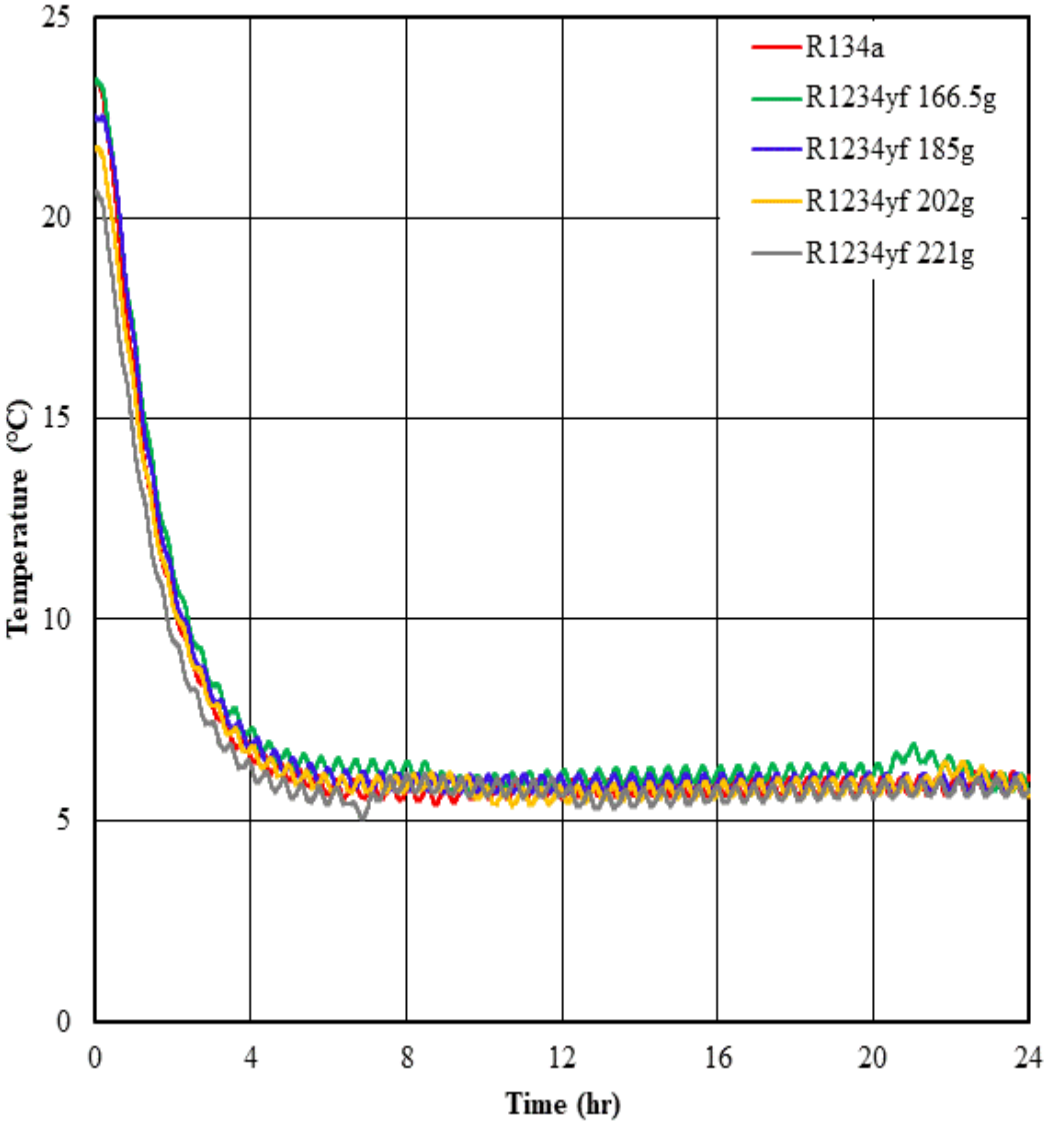

Figure 4.1: Refrigerator air temperature profile at the low thermostat point.

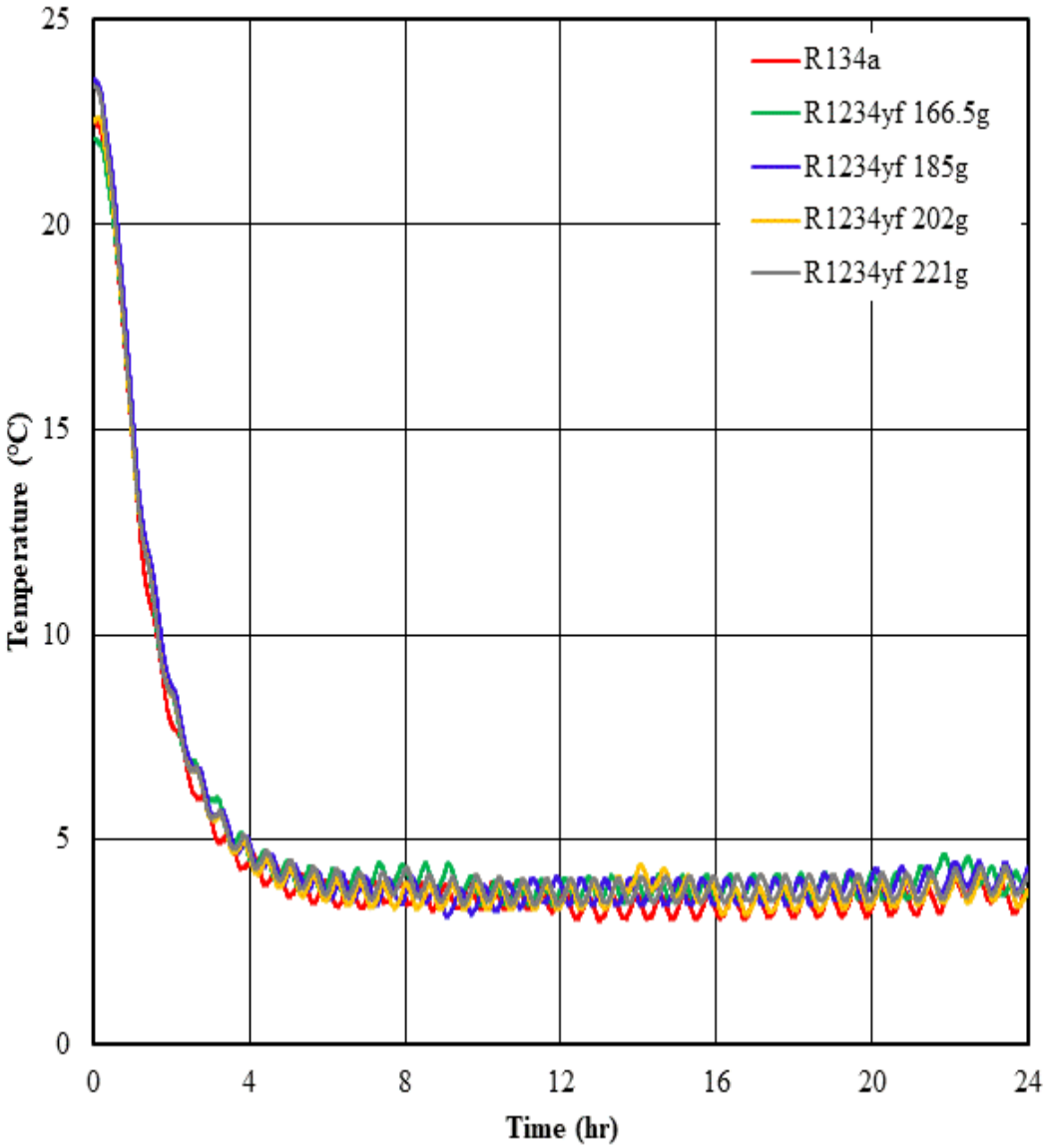

Figure 4.2: Refrigerator air temperature profile at the medium thermostat point.

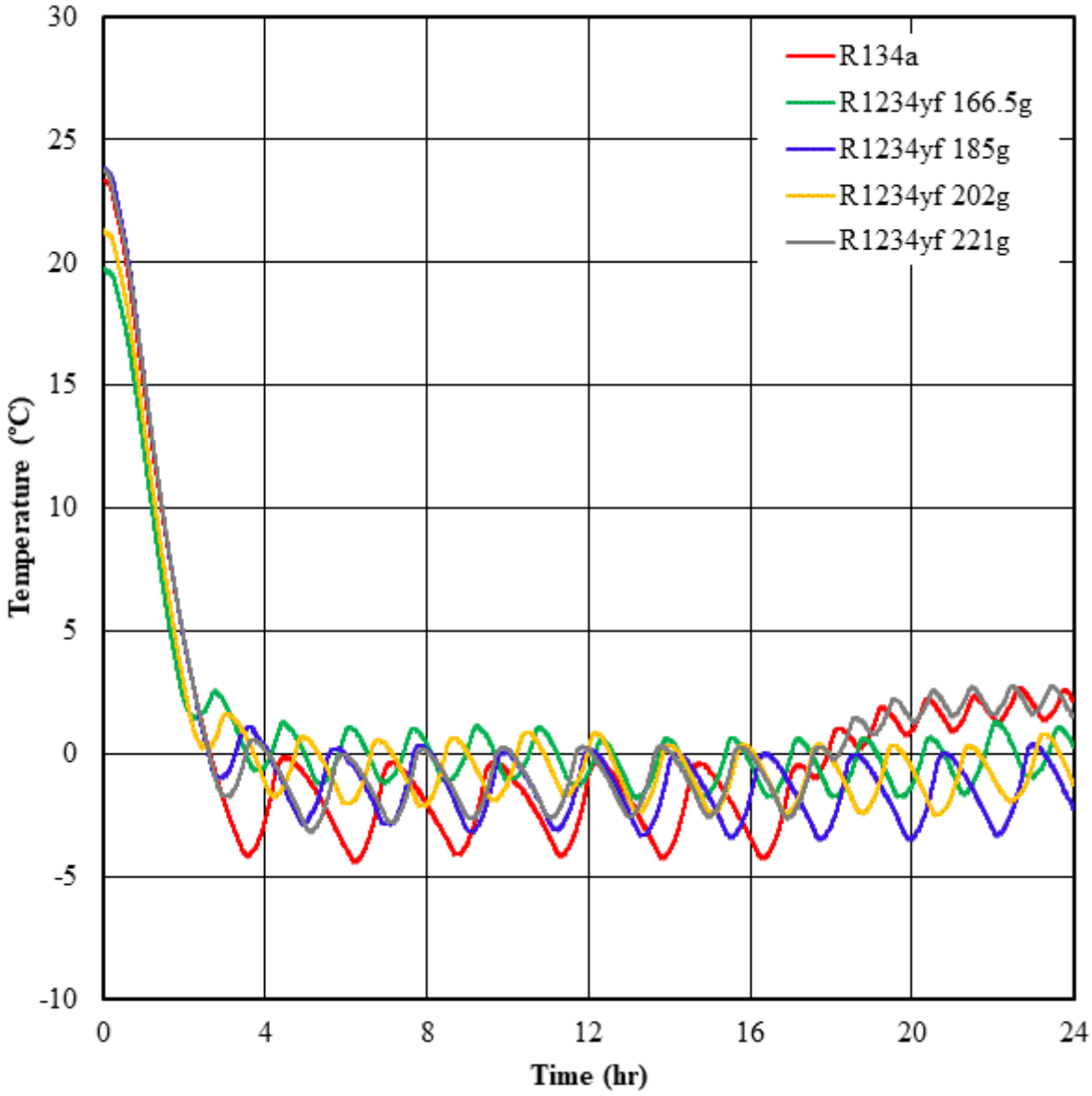

Figure 4.3: Refrigerator air temperature profile at the high thermostat point.

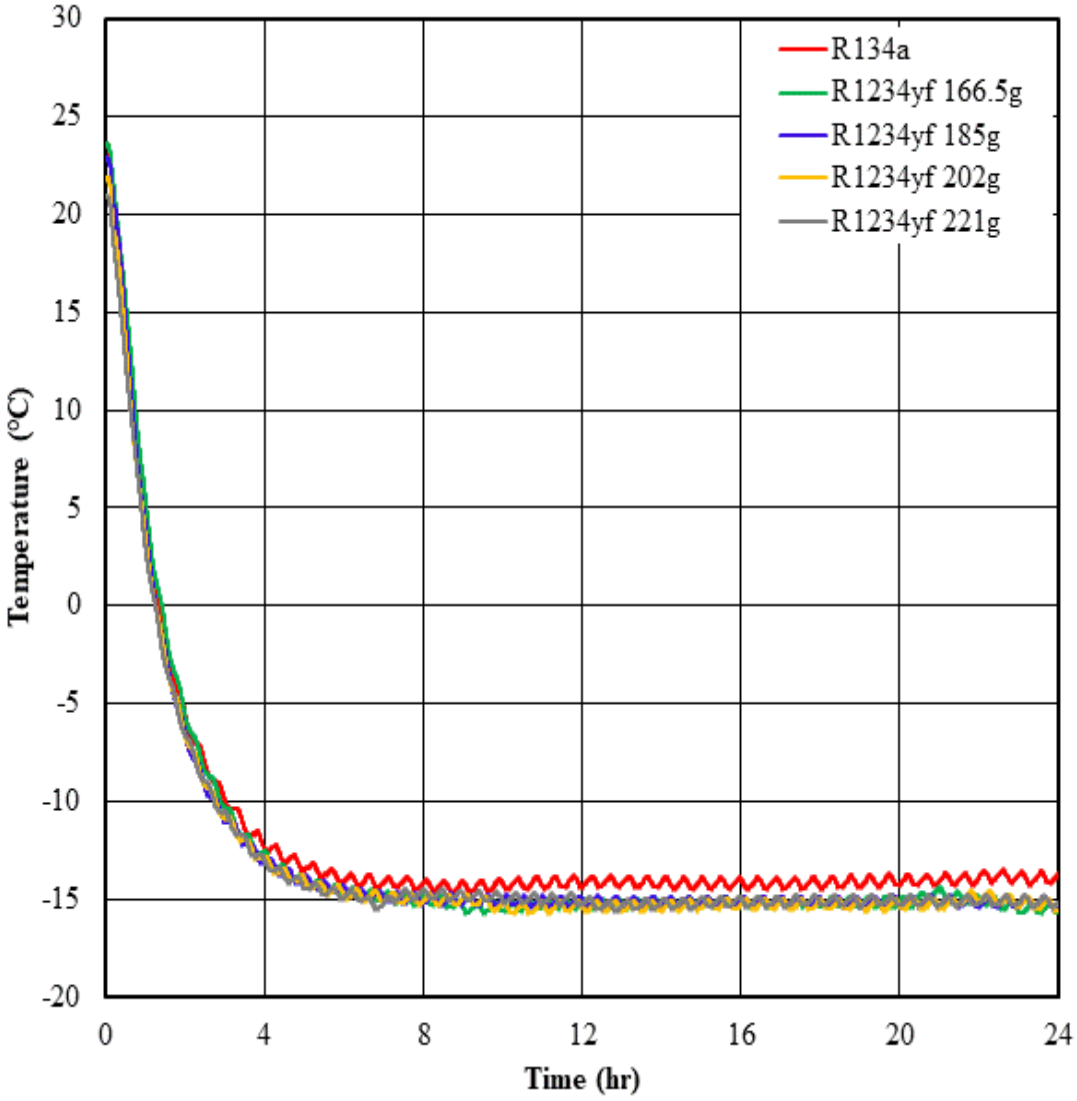

Figure 4.4: Freezer air temperature profile at the low thermostat point.

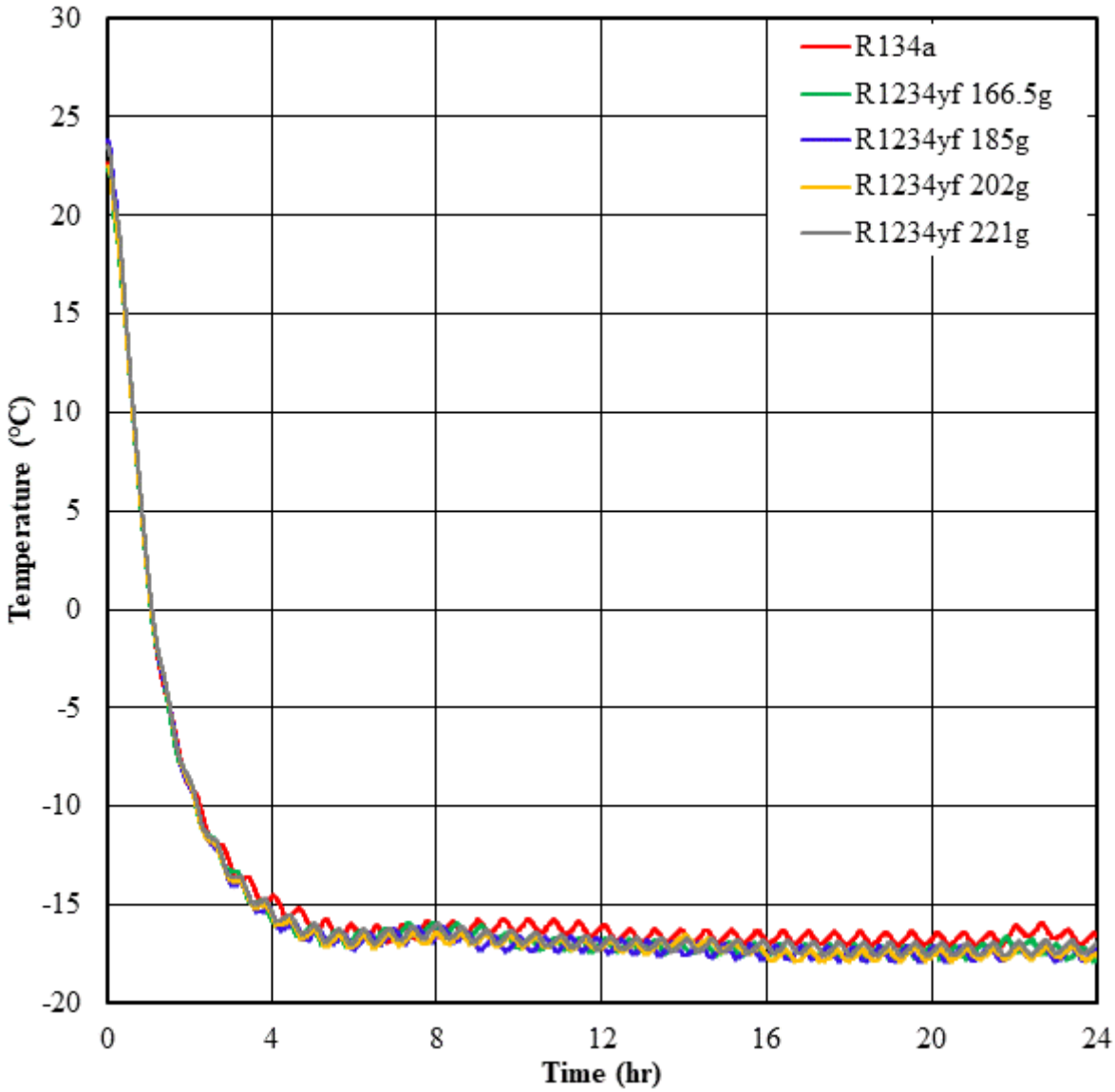

Figure 4.5: Freezer air temperature profile at the medium thermostat point.

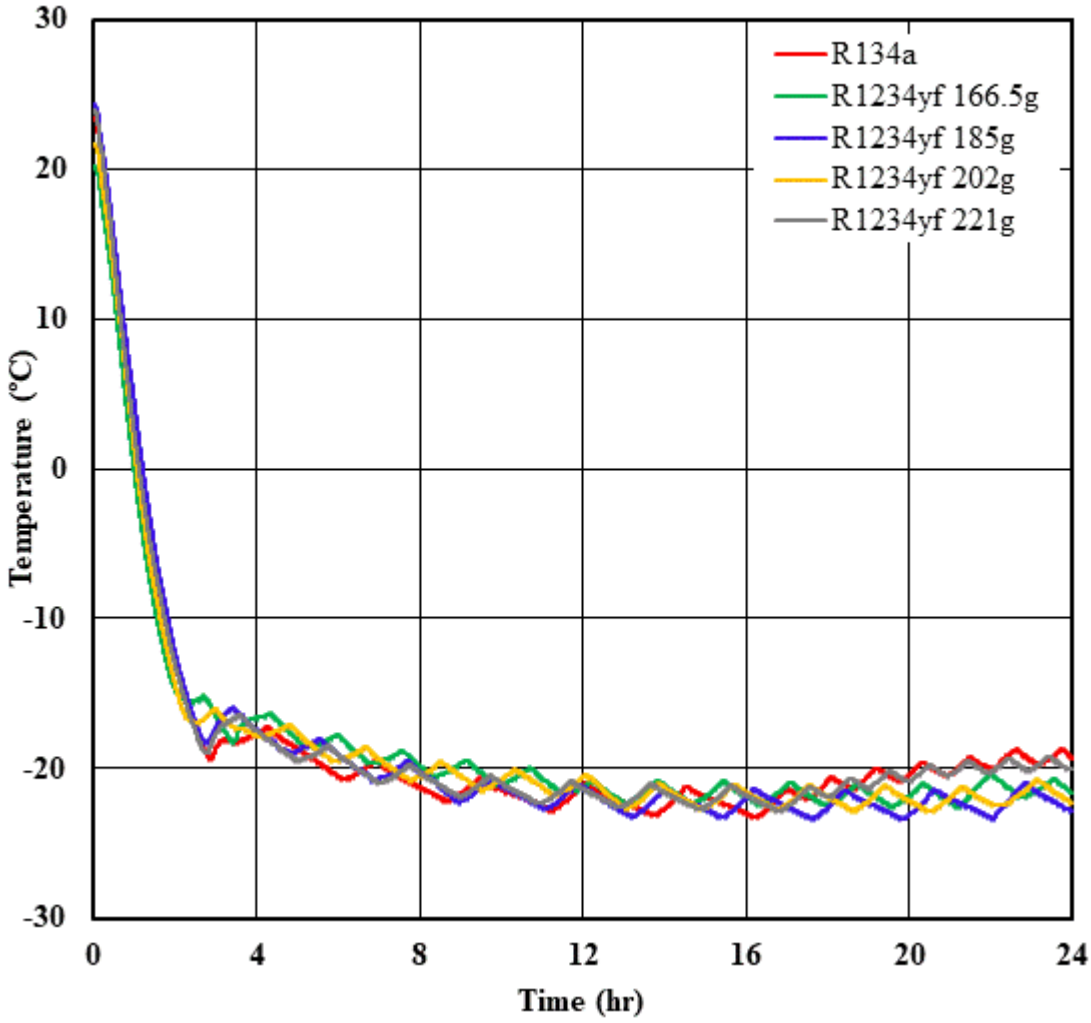

Figure 4.6: Freezer air temperature profile at the high thermostat point.

4.3. Evaporation Temperature

The evaporation temperature was measured using a surface-mount thermocouple at the evaporator inlet, as presented in figure 3.9. The R1234yf charges demonstrated lower evaporation temperatures than R134a at all thermostat points. Figure 4.7 presents the variation of the evaporation temperature of the tested charges with the thermostat points.

At the low thermostat point, the 185g charge of R1234yf achieved the lowest evaporation temperature (-23.58°C) followed by 202g charge (-23.46°C), then the 166.5g charge (-23.42°C) and the 221g (-23.28°C), and finally the R134a (-22.91°C).

At the medium thermostat point, the 202g charge of R1234yf achieved the lowest evaporation temperature (-26.30°C) followed by 166.5g charge (-26.20°C), then the 185g charge (-26.14°C) and the 221g (-25.81°C), and finally the R134a (-25.56°C).

At the high thermostat point, the 166.5g charge of R1234yf achieved the lowest evaporation temperature (-31.86°C) followed by 202g charge (-31.47°C), then the 185g charge (-31.09°C) and the 221g (-30.97°C), and finally the R134a (-25.56°C).

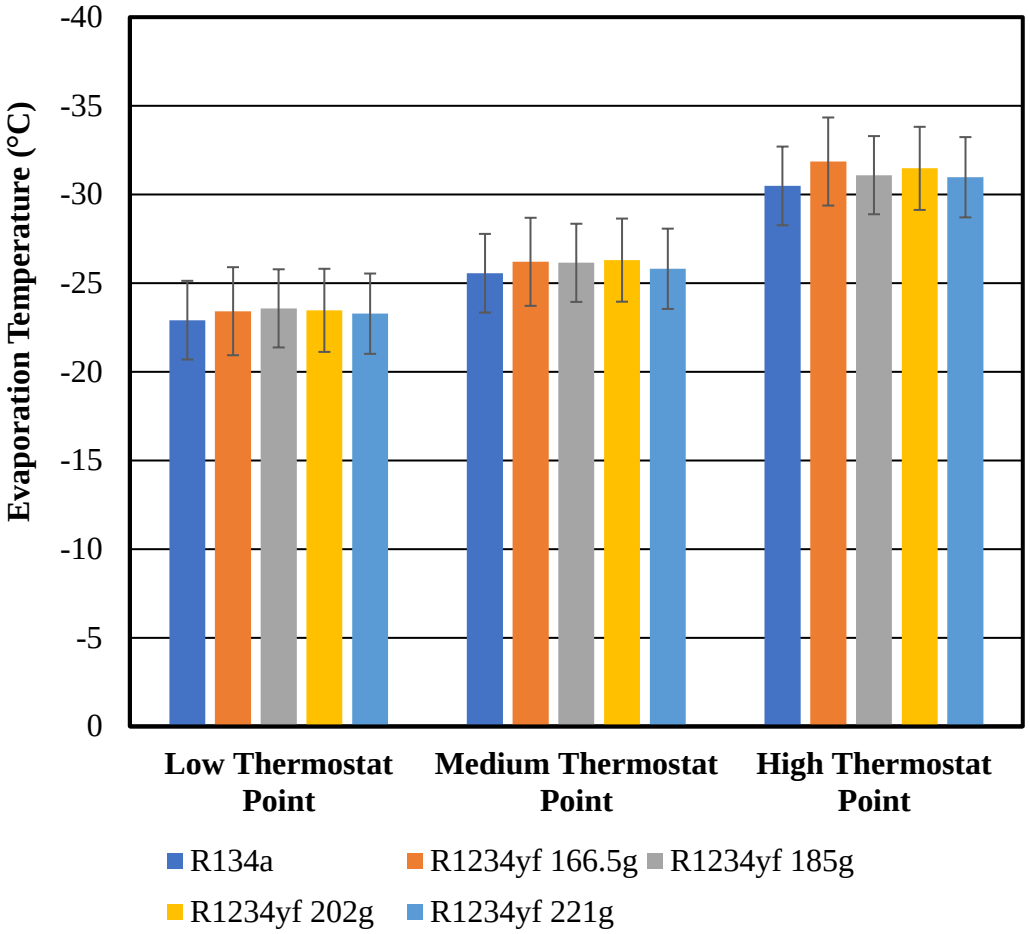

Figure 4.7: Evaporation temperature of the tested charges and R134a.

4.4. Condensation Temperature

The condensation temperature was calculated using the compressor discharge pressure. It is the saturation temperature of the discharge pressure. Figure 4.8 presents the variation of the condensation temperature of the tested charges with the thermostat points.

At the low thermostat point, the 166.5g charge of R1234yf achieved the highest condensation temperature (42.19°C) followed by the 185g charge (42.01°C), then R134a (41.03°C) and the 205g (40.38°C), and finally the 221g charge (40.20°C).

At the medium thermostat point, the 185g charge of R1234yf achieved the highest condensation temperature (40.93°C) followed by the 221g charge (40.43°C), then the 166.5g (40.31°C) and R134a (38.54°C), and finally the 202g charge (38.20°C).

At the high thermostat point, the 185g charge of R1234yf achieved the highest condensation temperature (37.57°C) followed by the 221g charge (37.16°C), then R134a (36.67°C) and the 202g charge (34.96°C), and finally, the 166.5g charge (33.72°C).

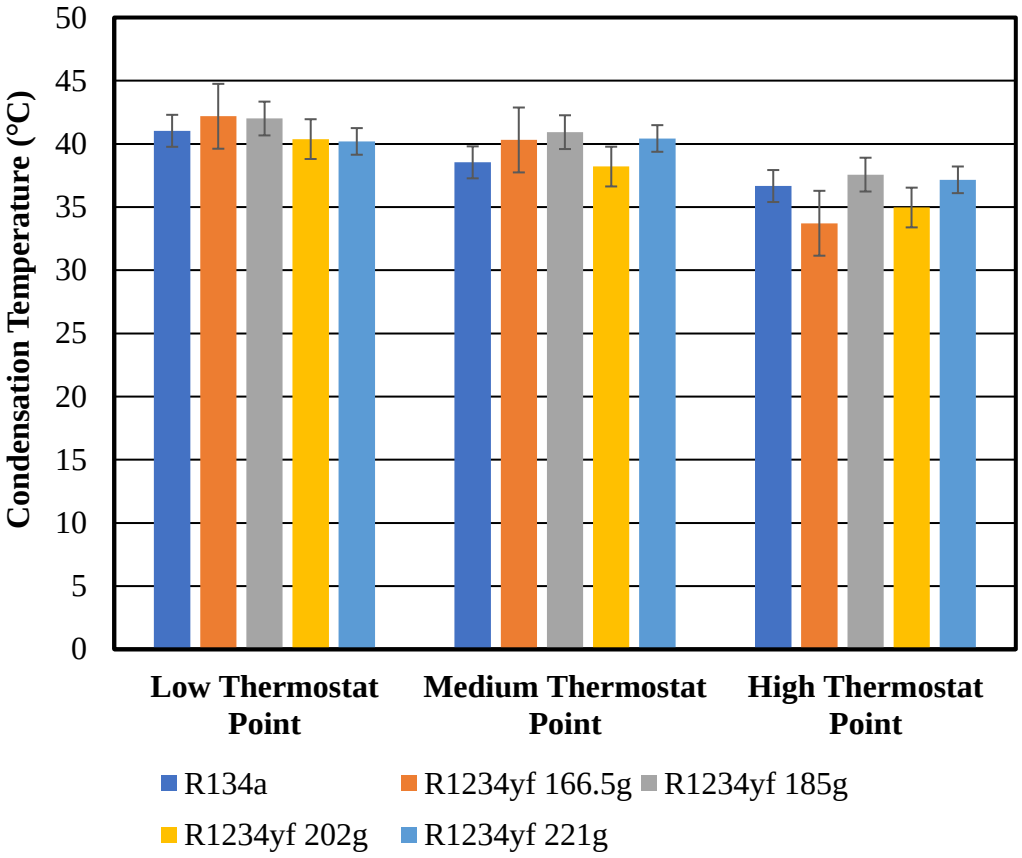

Figure 4.8: Condensation temperature of the tested charges and R134a.

4.5. Discharge pressure

The discharge pressure measured using a 0-16bar pressure transducer mounted at the compressor discharge line, as presented in figure 3.19. The variation of the discharge pressure of the tested charges with the thermostat points is presented in figure 4.9.

At the low thermostat point, the 166.5g charge of R1234yf achieved the highest discharge pressure (10.760bar) followed by the 185g charge (10.713bar), then R134a (10.451bar) and the 202g (10.282bar), and finally the 221g charge (10.235bar).

At the medium thermostat point, the 185g charge of R1234yf achieved the highest discharge pressure (10.426bar), followed by the 221g charge (10.295bar), then the 166.5g (10.264bar) and R134a (9.773bar), and finally the 202g charge (9.728bar).

At the high thermostat point, the 185g charge of R1234yf achieved the highest discharge pressure (9.570bar), followed by the 221g charge (9.469bar), then R134a (9.262bar) and the 202g charge (8.940bar), and finally the 166.5g charge (8.655bar).

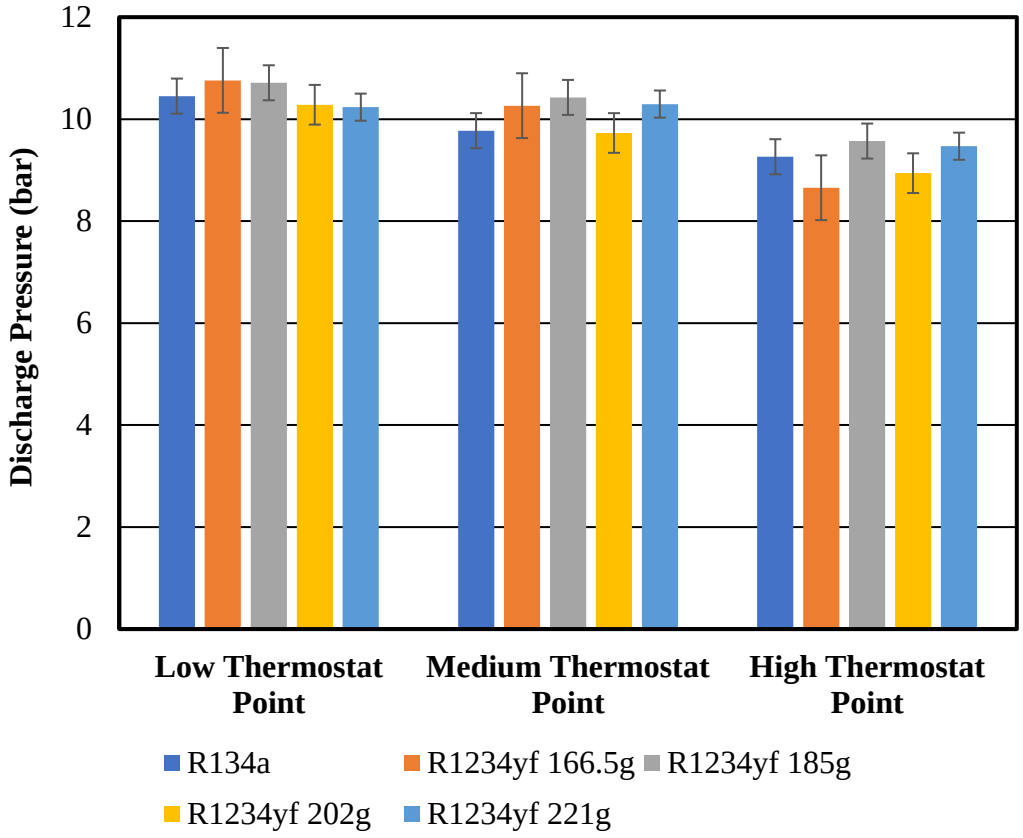

Figure 4.9: Discharge pressure of the tested charges and R134a.

4.6. Compression ratio

The compressor pressure ratio was calculated by dividing the discharge pressure by the suction pressure. R134a exhibited a higher compression ratio than all R1234yf charges at all thermostat points. The 166.5g charge of R1234yf showed a higher compression ratio among the other R1234yf charges at all thermostat points. Figure 4.10 shows the compression ratio variation of the charges under investigation with the thermostat points.

At the low thermostat point, the R134a obtained the highest pressure ratio with the value of 11.480, followed by the 166.5g charge of R1234yf (11.217) and the 202g charge (10.822), then the 221g charge (10.443), and finally the 185g charge (10.499).

At the medium thermostat point, the R134a obtained the highest pressure ratio with the value of 12.459, followed by the 166.5g charge of R1234yf (11.831) and the 202g charge (11.448), then the 221g charge (11.235), and finally the 185g charge (11.170).

At the high thermostat point, the R134a obtained the highest pressure ratio with the value of 13.528, followed by the 166.5g charge of R1234yf (12.405) and the 202g charge (12.344), then the 185g charge (12.192), and finally the 221g charge (12.189).

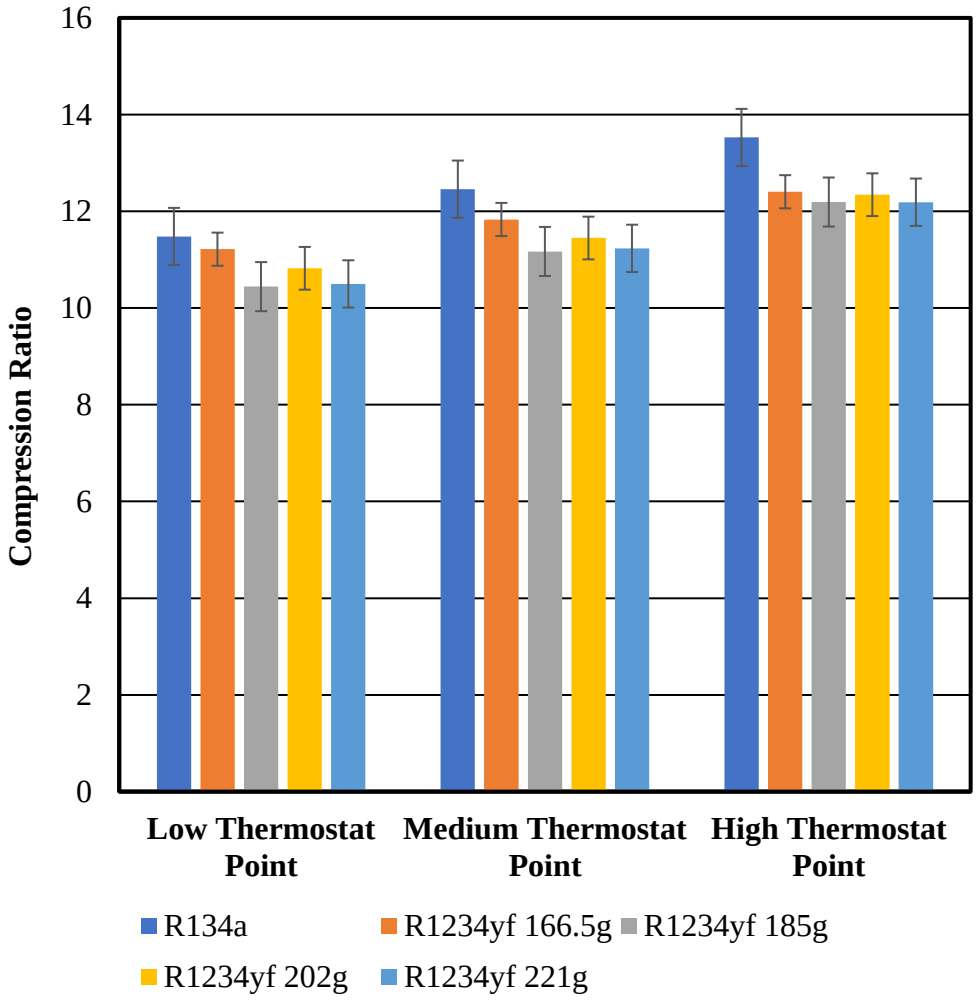

Figure 4.10: Compression ratio of the tested charges and R134a.

4.7. Power Draw

The power was calculated using the current and voltage measurements according to equation (4.1). It is noteworthy that the used refrigerator has an energy class E (the worst level in the power classification tag). Furthermore, the power factor measured during all tests to be 0.55.

$$\text{Power} = I * V * P.F \tag{4.1}$$

Figures 4.11 – 4.13 present the power draw for the investigated refrigerant charges at the low, medium, and high thermostat points, respectively.

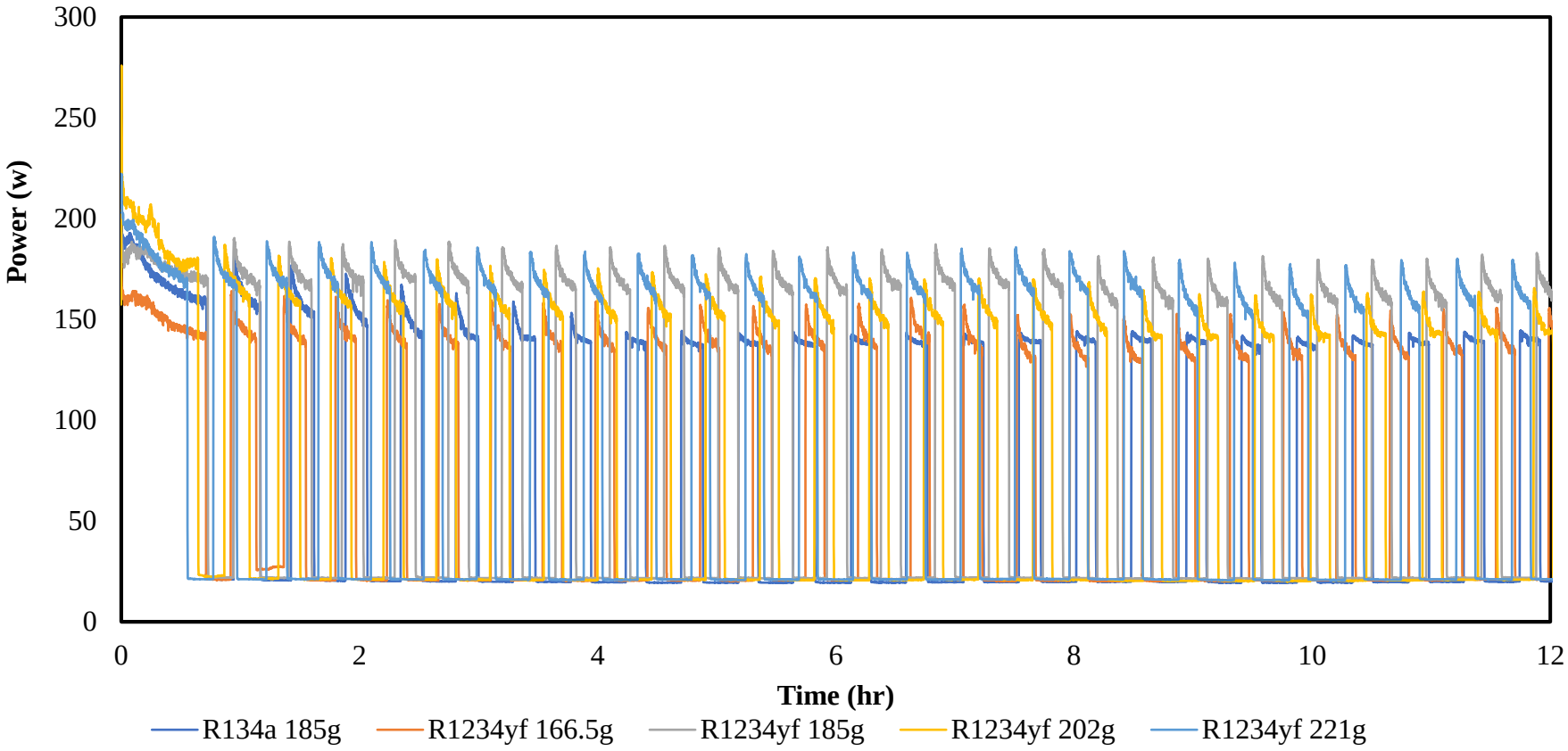

Figure 4.11: Power draw profile at the low thermostat point.

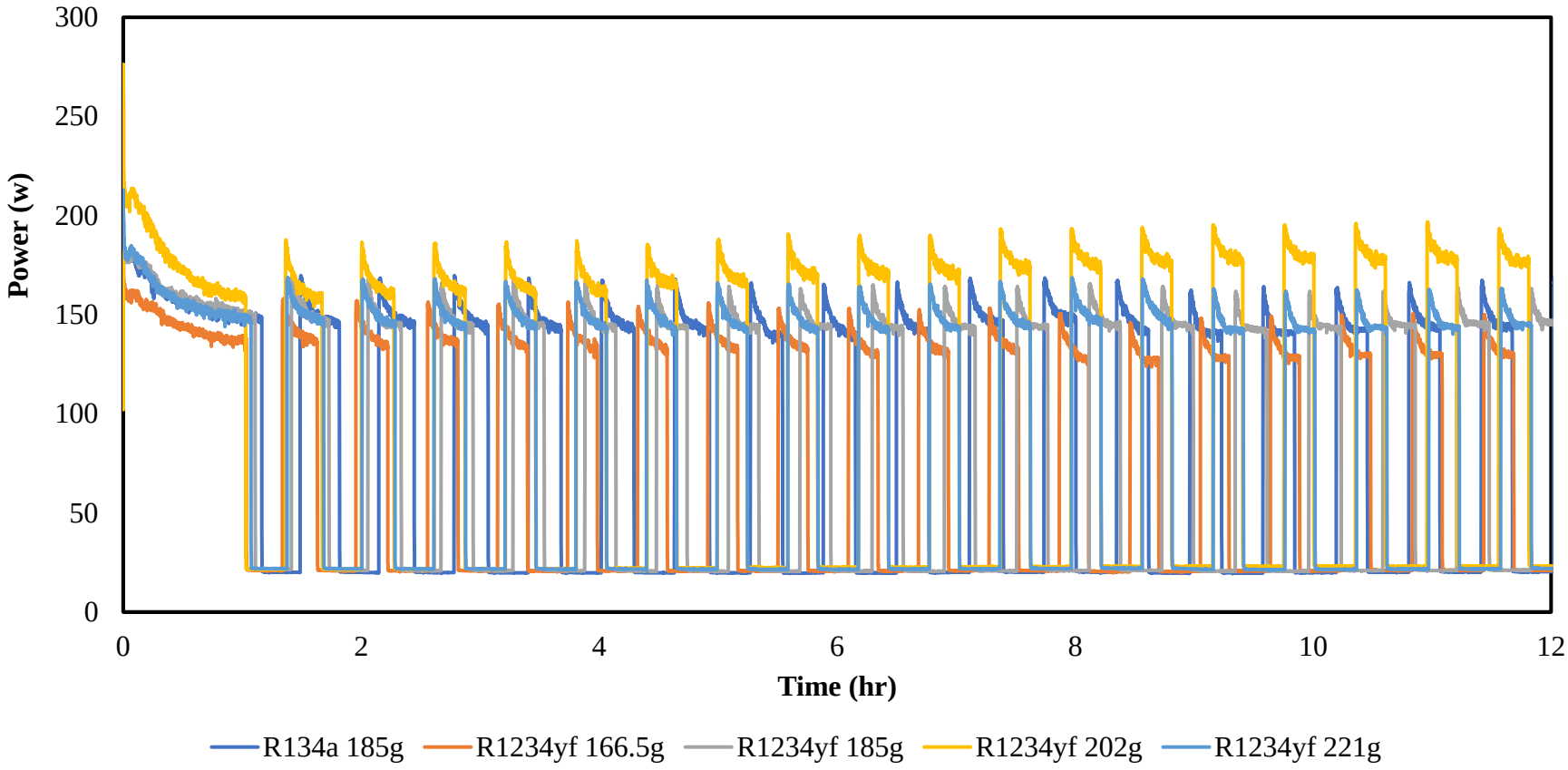

Figure 4.12: Power draw profile at the medium thermostat point.

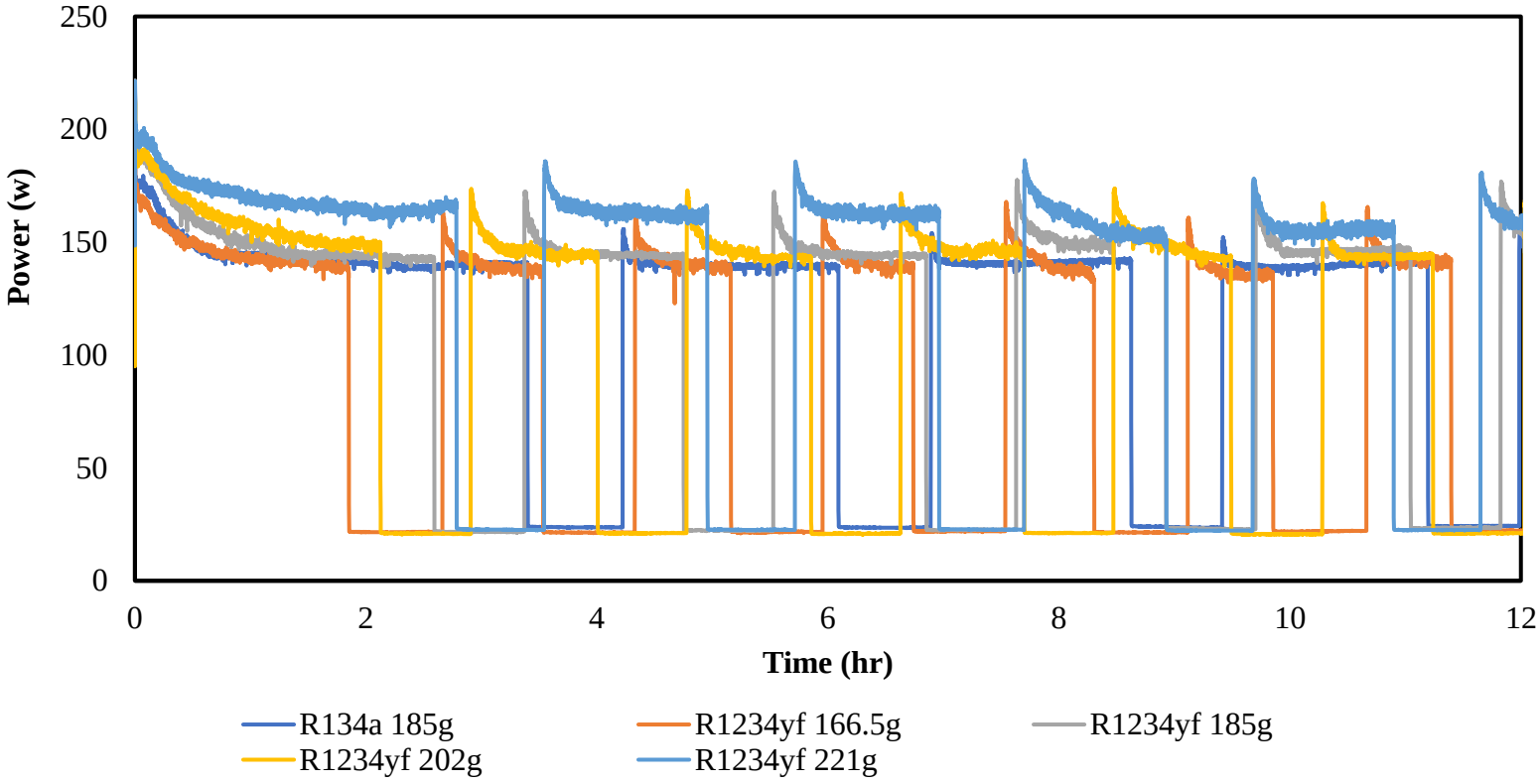

Figure 4.13: Power draw profile at the high thermostat point.

4.8. Daily Energy Consumption

The energy consumption in this study was calculated by integrating the power over the test duration.

Table 4.3 presents the experimental 24-hours energy consumption for the R1234yf and R134a charges.

Table 4.3: Experimental 24-hours energy consumption.

Thermostat Point	24-hours energy consumption (Wh)				
	R134a	R1234yf			
		166.5g	185g	202g	221g
Low	1665	1785	1872	1755	1800
Medium	2007	1950	1990	2069	1952
High	2538	2336	2794	2479	2676

These energy consumption values consumed by each refrigerant charge to achieve different air temperatures. Therefore, this data has been normalized at a specific temperature for each thermostat point to judge the refrigerant charges at the same air temperature.

The energy and freezer air temperature data mentioned in tables 4.3 and 4.1, respectively, is used to establish linear-fit interpolation to quantify the possible daily energy consumption if the freezer air temperature for all the charges was -16°C at the low thermostat point, -18°C at the medium thermostat point, and -21°C at the high thermostat point. The interpolation results and the normalized (resulting from the interpolation) daily energy consumption are presented in table 4.4 and 4.5. Figures 4.14 and 4.15 graphically present the normalized daily energy consumption as values in Wh and as a percentage of the baseline R134a.

Table 4.4: Linear fit interpolation for the daily energy consumption.

Charge		Thermostat Point	Pull-down freezer air Temp. (C)	Experimental 24-hours energy consumption (Wh)	Linear fit interpolation result	
					Intercept	Slope
R134a		Low	-14.24	1665	312.255	-97.359
		Medium	-16.90	2006		
		High	-23.02	2538		
R1234yf	166.5g	Low	-15.24	1785	602.040	-77.449
		Medium	-17.45	1950		
		High	-22.38	2336		
	185g	Low	-15.21	1872	-9.986	-119.370
		Medium	-17.54	1990		
		High	-23.27	2794		
	202g	Low	-15.36	1755	317.676	-95.922
		Medium	-17.71	2069		
		High	-22.71	2479		
	221g	Low	-15.17	1800	-90.399	-121.619
		Medium	-17.34	1952		
		High	-22.59	2676		

Table 4.5: Normalized 24-hours energy consumption.

Thermostat Point	24-hours energy consumption (Wh)				
	R134a	R1234yf			
		166.5g	185g	202g	221g
Low	1870	1841	1900	1852	1856
Medium	2065	1996	2139	2044	2099
High	2357	2228	2497	2332	2464

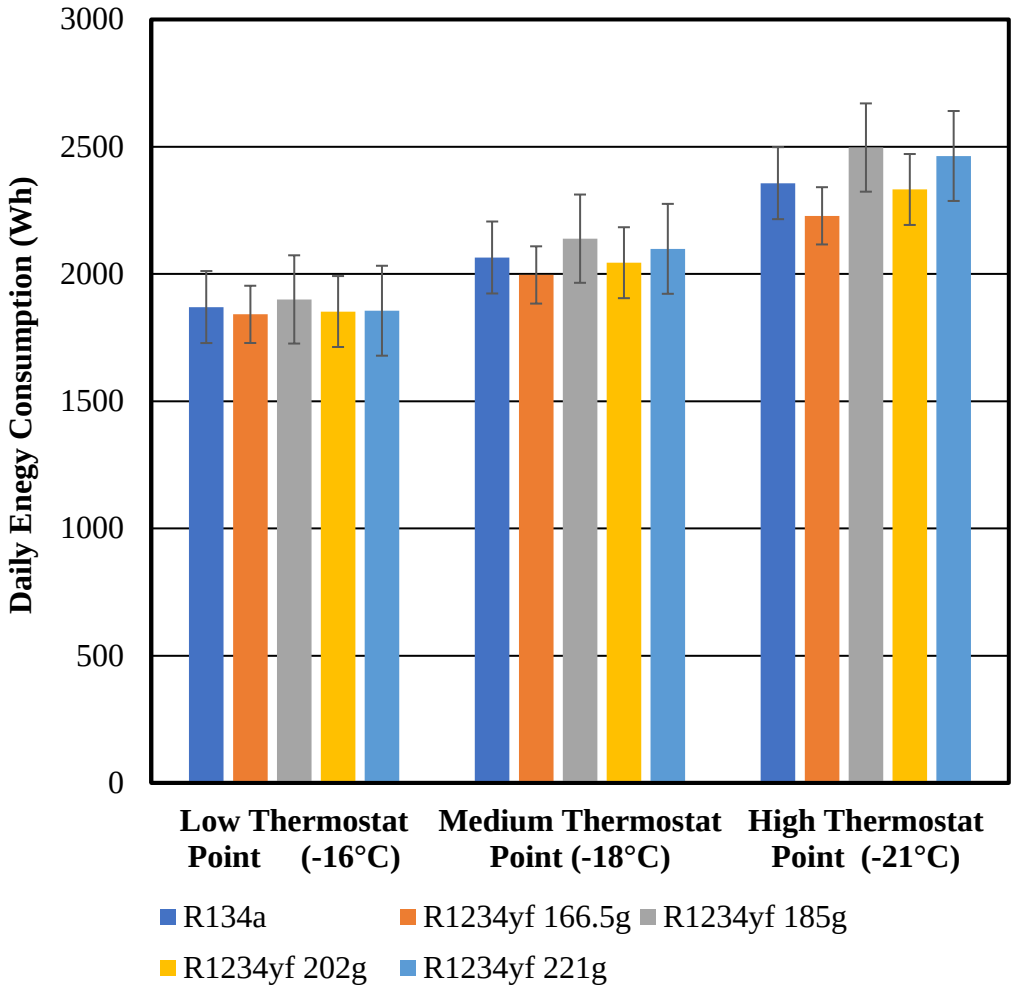

Figure 4.14: Daily energy consumption in Wh.

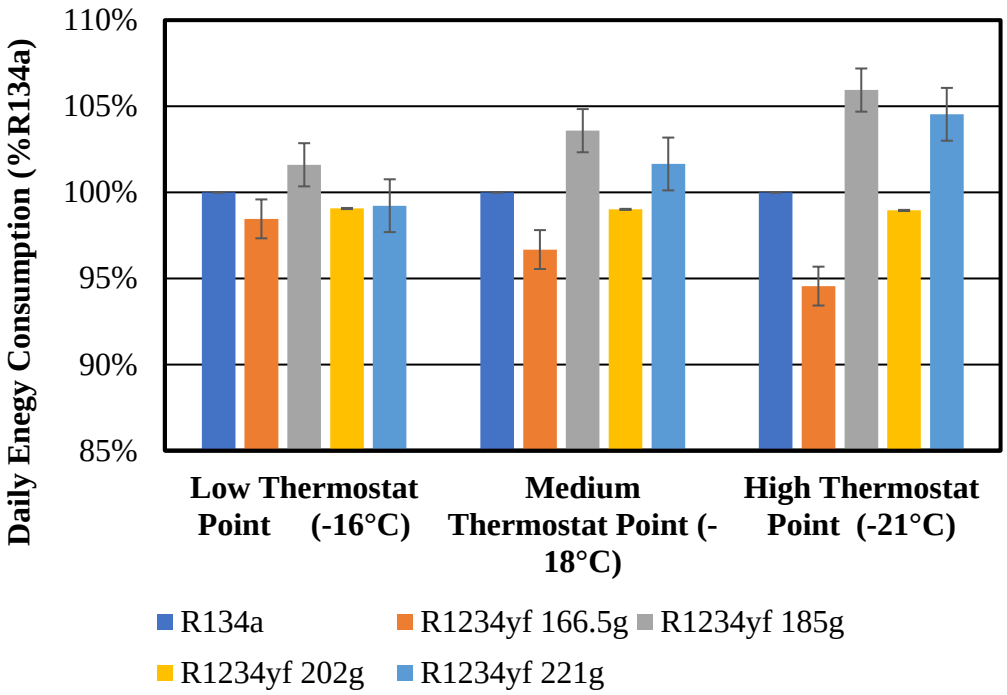

Figure 4.15: Daily energy consumption Percentage of R134a.

As Figure 4.15 shows, R1234yf with a charge of 166.5g in the lowest energy consumer at all thermostat points demonstrating 2-5% less energy consumption than R134a.

At the low thermostat point, R1234yf with a charge of 166.5g was the lowest energy consumption with 98% of R134a energy consumption flowed by the 202g charge, the 221g, and the 185g charge with 99%, 99%, and 102%, respectively.

At the medium thermostat point, R1234yf with a charge of 166.5g was the lowest energy consumption with 97% of R134a energy consumption flowed by the 202g charge, the 221g, and the 185g charge with 99%, 102%, and 104%, respectively.

At the high thermostat point, R1234yf with a charge of 166.5g was the lowest energy consumption with 95% of R134a energy consumption flowed by the 202g charge, the 221g, and the 185g charge with 99%, 105%, and 106%, respectively.

4.9. LCCP

The LCCP evaluates the total direct and indirect CO_2 emissions throughout the refrigerant's lifetime as described in section 2.3.3. The LCCP is calculated using equations [2.4-2.8] with the following assumption:

1) 1% ALR [57]
2) 15 years system's life [57]
3) 100% EOLL
4) The Cairo, Egypt electricity network emissions = 0.5164 $kgCO_2/kWh$ [58]

The system's material manufacturing and recycling emissions have not been considered the same refrigerator used for all tests without any changes. Figures 4.9 and 4.10 show the LCCP results.

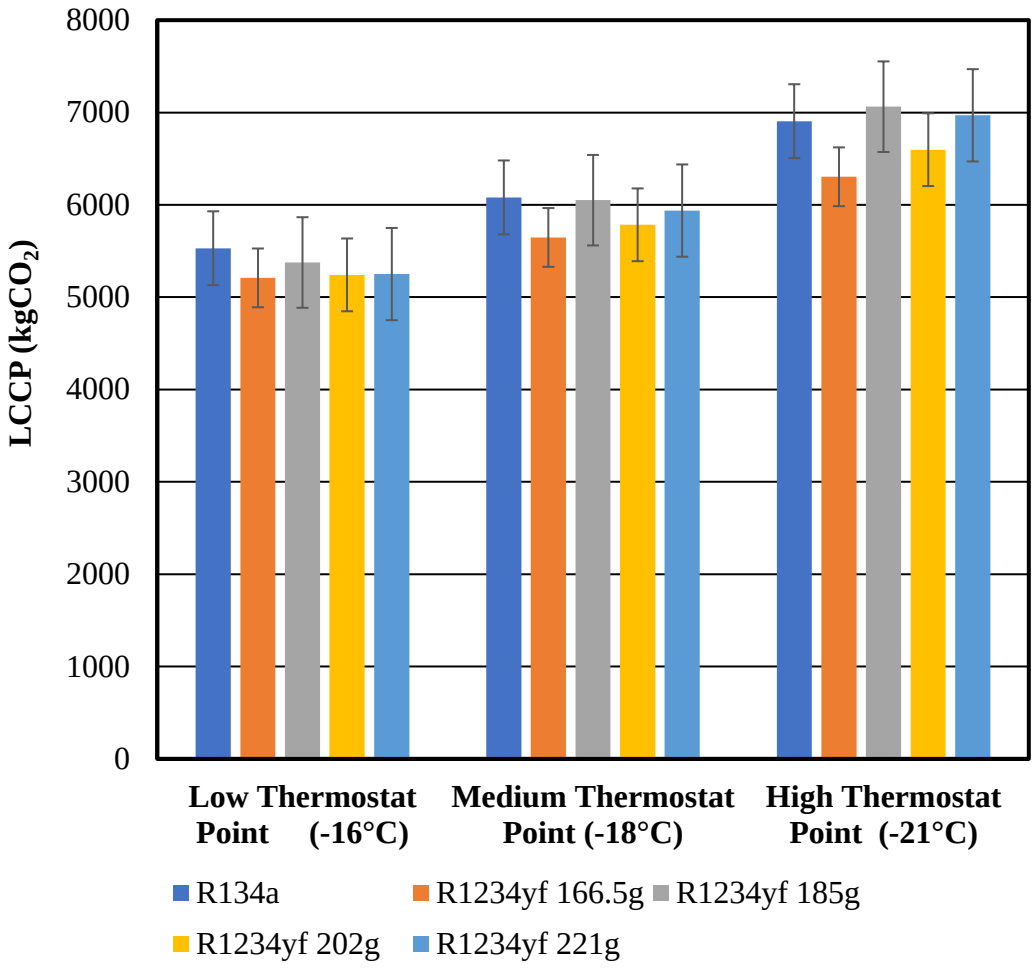

Figure 4.16: LCCP variation with the thermostat point in kgCO_2.

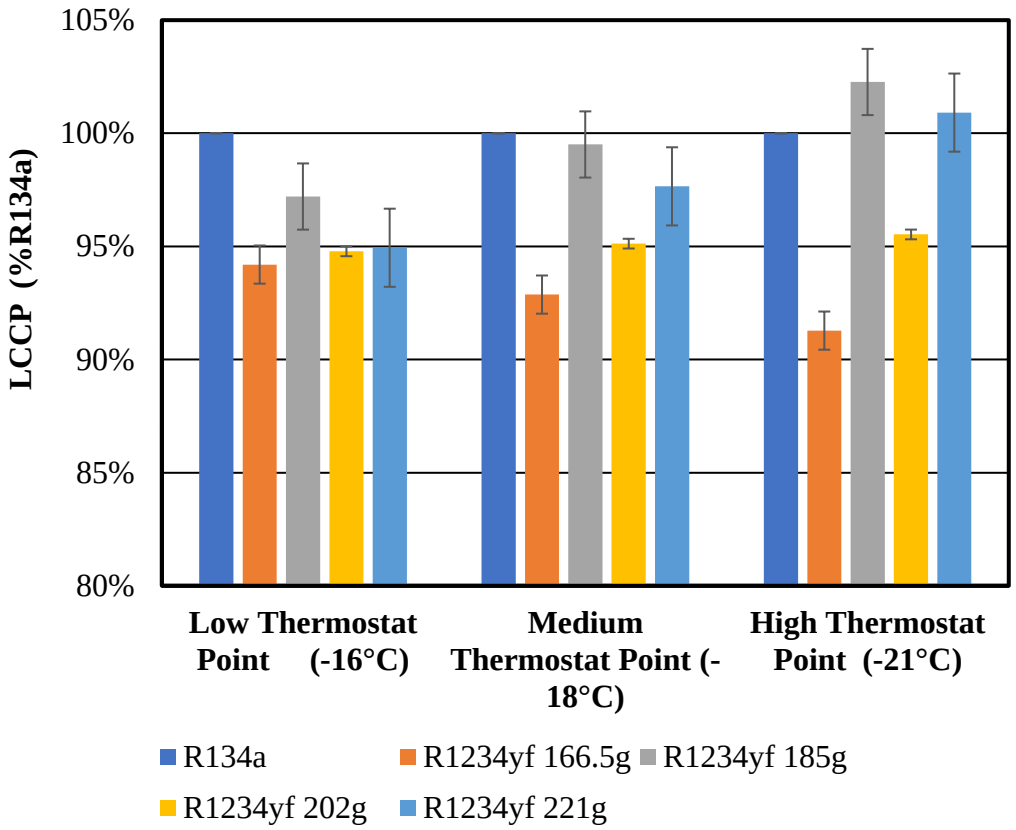

Figure 4.17: LCCP variation with the thermostat point in kgCO_2.

As Figure 4.17 shows, R1234yf with a charge of 166.5g in the charge with the lowest LCCP CO_2 emissions at all thermostat points exhibiting 6-9% LCCP CO_2 emissions savings than R134a.

At the low thermostat point, R134a showed higher LCCP CO_2 emissions than all R1234yf charges. R1234yf with a charge of 166.5g had the lowest value of LCCP CO_2 emissions with 94% of the R134a LCCP CO_2 emissions by the 202g charge, the 221g, and the 185g charge with 95%, 95%, and 97%, respectively.

At the medium thermostat point, R134a showed higher LCCP CO_2 emissions than three R1234yf charges. Also, R1234yf with a charge of 166.5g had the lowest value of LCCP

CO_2 emissions with 93% of the R134a LCCP CO_2 emissions flowed by the 202g charge, the 221g, and the 185g charge with 95%, 98%, and 100%, respectively.

At the high thermostat point, R134a showed higher LCCP CO_2 emissions than two R1234yf charges. Again, R1234yf with a charge of 166.5g kept its ranking as the charge with the lowest value of LCCP CO_2 emissions with 91% of the R134a LCCP CO_2 emissions. The 202g charge, the 221g charge, and the 185g charge exhibited 96%, 101%, and 102% of the R134a LCCP CO_2 emission, respectively.

Chapter 5 Conclusions and Recommendations

5.1. Conclusions

This study tested four different charges of R1234yf (166.5g, 185g, 202g, and 221g) as drop-in alternatives for the manufacturer-recommended charge of R134a (170g +15g to account for the cycle extensions to attach the measuring system) in a baseline domestic refrigerator. The used baseline refrigerator has a flat-plate evaporator, wire-on-tube condenser, one separate freezer cabinet, single-door refrigerator cabinet, and a LSHX. The investigated R1234yf charges and the manufacturer-recommended charge of R134a were tested against each other at three thermostat points (low, medium, and high). The carried tests aimed to study the daily energy consumption and the lifetime CO_2 emissions for the charges under investigation. Each of the alternative R1234yf charges was tested for 24 hours at every thermostat point. The test measurements (temperature, pressure, current, and voltage) were recorded every 4 seconds on a datalogger.

The results of this study proved the R1234yf ability to achieve freezing temperatures as much as R134a does. At low and medium thermostat points, R1234yf charges achieved lower freezer air temperature than that of R134a. for the evaporation temperature, all R1234yf charges achieved lower evaporation temperatures than R134a charge that the refrigerator is originally designed to work on.

For the pressure ratio, R134a showed a higher pressure ratio than R1234yf charges. Among the R1234yf charges, the 166.5g charge was the charge with the higher pressure ratio.

Regarding the daily energy consumption, a linear-fit interpolation using the steady-state freezer air temperature and the experimental 24-hours energy consumption was necessary for each charge. This normalization was to allow energy consumption comparison between the tested charges on the same freezer air temperature. Thus, each refrigerant charges' energy consumption was compared to each other at -16°C, -18°C, and -21°C representing the low, medium, and high thermostat points, respectively. The energy consumption results of this study yielded that the 166.5g charge of R1234yf is the optimum alternative charge for R134a. This charge led to the minimum daily energy consumption among the other tested charges. This R1234yf charge led to 2-5% less energy consumption than that of the manufacturer's recommended charge of R134a.

Concerning the LCCP, the energy consumption emissions were calculated based on the Cairo, Egypt electricity grid. Other assumptions have been taken into account to calculate LCCP. These assumptions like 1% ALR, 15 years system's life, and 100% EOLL. The LCCP results showed that the R1234yf charge of 166.5g saved 6-9% lifetime CO_2 emissions than R134a. The saved emissions were 6% at the low thermostat point and increased to 9% as the thermostat point moved to the high thermostat point.

5.2. Recommendations

Cycle modification is still needed to maximize the reduction of CO_2 emissions. Also, Further COP and cooling capacity investigations are recommended to be done.

References

[1] J. Navarro-Esbrí, J. M. Mendoza-Miranda, A. Mota-Babiloni, A. Barragán-Cervera, and J. M. Belman-Flores, "Experimental analysis of R1234yf as a drop-in replacement for R134a in a vapor compression system," *International Journal of Refrigeration*, vol. 36, no. 3, pp. 870–880, May 2013, doi: 10.1016/j.ijrefrig.2012.12.014.

[2] R. J. Dossat, *Principles of Refrigeration.* (4th ed.) Upper Saddle River, N.J: Prentice Hall International, 1997.

[3] C. T. Olivo and R. W. Marsh, *Principles of Refrigeration.* (3rd ed.) Albany, N.Y: Delmar Publishers, 1990.

[4] S. Benhadid-Dib and A. Benzaoui, "Refrigerants and their Environmental Impact Substitution of Hydro Chlorofluorocarbon HCFC and HFC Hydro Fluorocarbon. Search for an Adequate Refrigerant," *Energy Procedia*, vol. 18, pp. 807–816, Jan. 2012, doi: 10.1016/j.egypro.2012.05.096.

[5] B. O. Bolaji and Z. Huan, "Ozone depletion and global warming: Case for the use of natural refrigerant – a review," *Renewable and Sustainable Energy Reviews*, vol. 18, pp. 49–54, Feb. 2013, doi: 10.1016/j.rser.2012.10.008.

[6] I. Sarbu, "A review on substitution strategy of non-ecological refrigerants from vapour compression-based refrigeration, air-conditioning and heat

pump systems," *International Journal of Refrigeration*, vol. 46, pp. 123–141, Oct. 2014, doi: 10.1016/j.ijrefrig.2014.04.023.

[7] M. Mohanraj, S. Jayaraj, and C. Muraleedharan, "Environment friendly alternatives to halogenated refrigerants—A review," *International Journal of Greenhouse Gas Control*, vol. 3, no. 1, pp. 108–119, Jan. 2009, doi: 10.1016/j.ijggc.2008.07.003.

[8] M. O. McLinden, A. F. Kazakov, J. Steven Brown, and P. A. Domanski, "A thermodynamic analysis of refrigerants: Possibilities and tradeoffs for Low-GWP refrigerants," *International Journal of Refrigeration*, vol. 38, pp. 80–92, Feb. 2014, doi: 10.1016/j.ijrefrig.2013.09.032.

[9] S. Gupta, N. K. Karanam, R. Konijeti, and A. Dasore, "Thermodynamic Analysis and Effects of Replacing HFC by Fourth-Generation Refrigerants in VCR Systems," *Int. J. Air-Cond. Ref.*, vol. 26, no. 02, p. 1850013, Mar. 2018, doi: 10.1142/S201013251850013X.

[10] A. Mota-Babiloni, J. Navarro-Esbrí, Á. Barragán, F. Molés, and B. Peris, "Drop-in energy performance evaluation of R1234yf and R1234ze(E) in a vapor compression system as R134a replacements," *Applied Thermal Engineering*, vol. 71, no. 1, pp. 259–265, Oct. 2014, doi: 10.1016/j.applthermaleng.2014.06.056.

[11] O. US EPA, “Understanding Global Warming Potentials,” *US EPA*, 12-Jan-2016. [Online]. Available: https://www.epa.gov/ghgemissions/understanding-global-warming-potentials. [Accessed: 16-Jan-2019].

[12] "Regulation (EU) No 517/2014 of the European Parliament and of the Council of 16 April 2014 on fluorinated greenhouse gases and repealing Regulation (EC) No 842/2006 Text with EEA relevance", *Official Journal of the European Union*, pp. 195-230, 2014. Available: https://eur-lex.europa.eu/legal-content/en/ALL/?uri=CELEX%3A32014R0517. [Accessed 18 January 2019].

[13] A. Sethi, E. Vera Becerra, and S. Yana Motta, “Low GWP R134a replacements for small refrigeration (plug-in) applications,” *International Journal of Refrigeration*, vol. 66, pp. 64–72, Jun. 2016, doi: 10.1016/j.ijrefrig.2016.02.005.

[14] Carrier Corporation, “New Refrigerants Impact Standards and Codes”, *Carrier Engineering Newsletter*, Vol. 3 issue 2. 2015

[15] Myhre, G., D. Shindell, F.-M. Bréon, W. Collins, J. Fuglestvedt, J. Huang, D. Koch, J.-F. Lamarque, D. Lee, B. Mendoza, T. Nakajima, A. Robock, G. Stephens, T. Takemura and H. Zhang, 2013: Anthropogenic and Natural Radiative Forcing. In: *Climate Change 2013: The Physical Science Basis. Contribution of Working Group I to the Fifth Assessment Report of the Intergovernmental Panel on Climate Change* [Stocker, T.F., D. Qin, G.-K.

Plattner, M. Tignor, S.K. Allen, J. Boschung, A. Nauels, Y. Xia, V. Bex and P.M. Midgley (eds.)]. Cambridge University Press, Cambridge, United Kingdom and New York, NY, USA.

[16] "Guideline for Life Cycle Climate Performance," IIR, 2015.

[17] Lemmon, E.W., Bell, I.H., Huber, M.L., McLinden, M.O. NIST Standard Reference Database 23: Reference Fluid Thermodynamic and Transport Properties-REFPROP, Version 10.0, National Institute of Standards and Technology, Standard Reference Data Program, Gaithersburg, 2018.

[18] ASHRAE. 2019. ASHRAE Standard 34-2019, *Designation and Safety Classification of Refrigerants.* Atlanta: ASHRAE.

[19] A. Baral, R. Minjares and R. A. Urban, "Upstream climate impacts from production of R-134a and R-1234yf refrigerants used in mobile air conditioning systems", The International Council on Clean Transportation, 2013.

[20] S. Daviran, A. Kasaeian, S. Golzari, O. Mahian, S. Nasirivatan, and S. Wongwises, "A comparative study on the performance of HFO-1234yf and HFC-134a as an alternative in automotive air conditioning systems," *Applied Thermal Engineering*, vol. 110, pp. 1091–1100, Jan. 2017, doi: 10.1016/j.applthermaleng.2016.09.034.

[21] S. Jarall, “Study of refrigeration system with HFO-1234yf as a working fluid,” *International Journal of Refrigeration*, vol. 35, no. 6, pp. 1668–1677, Sep. 2012, doi: 10.1016/j.ijrefrig.2012.03.007.

[22] D. Sánchez, R. Cabello, R. Llopis, I. Arauzo, J. Catalán-Gil, and E. Torrella, “Energy performance evaluation of R1234yf, R1234ze(E), R600a, R290 and R152a as low-GWP R134a alternatives,” *International Journal of Refrigeration*, vol. 74, pp. 269–282, Feb. 2017, doi: 10.1016/j.ijrefrig.2016.09.020.

[23] H. Cho and C. Park, “Experimental investigation of performance and exergy analysis of automotive air conditioning systems using refrigerant R1234yf at various compressor speeds,” *Applied Thermal Engineering*, vol. 101, pp. 30–37, May 2016, doi: 10.1016/j.applthermaleng.2016.01.153.

[24] C. Aprea, A. Greco, and A. Maiorino, “HFOs and their binary mixtures with HFC134a working as drop-in refrigerant in a household refrigerator: Energy analysis and environmental impact assessment,” *Applied Thermal Engineering*, vol. 141, pp. 226–233, Aug. 2018, doi: 10.1016/j.applthermaleng.2018.02.072.

[25] F. Molés, J. Navarro-Esbrí, B. Peris, A. Mota-Babiloni, and Á. Barragán-Cervera, “Theoretical energy performance evaluation of different single stage vapour compression refrigeration configurations using R1234yf and R1234ze(E) as working fluids,” *International Journal of Refrigeration*, vol. 44, pp. 141–150, Aug. 2014, doi: 10.1016/j.ijrefrig.2014.04.025.

[26] Z. Qi, “Performance improvement potentials of R1234yf mobile air conditioning system,” *International Journal of Refrigeration*, vol. 58, pp. 35–40, Oct. 2015, doi: 10.1016/j.ijrefrig.2015.03.019.

[27] C. Aprea, A. Greco, and A. Maiorino, “An experimental investigation on the substitution of HFC134a with HFO1234YF in a domestic refrigerator,” *Applied Thermal Engineering*, vol. 106, pp. 959–967, Aug. 2016, doi: 10.1016/j.applthermaleng.2016.06.098.

[28] S. E. Jørgensen, “Exergy,” in *Encyclopedia of Ecology*, S. E. Jørgensen and B. D. Fath, Eds. Oxford: Academic Press, 2008, pp. 1498–1509.

[29] Saeid Mokhatab, John Y. Mak, Jaleel V. Valappil, David A. Wood, Handbook of Liquefied Natural Gas, Gulf Professional Publishing, 2014, Pages 185-228, ISBN 9780124045859, https://doi.org/10.1016/B978-0-12-404585-9.00004-0.
(http://www.sciencedirect.com/science/article/pii/B9780124045859000040)

[30] A. Yataganbaba, A. Kilicarslan, and İ. Kurtbaş, “Exergy analysis of R1234yf and R1234ze as R134a replacements in a two evaporator vapour compression refrigeration system,” *International Journal of Refrigeration*, vol. 60, no. Supplement C, pp. 26–37, Dec. 2015.

[31] J. M. Belman-Flores, A. P. Rodríguez-Muñoz, C. G. Pérez-Reguera, and A. Mota-Babiloni, “Experimental study of R1234yf as a drop-in replacement

for R134a in a domestic refrigerator," *International Journal of Refrigeration*, vol. 81, pp. 1–11, Sep. 2017, doi: 10.1016/j.ijrefrig.2017.05.003.

[32] S. Golzari, A. Kasaeian, S. Daviran, O. Mahian, S. Wongwises, and A. Z. Sahin, "Second law analysis of an automotive air conditioning system using HFO-1234yf, an environmentally friendly refrigerant," *International Journal of Refrigeration*, vol. 73, pp. 134–143, Jan. 2017, doi: 10.1016/j.ijrefrig.2016.09.009.

[33] Japanese Industrial Standard, JIS D1618-1986, 1986.

[34] J. M. Belman-Flores, V. H. Rangel-Hernández, S. Usón, and C. Rubio-Maya, "Energy and exergy analysis of R1234yf as drop-in replacement for R134a in a domestic refrigeration system," *Energy*, vol. 132, pp. 116–125, Aug. 2017.

[35] S.A. Klein, *Engineering Equation Solver*. F-Chart Software.

[36] P. Makhnatch and R. Khodabandeh, "The role of environmental metrics (GWP, TEWI, LCCP) in the selection of low GWP refrigerant," in *International Conference on Applied Energy, Icae2014*, vol. 61, J. Yan, D. J. Lee, S. K. Chou, U. Desideri, and H. Li, Eds. Amsterdam: Elsevier Science Bv, 2014, pp. 2460–2463.

[37] K. P. Shine, J. S. Fuglestvedt, K. Hailemariam, and N. Stuber, "Alternatives to the Global Warming Potential for Comparing Climate Impacts of

Emissions of Greenhouse Gases," *Climatic Change*, vol. 68, no. 3, pp. 281–302, Feb. 2005.

[38] S. J. Smith and M. L. Wigley, "Global Warming Potentials: 1. Climatic Implications of Emissions Reductions," *Climatic Change*, vol. 44, no. 4, pp. 445–457, Mar. 2000.

[39] S. K. Fischer, "Total equivalent warming impact: a measure of the global warming impact of CFC alternatives in refrigerating equipment," *International Journal of Refrigeration*, vol. 16, no. 6, pp. 423–428, Jan. 1993.

[40] S.K. Kalla*, J.A. Usmani," Alternative Refrigerants: A review," *International Journal of Engineering Science & Research Technology*, Vol.3 ,(6),PP. 397-401: June, 2014.

[41] R. G. Richels and A. S. Manne, "An alternative approach to establishing trade-offs among greenhouse gases," *Nature (London)*, vol. 410, *(6829)*, pp. 675-677, 2001.

[42] "Methods of calculating Total Equivalent Warming Impact (TEWI)," The Australian Institute of Refrigeration, Air Conditioning and Heating, 2012.

[43] Fischer, S.K., Hughes, P.J., Fairchild, P.D., Kusik, C.L., Dieckmann, J.T., McMahon, E.M., & Hobday, N. "Energy and global warming impacts of CFC alternative technologies", Arlington, VA: U.S. Department of Energy and AFEAS, 1991.

[44] Md. A. Islam, K. Srinivasan, K. Thu, and B. B. Saha, “Assessment of total equivalent warming impact (TEWI) of supermarket refrigeration systems,” *International Journal of Hydrogen Energy*, vol. 42, no. 43, pp. 26973–26983, Oct. 2017, doi: 10.1016/j.ijhydene.2017.07.035.

[45] S. Papasavva and S. O. Andersen, “Green-MAC-LCCP©: Life-cycle climate performance metric for mobile air conditioning technology choice,” *Environmental Progress & Sustainable Energy*, vol. 30, no. 2, pp. 234–247, 2011, doi: https://doi.org/10.1002/ep.10465.

[46] Koban, M., “HFO-1234yf Low GWP Refrigerant LCCP Analysis (2009-01-0179 Technical Paper)- SAE Mobilus.” https://saemobilus.sae.org/content/2009-01-0179/ (accessed May 19, 2019).

[47] H. Lee, S. Troch, Y. Hwang, and R. Radermacher, “LCCP evaluation on various vapor compression cycle options and low GWP refrigerants,” *International Journal of Refrigeration*, vol. 70, pp. 128–137, Oct. 2016, doi: 10.1016/j.ijrefrig.2016.07.003.

[48] *Italian National Unification*, UNI-EN ISO 15502, 2006.

[49] IEC 62552-2:2015, Household refrigerating appliances – Characteristics and test methods – Part 2: Performance requirements

[50] CMS3005ABA-KA current sensor datasheet

[51] CMk3005ABA-KA demoboard datasheet

[52] Campbellsci, “https://www.campbellsci.com/cr3000,” Data logger CR3000.

[53] Campbellsci, “https://www.campbellsci.com/am25t,” 25-Channel Solid-State Thermocouple Multiplexer AM25T.

[54] Omega, “https://www.omega.com/index.html,” Omega Stamford CT 06907.

[55] https://www.tek.com/tektronix-and-keithley-digital-multimeter/2001-series-7%C2%BD-digit-multimeter-scanning, Aug. 10th 2020.

[56] Clifford, A. A. (1973). Multivariate error analysis: a handbook of error propagation and calculation in many-parameter systems. John Wiley & Sons. *ISBN 978-0470160558*.

[57] O. Abdelaziz, N. Cotton and P. Cazelles, "Guidance Report on net benefits and cost for energy efficient refrigeration design options", International Copper Association, 2020.

[58] AUC Office of Sustainability, "CARBON FOOTPRINT 2019 REPORT", The American University in Cairo, Cairo, Egypt, 2019.

Chapter 6 Appendix

6.1. Pressure Transducers Calibration

Table 6.1: Compressor suction pressure transducer calibration data.	
Actual Pressure (bar gauge)	**Measured Voltage (V)**
0	1.0217
0.689476	1.448
1	1.6355
1.189476	1.7526
1.5	1.9453
1.5	1.9453
1.189476	1.7527
1	1.6364
0.689476	1.4477
0	1.0217

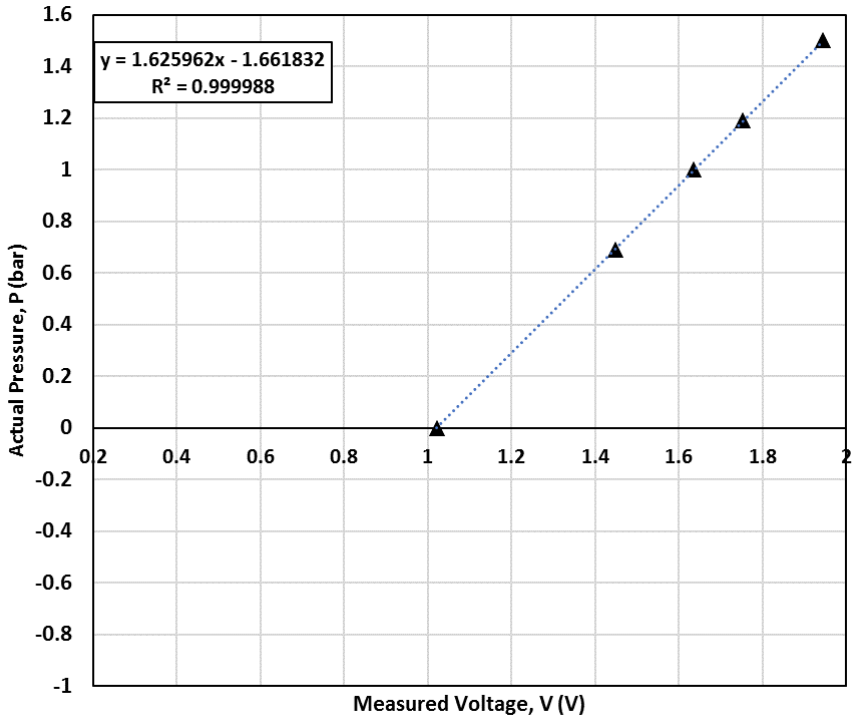

Figure 6.1: Compressor suction pressure transducer calibration curve.

Table 6.2: Compressor discharge pressure transducer calibration data.	
Actual Pressure (bar gauge)	**Measured Voltage (V)**
0	0.4024
1	0.503
2	0.604
3	0.7049
4	0.8056
5	0.9063
6	1.0067
7	1.107
8	1.2072
9	1.3078
10	1.408
11	1.508
12	1.6082
13	1.7077
14	1.8079
15	1.9076
16	2.0078
16	2.0078
15	1.901
14	1.8079
13	1.7078
12	1.6077
11	1.5078
10	1.4076
9	1.3073
8	1.2069
7	1.1066
6	1.0063
5	0.9061
4	0.8055
3	0.7048
2	0.604
1	0.503
0	0.4024

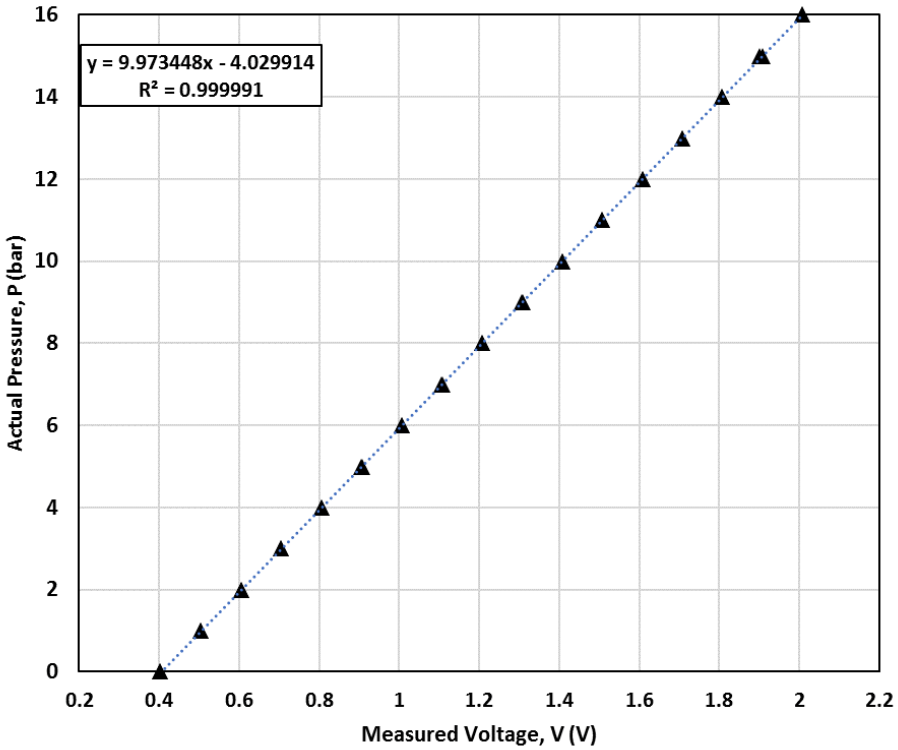

Figure 6.2: Compressor discharge pressure transducer calibration curve.

Table 6.3: Anti- Sweat tube outlet pressure transducer calibration data.	
Actual Pressure (bar gauge)	**Measured Voltage (V)**
0	0.3987
1	0.5526
1.5	0.6295
2	0.7069
3	0.8605
4	1.0144
5	1.1683
6	1.3221
7	1.4755
8	1.6289
9	1.7829
10	1.9349
10	1.9349
9	1.7819
8	1.6284
7	1.4752
6	1.3218
5	1.1679
4	1.0142
3	0.8617
2	0.7075
1.5	0.6303
1	0.5529
0	0.3987

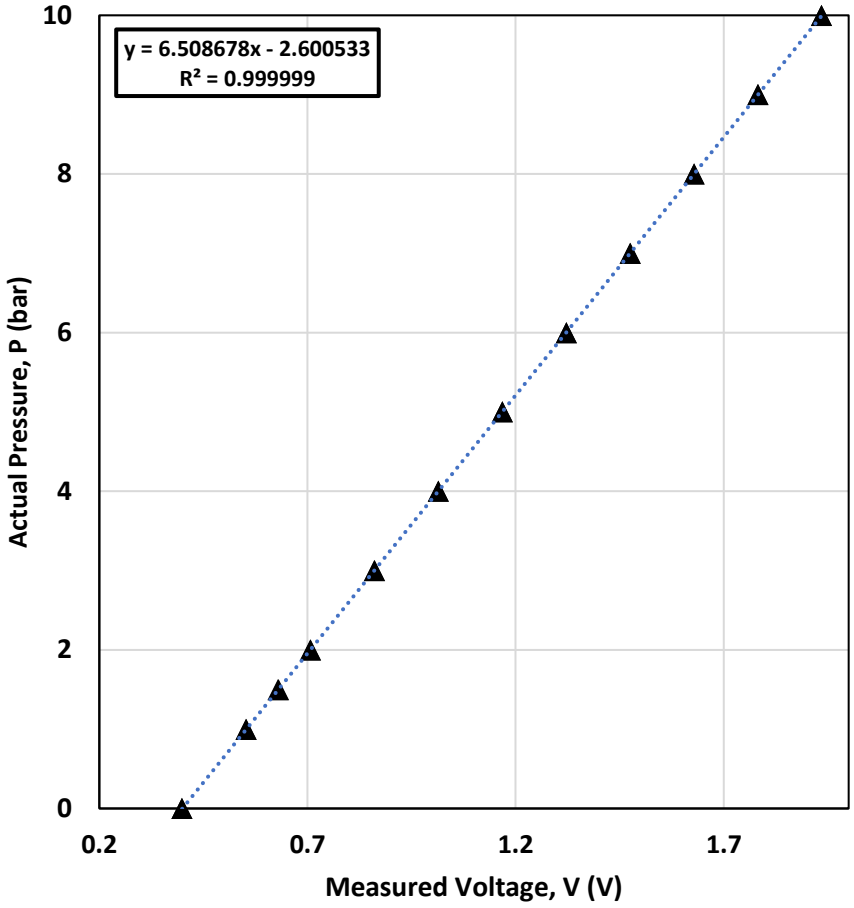

Figure 6.3: Anti-Sweat tube outlet pressure transducer calibration curve.

6.2. Thermocouple Calibration

6.2.1. Group A thermocouples calibration

Table 6.4: Group A thermocouples calibration.					
Actual Temperature (°C)	**A1 Reading (°C)**	**A2 Reading (°C)**	**A3 Reading (°C)**	**A4 Reading (°C)**	**A5 Reading (°C)**
1	0.1	-0.03	-0.02	0.05	0.11
1	0.05	-0.03	0.02	-0.01	0.08
1	0.02	-0.04	0.08	0.18	0.02
99	98.11	98.3	98.24	98.1	98.28
99	98.35	98.49	98.37	98.39	98.35
99	98.34	98.37	98.55	98.33	98.44

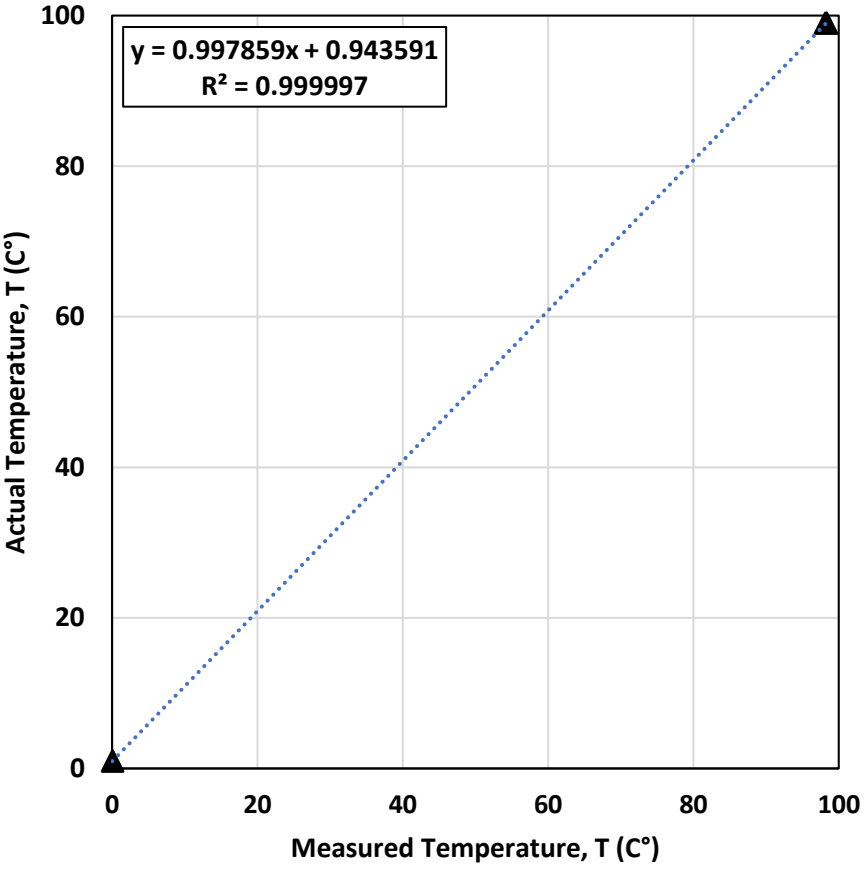

Figure 6.4: Thermocouple A1 calibration curve.

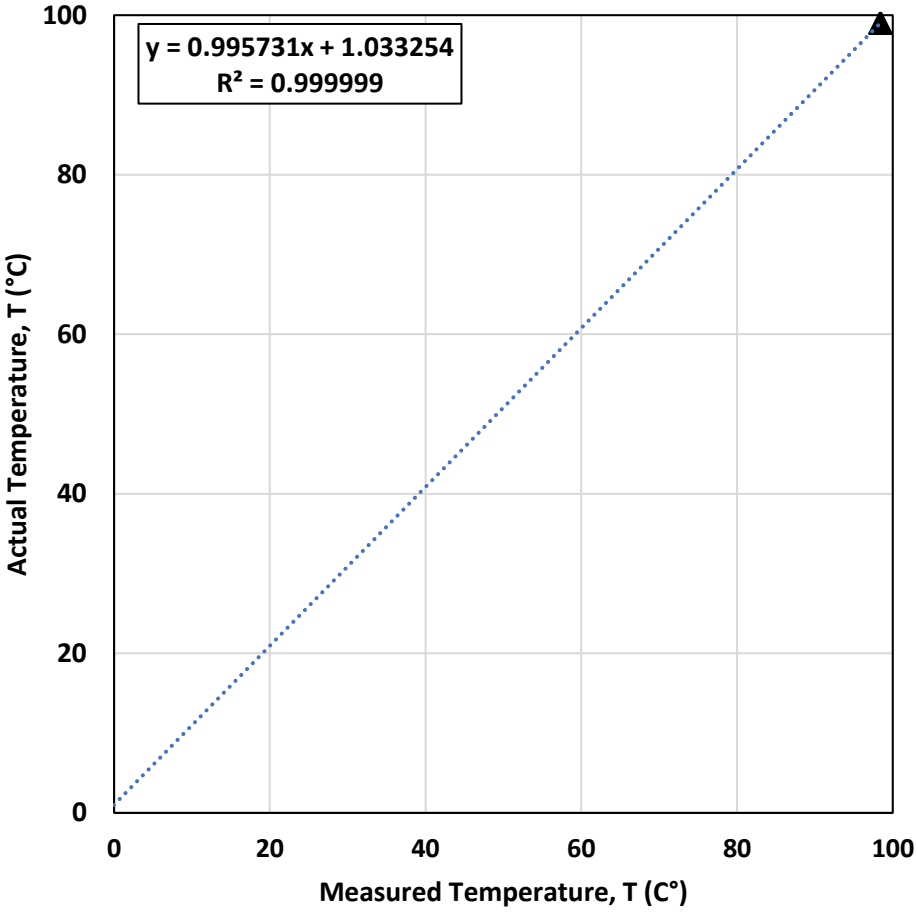

Figure 6.5: Thermocouple A2 calibration curve.

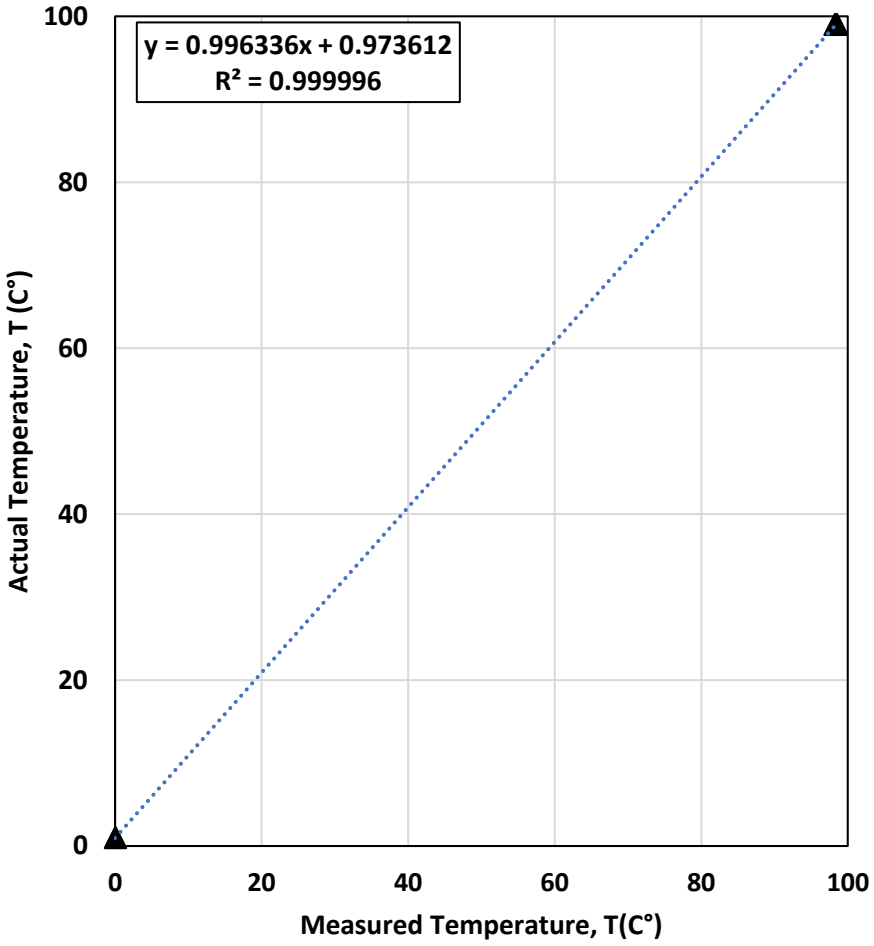

Figure 6.6: Thermocouple A3 calibration curve.

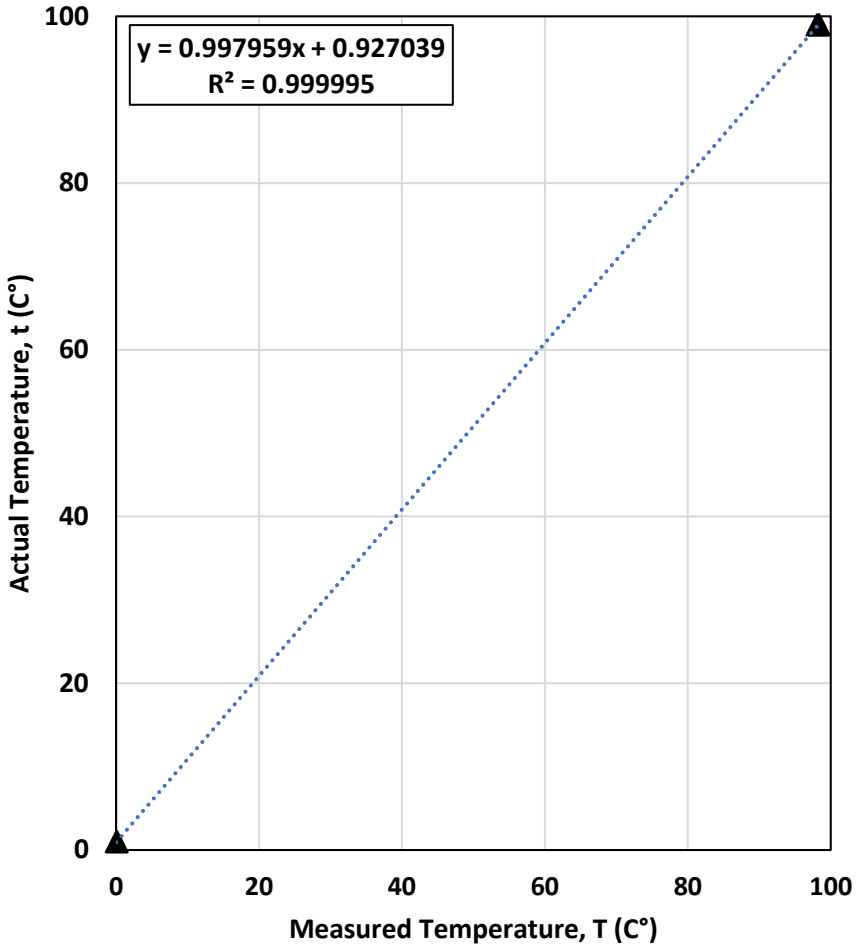

Figure 6.7: Thermocouple A4 calibration curve.

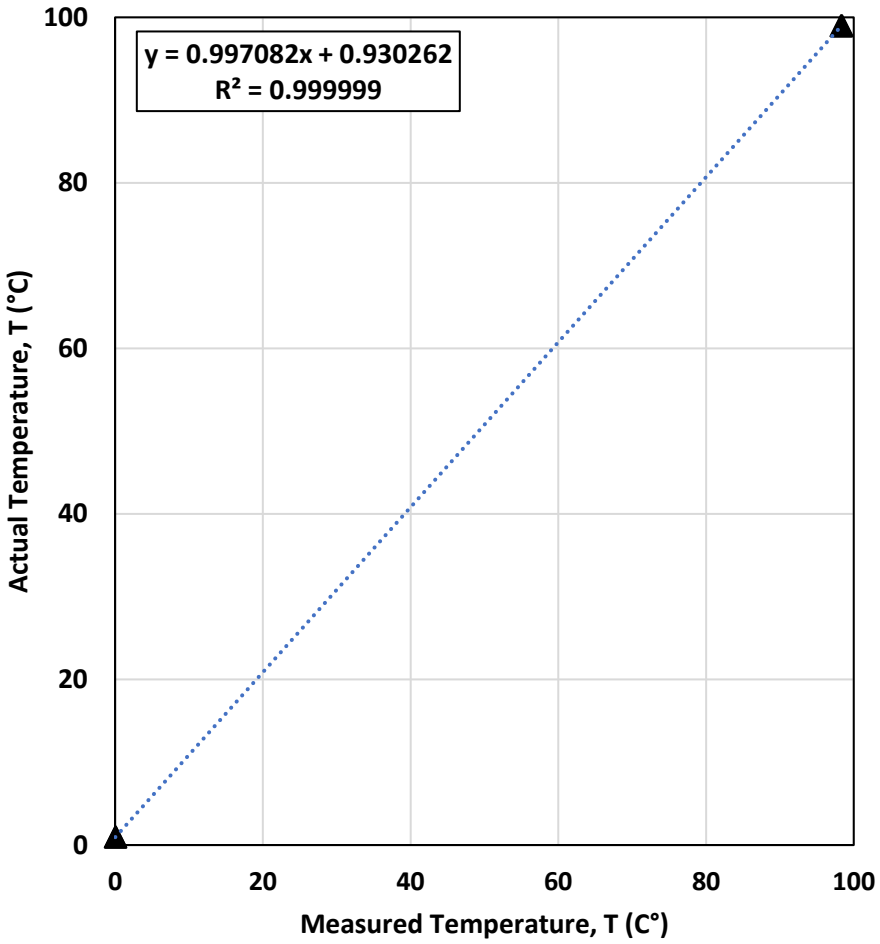

Figure 6.8: Thermocouple A5 calibration curve.

6.2.2. Group B thermocouples calibration

Table 6.5: Group B thermocouples calibration.

Actual Temperature (°C)	B3 Reading (°C)	B5 Reading (°C)
1	0.1	0
1	0.08	0.08
1	0.1	0.08
99	98.61	98.72
99	98.24	98.29
99	98.1	98.54

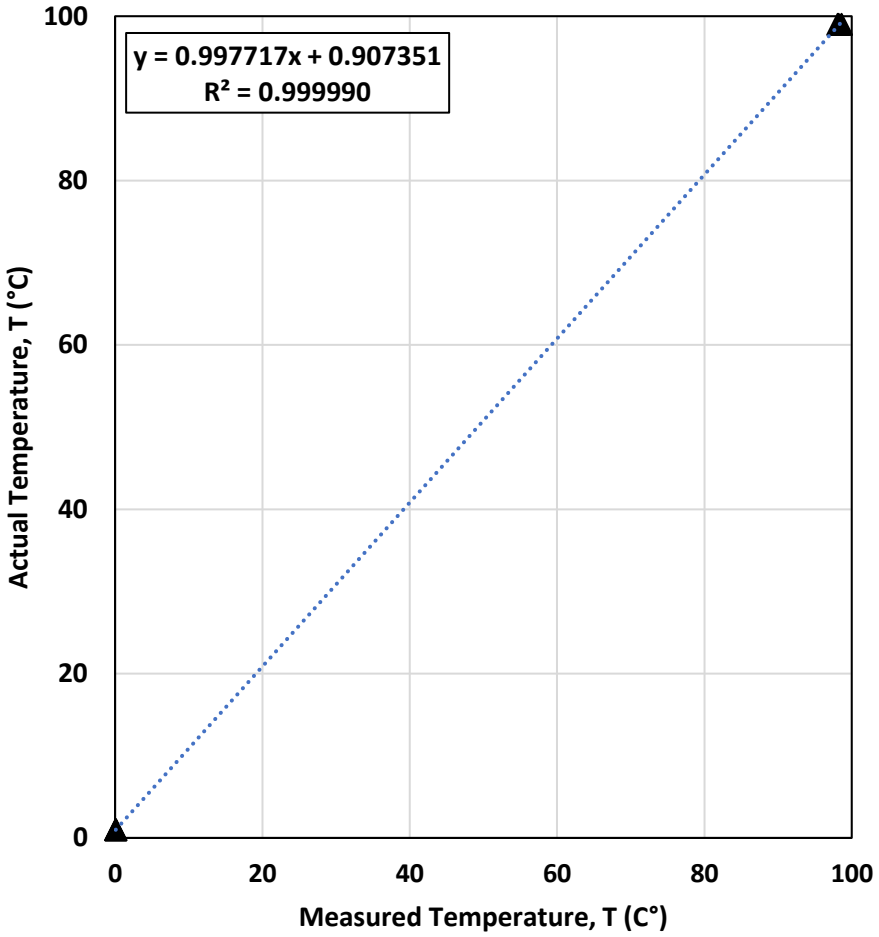

Figure 6.9: Thermocouple B3 calibration curve.

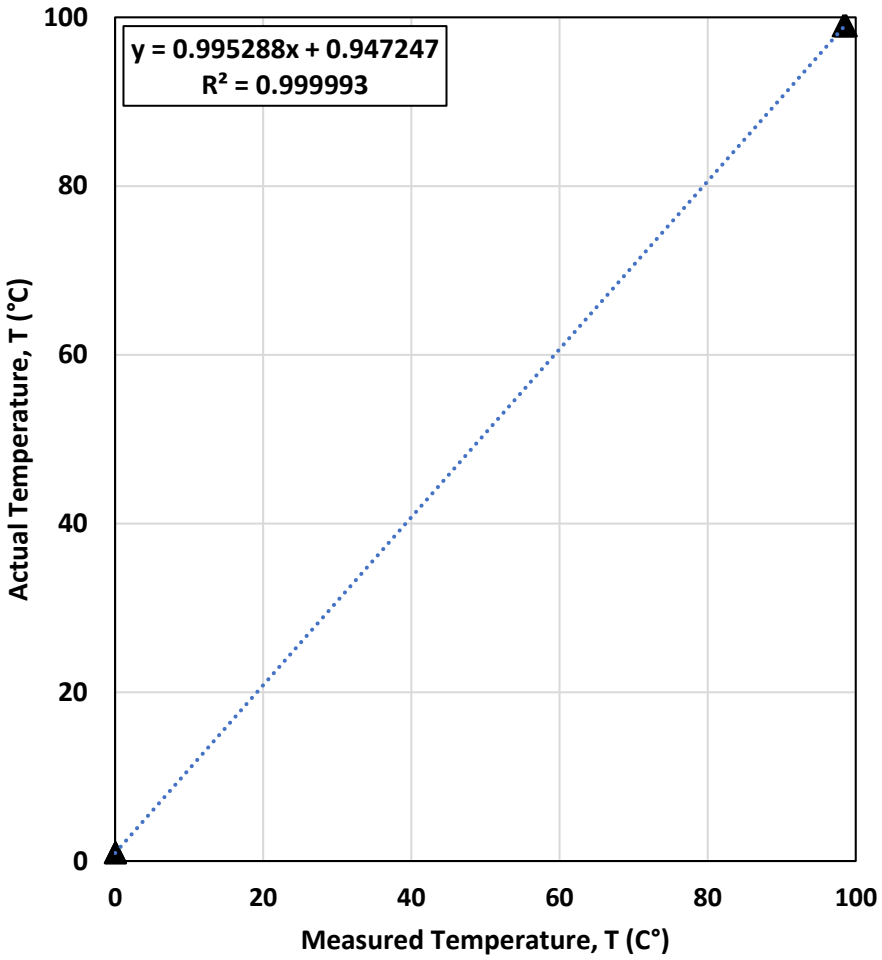

Figure 6.10: Thermocouple B5 calibration curve.

6.2.3. Group C thermocouples calibration

Table 6.6: Group C thermocouples calibration.

Actual Temperature (°C)	C1 Reading (°C)	C2 Reading (°C)	C3 Reading (°C)	C4 Reading (°C)	C5 Reading (°C)
1	-0.15	-0.17	0.11	0.08	0.1
1	0.1	0.14	0.25	0.31	-0.01
1	0.17	0.03	0.03	-0.01	0.05
99	98.6	98.64	98.5	98.7	98.39
99	98.09	98.25	97.97	97.91	98.37
99	97.79	97.9	97.92	97.9	98.37

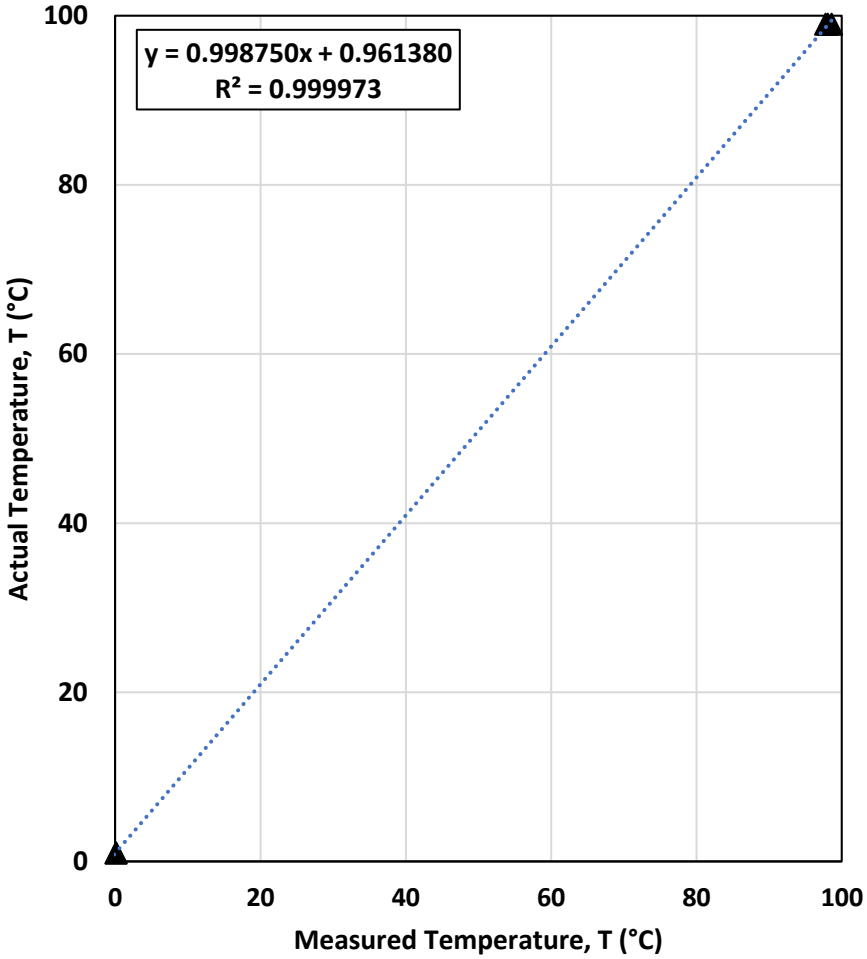

Figure 6.11: Thermocouple C1 calibration curve.

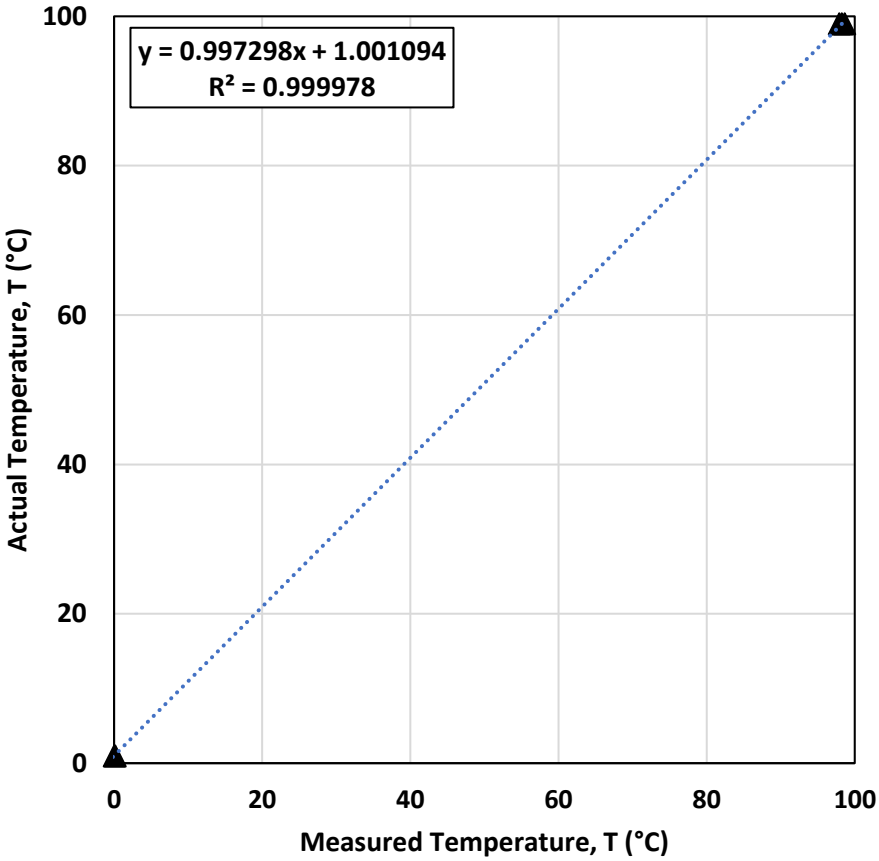

Figure 6.12: Thermocouple C2 calibration curve.

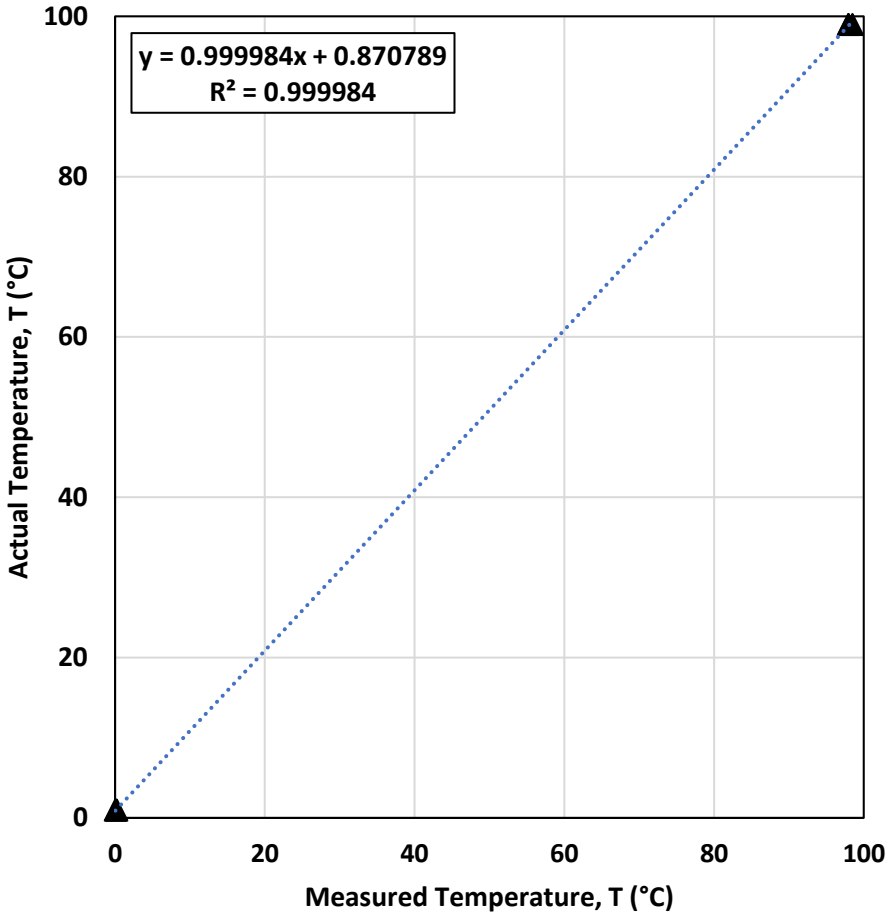

Figure 6.13: Thermocouple C3 calibration curve.

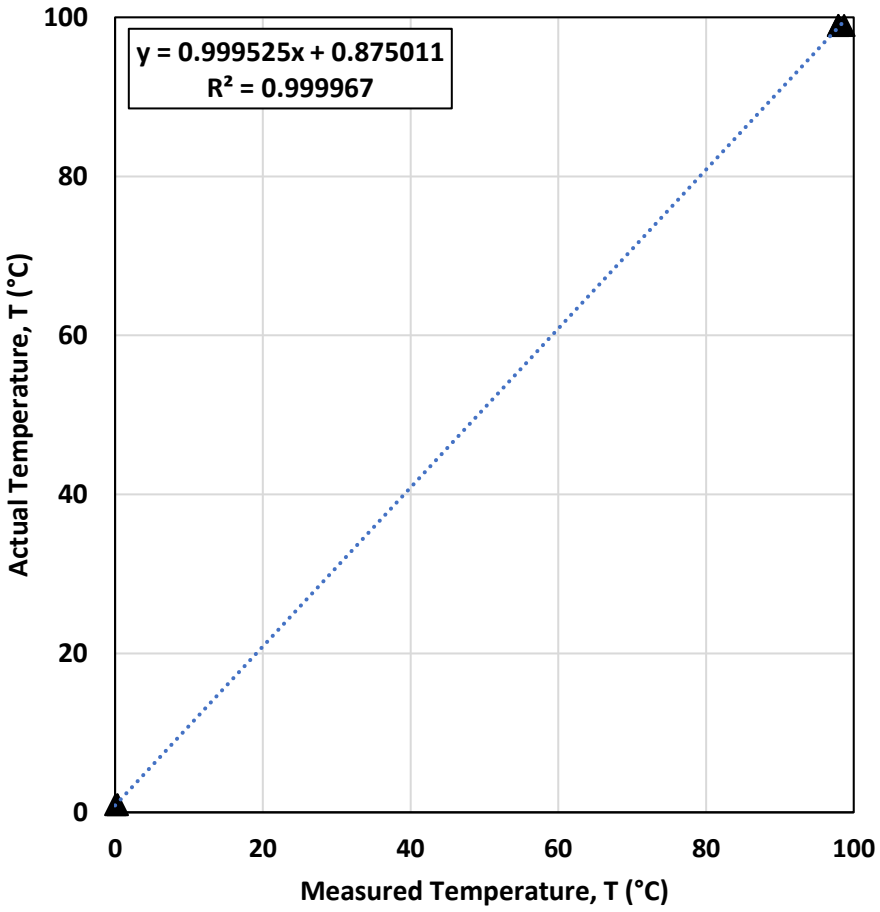

Figure 6.14: Thermocouple C4 calibration curve.

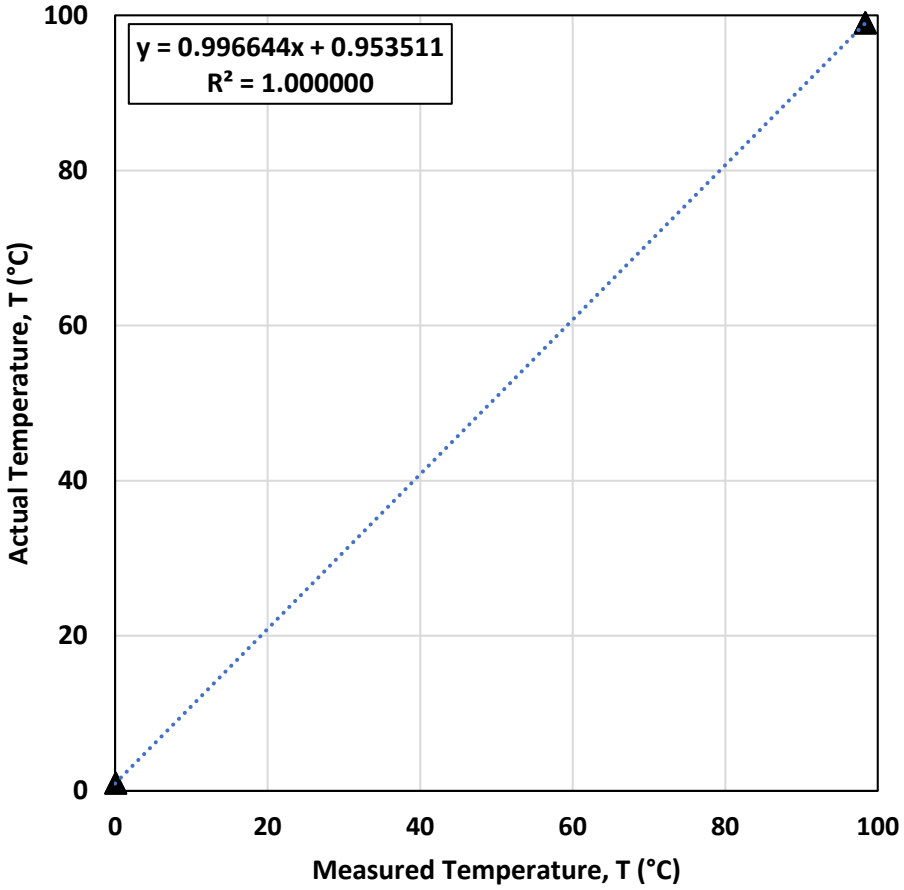

Figure 6.15: Thermocouple C5 calibration curve.

6.3. Current Sensor Calibration

Table 6.7: Current sensor calibration data.	
Actual Current (V)	**Measured Voltage (V)**
0	0.001
0.1776	0.33
0.3491	1.049
0.5195	1.691
0.6858	2.337
0.8557	2.794
1.0287	3.017
1.1976	3.109
1.3563	3.154
1.5308	3.192
1.6359	3.205
1.6951	3.217
1.8063	3.23
1.987	3.249
2.0819	3.253
2.2513	3.261
1.5334	3.19
1.3573	3.152
1.1991	3.106
1.0287	3.014
0.8532	2.79
0.6858	2.339
0.5195	1.692
0.3501	1.052
0.1776	0.32
0	0.001

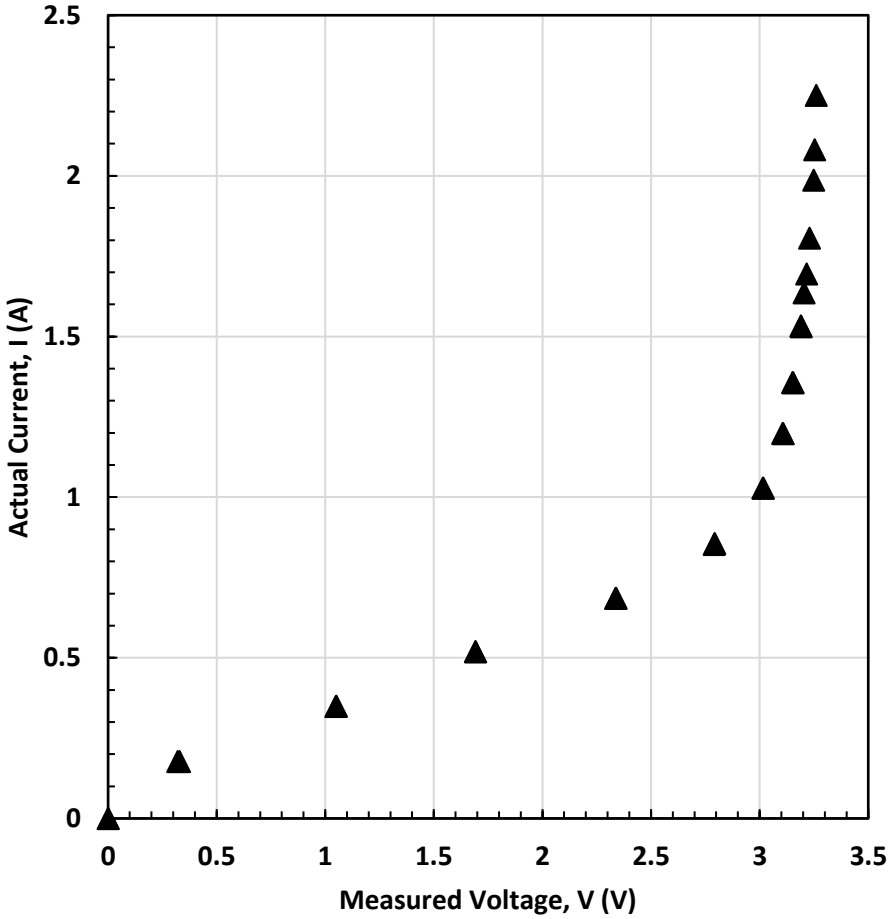

Figure 6.16: Current sensor calibration points.

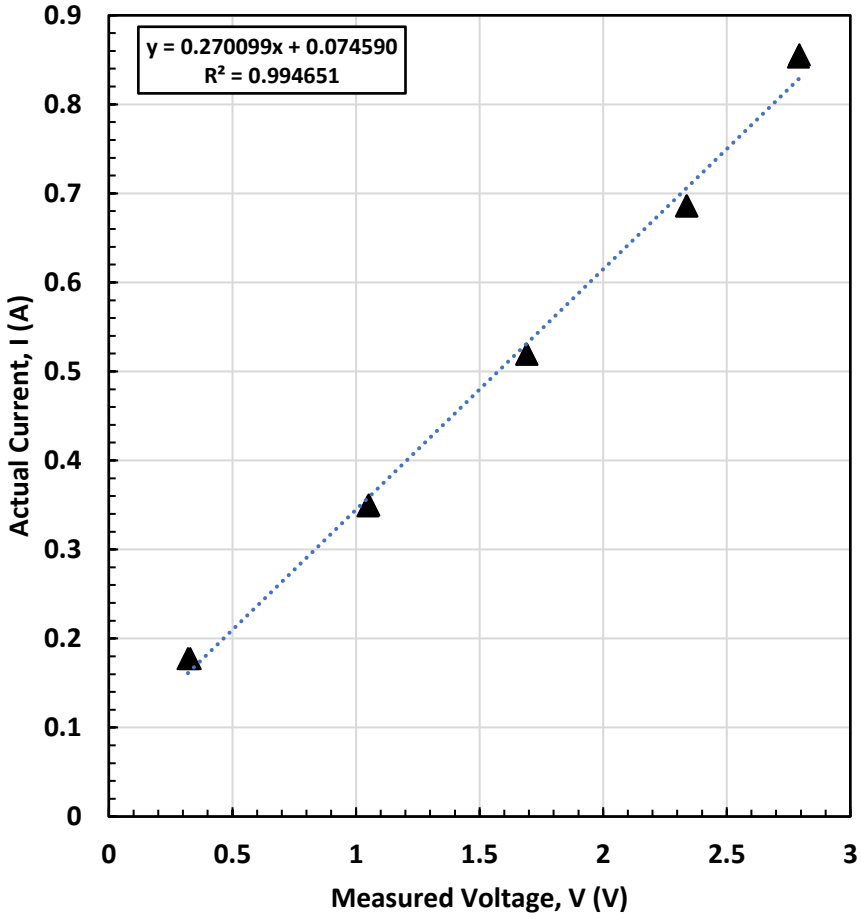

Figure 6.17: Current sensor calibration curve if the reading <2.79V (actual current <0.8532A).

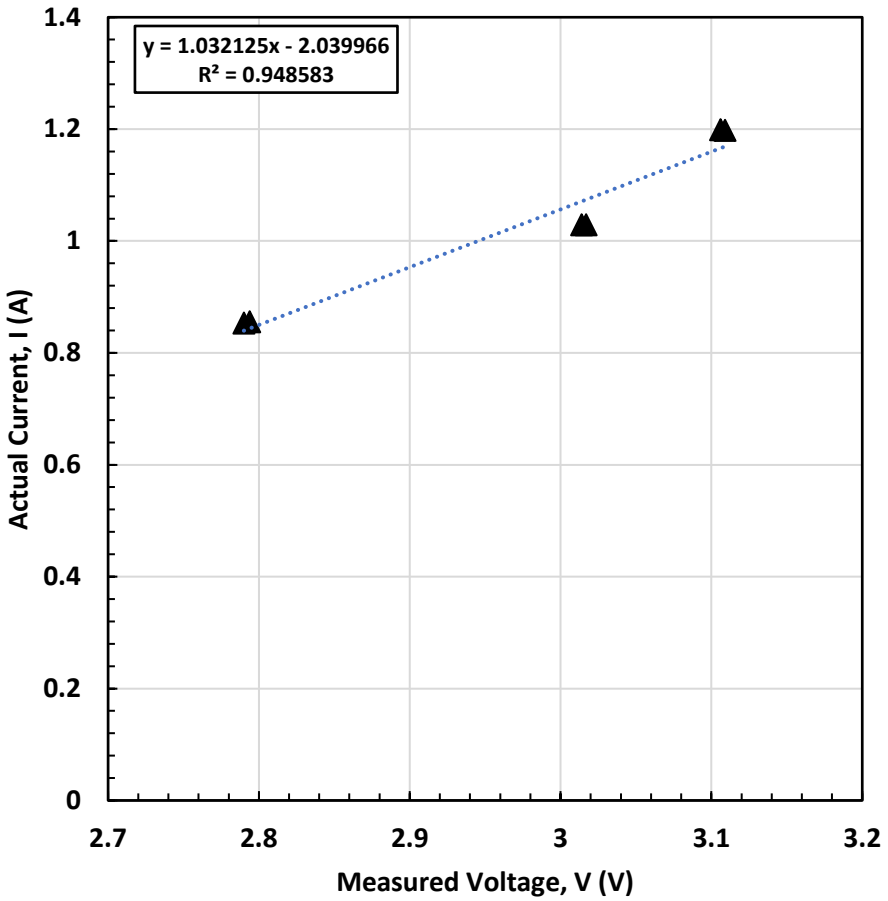

Figure 6.18: Current sensor calibration curve if the reading =[2.79V:3.109V[(actual current = [0.8532A : 1.1976[ ).

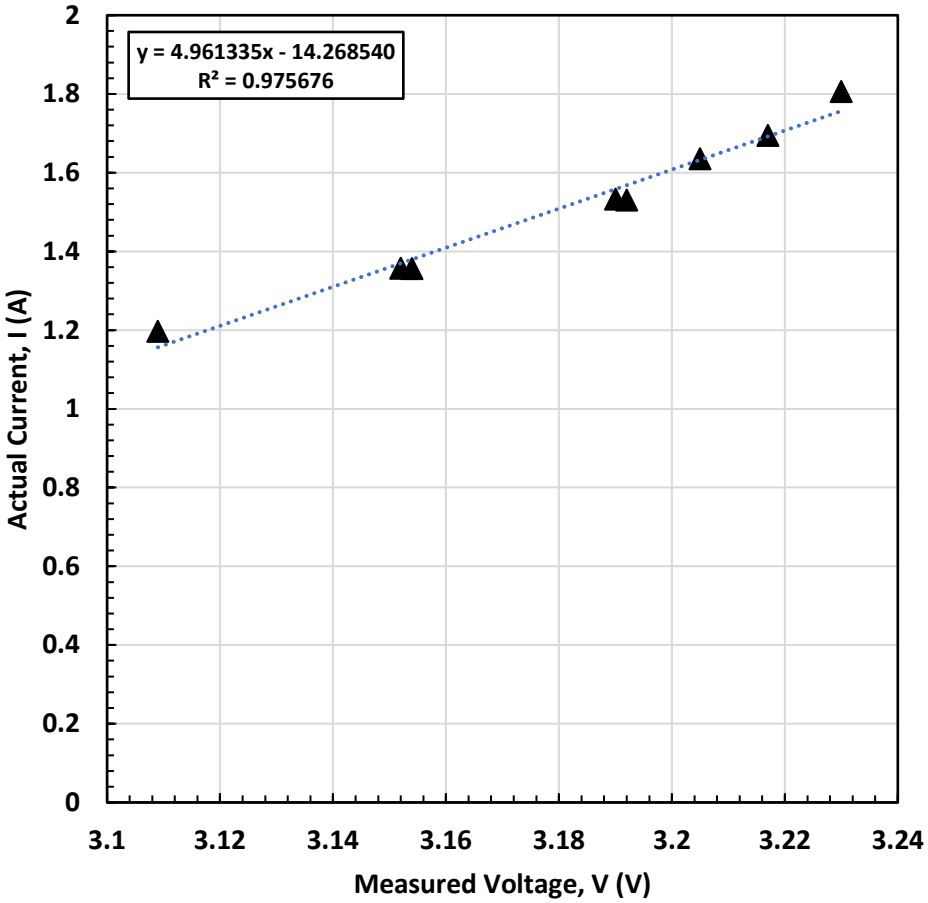

Figure 6.19: Current sensor calibration curve if the reading = [3.109V:3.23] (actual current = [1.1976A:1.8063A]

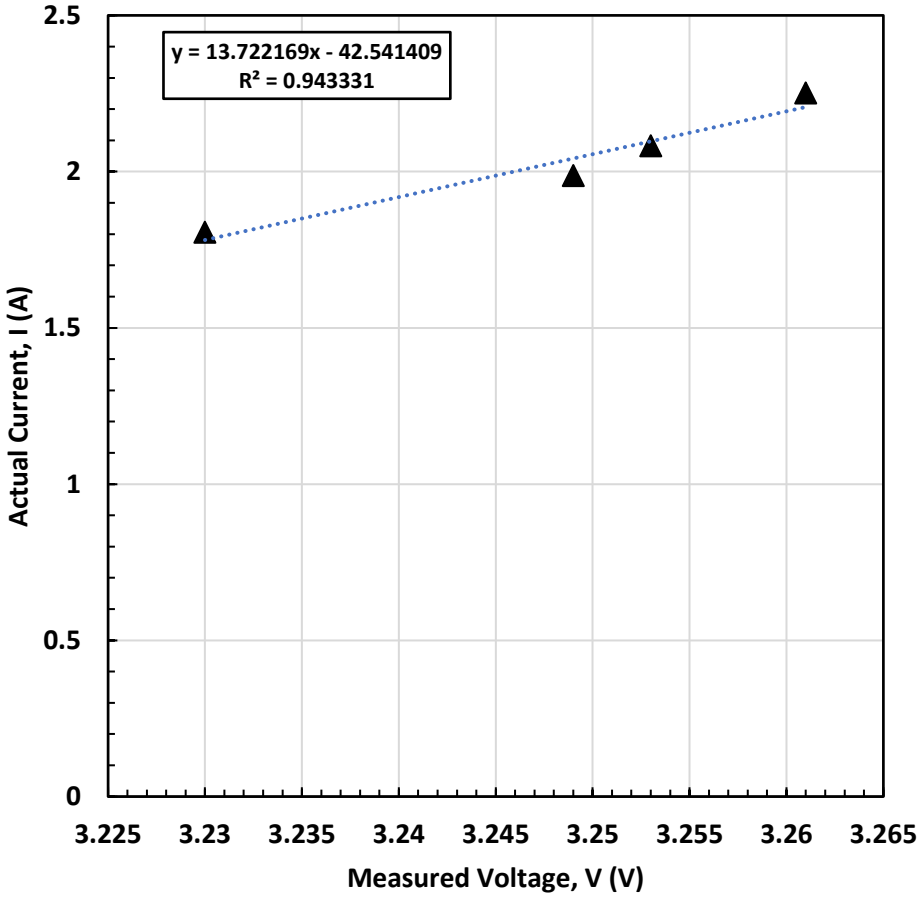

Figure 6.20: Current sensor calibration curve if the reading > 3.23V (actual current > 1.8063A)

6.4. Voltage Sensor Calibration

Table 6.8: Voltage sensor calibration data.	
Actual Voltage (V)	**Measured Voltage (mV)**
206	353.21
208	352.95
210	352.87
212	352.60
214	352.37
216	352.12
218	351.89
220	351.63
222	351.39
224	351.11
226	350.88
228	350.63
230	350.42
232	350.14
234	349.94
236	349.737
238	349.627
240	349.426
238	349.638
236	349.753
234	349.91
232	350.16
230	350.39
228	350.63
226	350.86
224	351.10
222	351.41
220	351.61
218	351.78
216	352.14
214	352.37
212	352.59
210	352.90
208	353.00
206	353.22

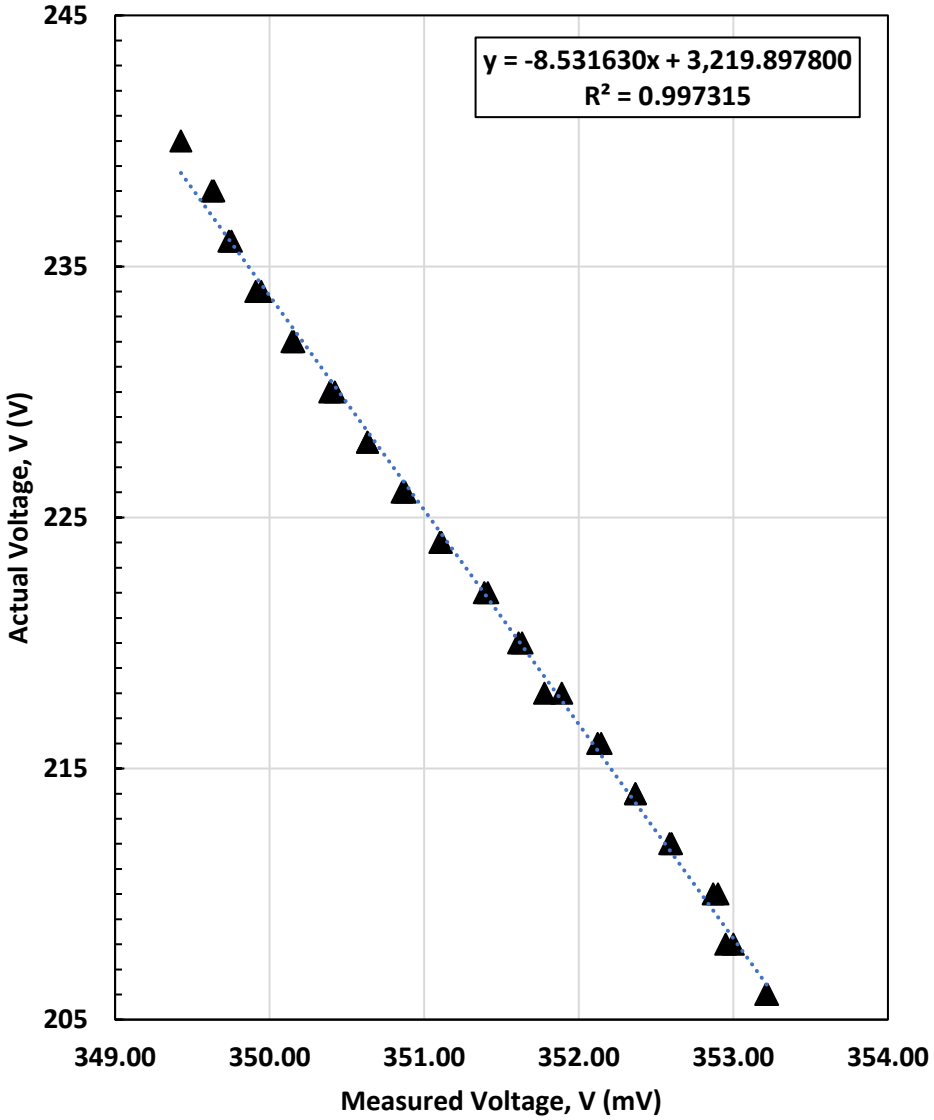

Figure 6.21: Voltage sensor calibration curve.